Corrosion Effects on Bond Strength in Reinforced Concrete

by

Kyle Stanish

A thesis submitted in conformity with the degree requirements
for the degree of Master's of Applied Science
Graduate Department of Civil Engineering
University of Toronto

0-612-29397-1

Abstract

AUTHOR: Kyle Stanish

DEGREE: Master's of Applied Science

DEPARTMENT: Civil Engineering, University of Toronto

SUPERVISORS: Professors R.D. Hooton and S.J. Pantazopoulou

TITLE: Corrosion Effects on Bond Strength in Reinforced Concrete

COMPLETION DATE: September, 1997

Corrosion of the reinforcing steel in reinforced concrete will effect its structural performance. This is in two ways: loss of steel section and deterioration of steel-concrete bond. In this, bond effects are investigated using two methods for different influences. The first technique looks at the effect of spalling concrete. This would affect bond by lessening the confinement. This is simulated by debonding proportions of the perimeters of steel bars in a reinforced concrete member and testing in flexure. The second looks at the effect of corrosion products. This was accomplished by casting reinforced concrete slabs with the ends of the reinforcing bars anchored in the concrete for a known length; the centre portion unbonded. The ends were corroded to various corrosion levels and then tested in flexure. Also included is a test of the predictive power of this work.

Acknowledgements

My first thanks must go to my supervisors, Prof. R.D. Hooton and Prof. S.J. Pantazopoulou. Without their support, both in terms of advice and financially, this work would not have even been begun, never mind completed. I would also like to thank the lab technicians who were so helpful along the way, principally Urszula Nytko, Giovanni Buzzeo and John MacDonald. They created an atmosphere where it was possible to accomplish a great deal. I would also like to thank my fellow students who provided a pleasant atmosphere in the labs and made it a pleasure to come in to work.

I would like to thank NSERC for their scholarship support of me through my graduate work. I would like to thank St. Mary's Cement and Lafarge cement for providing some of the materials I needed.

Finally, I would like to thank my parents for allowing my curiosity to grow from a young age. They placed my feet on the path I have chosen and were always ready to give me support along the way. Without them I would not be the person I am today and words cannot express how grateful I am. Thank You.

Table of Contents

Appendices

List of Tables

List of Figures

1.0 Introduction

Corrosion damage of reinforced concrete is a serious problem that needs to be addressed. This damage is a large drain on the economy. For example, in 1986 the Ontario Ministry of Housing estimated there was a $1 billion plus cost for repair in the approximately 3000 existing parking structures.[1-1] Most of this damage is due to reinforcement corrosion. This is only one province and only refers to one type of structure, but shows the magnitude of the problem. Another example would be the West Asia Gulf region where repairs, maintenance and reconstruction programs run into the billions of dollars.[1-2] Reinforced concrete corrosion is especially important as concrete is a widely used building material. By some estimates, approximately one ton of concrete is produced per person in the world per year.[1-3]

One reason for this large repair cost is that the role of chlorides in corrosion was ignored in standards until the 1970's. In the United Kingdom, there was no limit on the chloride content of concrete mix water until 1972, while the ACI code did not limit it until 1974. Limits on the chloride content of admixtures and of the concrete mix did not exist until the 1980's.[1-4] Before this time there were a large number of buildings and parking garages erected, especially during the 1970's construction boom. This has led to an ageing infrastructure, with these buildings now running into difficulty. Thus, the repair bill is taking larger and larger proportions of the construction dollar. Twenty years ago, approximately 30 % of construction expenditures were for repairs. This compares to the current level of 50 %, with indications that this will increase to the year 2000 and beyond.[1-5] Given this large expenditure, any improvement in the efficiency of evaluation techniques has the potential for large savings. Thus more information regarding how different corrosion levels corrosion affect a structural member's capacity would be useful. It would help in evaluating corroded structures and determining the optimum time for repair when performing a life-cycle cost analysis.

Parking garages are a type of structure that often run in to problems with corrosion. They are normally unheated; so to prevent ice formation de-icing salts are employed. These de-icing salts contain chlorides that dissolve in the melt water. Also, water often is allowed to collect because of poor drainage conditions. This lack of drainage may be due to poor design - e.g. insufficient slope of the slabs, improper construction practices - e.g. misplaced drains, or lack of maintenance - e.g. not cleaning out the drains properly. Chlorides will then penetrate the concrete from the water and are able to attack the reinforcing steel. This causes corrosion. The common parking garage structure is a continuous flat slab. Thus, the only steel contained in the slab is the flexural reinforcement. Once the steel is attacked, the moment capacity of the slab will be affected. This is a condition regarding which more information is needed. Thus, an investigation on the effect of corrosion on the flexural capacity of reinforced concrete slabs was undertaken.

There are two mechanisms occurring. The first is the loss of the section properties. This refers to any weakening that may be occurring due to loss of steel at a cross-section and this influence on the sectional moment capacity. This influence has been studied, for example by J. Phillips as part of his doctoral work at the University of Toronto.[1-6] The effect was found to be equivalent to a loss of steel area equal to the amount of steel corroded. A less studied influence is the effect of corrosion on the bond between the steel and the concrete. This work shall examine this issue.

To examine the effect of corrosion on bond, two influences on bond were studied. The first issue is the effect of spalling. Spalling will reduce bond by removing the concrete cover. This will lessen the confinement and thus reduce the bond. This influence was simulated for various proportions of the bars' perimeter along the entire length of the bar. The second effect is due to the creation of corrosion products. This has the effects of both changing the surface properties of the bar and exerting tensile stresses in the concrete, which leads to cracking. This influence was investigated for a variety of levels of corrosion and for two concrete mix designs. The mix designs chosen were typical of those used in properly designed parking garages.

Finally, a test of the predictive power of this work was performed. A normal slab was corroded and, after predicting the capacity based on the work done herein and by others, tested to failure. It was hoped to be able to predict both the load at ultimate capacity and the mode of failure. What follows are an investigation of the literature, the details of the experimental procedure undertaken, the results of this experimental program and a discussion of these results.

References

[1-1] *Report of the Advisory Committee on the Deterioration, Repair and Maintenance of Parking Garages* Ministry of Housing, Ontario Buildings Branch, July 1988, pg. i

[1-2] *Corrosion Damage to Concrete Structures in Western Asia* United Nations Centre for Human Settlements (Habitat), Nairobi, 1990, pg. i

[1-3] N.P. Mailvaganan *Repair and Protection of Concrete Structures* CRC Press c1992, pg. i (prologue)

[1-4] P. Pullar-Strecker, *Corrosion Damaged Concrete: Assessment and Repair* Anchor Brendon Ltd., Tiptree Essex, England c1987 pg. 91-6

[1-5] N.P. Mailvaganan *Repair and Protection of Concrete Structures* CRC Press c1992, pg. i (prologue)

[1-6] J. Phillips, *The Effect of Corrosion on the Structural Performance of New and Repaired One-Way Slabs,* Ph.D. Thesis, University of Toronto, c1993

2.0 Literature Review

When investigating the effects of corrosion on bond strength, there are a few subjects that must be examined before looking at the area as a whole. First, the process of corrosion must be understood. This includes why corrosion occurs and what affects it. Next, bond in normal, uncorroded specimens must be examined to see what is occurring in that situation. This allows us to focus on the potential differences between the two situations. Then, any structural effects of corrosion besides those on bond must be examined to determine what influence these could have. Finally, but most importantly, previous work on this subject must be examined for comparison. These subjects are all examined in this section.

2.1. Corrosion

Corrosion of the steel rebar in reinforced concrete occurs when the iron atoms combine with oxygen or chloride atoms to form a new compound. This is an electrochemical reaction that depends on the presence of water in the pores to act as an electrolyte.

Initially, the rusting of steel in a normal environment, without the presence of concrete, will be discussed. There are three distinct chemical reactions that occur:

$$Fe \rightarrow Fe^{2+} + 2e^- \qquad (2\text{-}1)$$

$$O_2 + 4\,e^- + 2\,H_2O \rightarrow 4\,OH^- \qquad (2\text{-}2)$$

$$2\,Fe^{2+} + 1/2\,O_2 + 4\,OH^- \rightarrow 2\,FeO.OH + H_2O \qquad (2\text{-}3)$$

Each of these reactions occurs at a different location in the chemical system. The iron disassociates at the anode (Reaction 2-1), and the oxygen and water react in the electrolyte (Reaction 2-2). These then react at the cathode to form corrosion products at the cathode. Reaction 2-3 is one typical cathodic reaction, but there are other possibilities.[2-1] This is a normal course for corrosion reactions of any metal.

Once concrete is involved, there are some differences. The concrete initially prevents corrosion by creating a basic environment. This passivates the steel by changing the form of corrosion products. Instead of producing the loose product FeO.OH, the FeO_2 and FeO_3 are produced. These substances adhere more closely to the surface of the bar. The progress of corrosion is thus limited by restricting oxygen access.[2-2] The protection of the alkalinity can be overcome through either carbonation, or chloride ingress. The steel then begins to rust. The reason for loss of protection with carbonation is loss of alkalinity. The corrosion products are then similar to those found in the bare steel situation. With loss of protection due to chloride ingress, the corrosion reactions are then slightly different, as the pH has not been reduced. Instead it is $FeCl_2$ that is initially produced and this then forms $Fe(OH)_2$, or other more complex oxides and chloride compounds

So what effect does this have on the mechanical properties of the steel? The first effect is that there is smaller area of steel. Some steel has become this weak corrosion product. Furthermore, the corrosion products have a larger volume than the original steel. This leads to stresses in the surrounding concrete and the potential for cracking. This obviously will have some effect on the performance of the reinforced concrete structure. It can also result in spalling of concrete cover.

Various factors affect the rate of corrosion in concrete. These include the concrete quality, the thickness of cover, any cracking that may exist, the water and oxygen content of the pore system and either the chloride concentration or the depth of carbonation; depending upon what is causing corrosion. The concrete quality affects corrosion rate by limiting the access of any deleterious substances as well as oxygen. The quality can be improved by both reducing the water-cement ratio and the inclusion of supplementary cementing materials. Increasing the concrete cover thickness has a similar effect of reducing the amount of aggressive substances that can enter. Cracks increase the amount of corrosion by providing pathways for deleterious chemicals and oxygen or water. The oxygen content and water content of the concrete are important as corrosion is an electrochemical process requiring the presence of both these substances to occur. If either of these substances are not present, then corrosion cannot occur.

2.2. Reinforcement-Concrete Bond

The bond between reinforcing steel and concrete is not fully understood, though a good working theory has been produced. Most of the main concepts are agreed upon, though some of the details are still being discussed. The reason for this is that the force transfer called bond is a complicated, multipart phenomenon. A useful method of describing the main forces is contained in Treece and Jirsa.[2-3] They divide the main components into two main categories. The first is the bearing component on the lugs. This is what will cause splitting of the concrete. The second category is the friction component. This is both true friction and the effect of any secondary chemical bonding effects.

A good summary of the major influences on bond is contained in Nawy.[2-4] The major factors are, according to Nawy:

1. Adhesion between the concrete and the reinforcing elements.
2. Gripping effect resulting from the drying shrinkage of the surrounding concrete
3. Frictional resistance to sliding and interlock on the reinforcing elements subjected to tensile stress.
4. Effect of concrete quality and strength in tension and compression.
5. Mechanical anchorage effects of the ends of the bars through the development length, splicing, hooks and crossbars.
6. Diameter, shape and spacing of reinforcement as they affect crack development.

It is suggested that factors 2, 3 and 4 are most important. This list is not universally agreed upon, however, and current literature contains models for bond that focus more on the effects of bond rather than on absolute mechanisms. A typical model is presented by Cairns and Jones[2-5, 2-6] and Cairns and Bin Abdullah[2-7]. They view bond as containing both a splitting and a non-splitting component. The splitting component varies with the amount of confinement that the bar experiences, while the non-splitting component is fixed. They do not explain what causes the non-splitting component, only that it is possibly similar to the cohesive effect in soils.

An other variable that affects bond and has not been discussed so far is concrete confinement. Increasing the confinement around a bar increases its bond strength.[2-8] This is true whether the confinement comes from transverse steel, e.g., stirrups, or from the stress field that exists in the concrete. This second situation can be explained best using an example. Where a beam intersects a column, the column load creates stresses that act perpendicular to the direction of the longitudinal beam steel. These stresses act to confine the steel and increase the bond strength. The influence of stress fields is not relied upon in design codes, [2-9,2-10,2-11] though it is well accepted. This is because it is impossible to ensure that a stress field will always exist.

Before discussing specific bond strengths, it is important to understand how bond is tested in reinforced concrete. There are three main tests for determining bond strength, according to Nawy.[2-12] These are: pull-out tests, embedded bar tests and beam tests. Each of these has its strengths and weaknesses, and will be further discussed. During this, however, it should be remembered what the purpose of the bond test is; to discover how well the steel transfers load to the concrete under service conditions. For most reinforced concrete applications, this is when the steel and the surrounding concrete are both in tension.

Pullout tests are relatively simple to perform. The steel is cast into a concrete sample to a known length. The steel is pulled upon while the concrete is restrained. This is continued until the steel either yields or is pulled out of the concrete. This test has the advantage of simplicity and ease of determination of the bond strength. It also allows the simultaneous measurement of slip between the concrete and the steel. Its disadvantage lies in the stress field that arises. The steel is in tension, but the concrete is in compression. This is important as it is known that concrete behaves differently in compression and tension. Concrete has little tensile strength and exhibits cracking at low tensile loads. These aspects are not represented in this type of test. A pull-out test has been standardized as ASTM C234-91a.[2-13] This test, however, is strictly for evaluating different concrete types. It is not designed to be used for establishing bond values for structural design purposes or for determining the influence of different bar sizes or types. It does suggest however that this test could be adapted for research purposes if it is desired to study one of these influences.

An embedded bar test consists of a bar extended through a section of concrete. The bar is then pulled at both ends. The concrete will then crack and, based upon the crack spacing and widths, the bond stresses can be determined. This test does accurately model the stress field and is relatively simple to prepare. It is difficult to accurately monitor the crack spacing and widths, however. It is also difficult to interpret the data to give a direct stress. A basic understanding of what is occurring and how this relates to stress is difficult to achieve, as well.

The third test is the beam test. This test is set up in a variety of ways, the aim of which is to model a section of a beam with a known length of reinforcing steel embedded inside. This is then caused to bend so that the steel and the surrounding concrete are in tension. If done properly, this models service conditions well. It is also simple to understand and interpret. It can be difficult to do, however, due to the possibly unusual geometry involved. This has lead to a variety of set ups presented in the literature as compared to a standardized test which all researchers use.

Typical bond strengths for normal, ribbed bars thus can vary depending on the conditions that are encountered in service. The Eurocode does give values for use in design, with a built in factor of safety of 1.5. These values are dependent on the concrete strength and vary from 1.6 MPa for a concrete strength of 12 MPa to 3.4 MPa for a concrete strength of 35 MPa to 4.3 MPa for a concrete strength of 50 MPa. This is then modified to account for such issues as casting direction, bar diameter and actual stress in the bar.[2-14] Some experimentally determined values reported by Cairns and Jones[2-15,2-16] range from 3 - 5 MPa. This was for specimens with concrete strength near 30 MPa and concrete specimen dimensions of either 320 mm x 225 mm or 100 mm x 225 mm. A formula has also been developed for bond strength, based on tests at the University of Texas.[2-17] It proposes that bond stress is given by:

$$u = \frac{9.5\sqrt{f_c'}}{d_b} \leq 800 psi \quad \text{(USCU)}$$

$$\text{or } u = \frac{20\sqrt{f_c'}}{d_b} \leq 5.52\, MPa \quad \text{(metric).}$$

Thus typical values would range from 1.5 MPa, with weak concrete and a large diameter bar, to 5.5 MPa, with strong concrete and small bars.

2.3. Effects of Corrosion on Structural Performance

Corrosion of the reinforcing steel will affect the structural performance of a reinforced concrete section. In this section, we will discuss effects other than loss of bond. Bond effects are discussed in the next section.

The first effect is the corrosion influence on the steel properties. This influence is in two ways. First, there is a loss of steel section. The corrosion reactions convert the iron atoms into some other molecule, as described previously. These molecules form a brittle, weak substance that does not participate in load sharing. Thus in can be assumed that the load the steel can take reduces in proportion to the steel loss, as has been done in many typical analyses.[2-18, 2-19] This assumption has been confirmed by the work of J. Phillips.[2-20] This would have an obvious influence on the capacity of the member and consequent effects on safety.

The second effect corrosion has on structural performance is related to spalling. This is loss of the concrete around a bar due to its expansion. Spalling creates two difficulties. First, it can lead to a loss of bond. This will be discussed more extensively in the next section on bond. It also has the effect of loss of concrete section. This is more critical when the section that is spalling off is in the compression region. This can occur if the steel that is rusting is not the primary reinforcement but is included to control other effects, such as shrinkage and thermal movement. Unlike the concrete in the tension region, all the concrete in the compression region is used to resist load. Thus, if concrete is lost, this will have the effect of reducing the capacity of the member. This may not be critical at low levels of concrete loss due to the design factors of safety. If allowed to continue, however, then a significant weakening can occur. The beams will then also be failing in compression, which is a brittle failure. This is undesirable.

2.4. Effects of Corrosion on Bond

The effects of corrosion on bond have not been studied extensively. Some of the articles investigate the effect of using corroded steel as reinforcement. This is a very different situation from that of interest here and the results are not necessarily transferable. There have also been some studies on the effects of corrosion after steel inclusion.

If the steel is corroded before it is placed, then there is little or no decrease in the bond strength at low corrosion levels, up to about 1.0 %.[2-21] There may even be an increase in bond strength. It was felt that this is because the corrosion products at this level adhere to the bar. They would also increase the surface roughness.

If the steel corrodes in the concrete, there is a different situation. The expansion of the steel can cause cracking of the concrete. This will affect the bond strength. Al-Sulaimani, et al.[2-22] conducted a series of tests on pullout specimens in which they measured the slip versus load for different size bars corroded to different levels. The bars were corroded using impressed current techniques. They found that before the appearance of visible cracks, corrosion increased the bond strength. When visible cracks begin to appear on the surface, then the bond strength dropped down to slightly below the original level. Once extensive cracking occurred at about 7-8 % of mass loss then the bond strength decreased to about one third to one quarter of its original level. The slip at ultimate corrosion strength was found to be approximately the same, however. They attributed this trend to the effect of increased surface roughness at low corrosion levels and the deterioration of the rebar lugs at higher levels of corrosion.

Another series of tests was reported by Almusallam, et al.[2-23] They electrochemically corroded a series of slab-shaped bending specimens to a variety of corrosion levels. They found that the mode of failure changed at different corrosion levels. At no or low corrosion, the slabs failed in flexure, as they were designed to do. At higher corrosion levels, from 10 to 25 %, the slabs, along with being weaker, failed in a combination of bond failure and shear cracking. This is of interest as these are brittle failure modes that are more dangerous.

There has been some work performed by Rodriguez, et al.[2-24] They tested cubes with four bars at the corners to better simulate the actual conditions that exist during service. They tested cubes with and without stirrups. It was determined that the concrete quality and the cover to bar diameter ratio were not relevant if the cover was badly cracked. They also used these test results to establish relationships between residual bond strength and depth of attack penetration. The experimental values of attack penetration ranged between 0.04 and 0.5 mm of depth, but the authors felt that this could reasonably be extrapolated to a penetration of 1.0 mm. The relationships developed were:

$$u = 5.28 - 2.72\,x \qquad \text{(with stirrups)}$$

or

$$u = 3.00 - 4.76\,x \qquad \text{(without stirrups)}$$

where: $u \equiv$ the bond strength in MPa
$x \equiv$ the attack penetration, in mm ($0.05 \le x \le 1.00$)

In this study, the stirrups were not corroded. An expression was also developed for the intermediate case when there were some stirrups, but were less than the minimum required in the anchorage length by the Eurocode.

The article by Rodriguez et al.[2-25] also discussed the effect of confinement on the bond strength of corroded rebar. They found that increasing confinement increases the bond strength, just as determined for a uncorroded bar.

Thus it can be seen that it is likely that corrosion will significantly affect bond. It is the aim of this work to study this influence and quantify it. Thus a few words on what the expected influence of certain factors is now appropriate.

The first effect is that of spalling. As bond develops due to both the bearing on the bar by the concrete and the friction between the concrete and the bar, how much does the loss of the concrete surrounding the bar affect this stress transfer? It is likely that the capacity will be reduced but by how much? Will the adhesion between the concrete and the steel be sufficient to provide some load transfer or will this effect be insufficient on its own to provide any significant load transfer?

The effect of the expansion of the bar due to the formation of the corrosion products must be considered. This will lead to cracking of the concrete in the neighbourhood of the bar. What influence will these cracks have on the forces that can be developed to share load between the steel and the concrete?

These questions form the crux of what is hoped to be accomplished in this experimental investigation. In the following section, the approach that was taken to explore these questions is outlined.

References

[2-1]P. Schiessl, ed. *Corrosion of Steel in Concrete,* Chapman and Hall, Ltd. c1988, pg. 8

[2-2]P. Schiessl, ed. *Corrosion of Steel in Concrete,* Chapman and Hall, Ltd. c1988, pg. 8

[2-3]R. A. Treece, and J. O. Jirsa, "Bond Strength of Epoxy Coated Reinforcing Bars", *ACI Materials Journal,* v. 86 n. 2, March-April 1989, pg. 167-174

[2-4]Edward G. Nawy *Reinforced Concrete: A Fundamental Approach* 3rd Ed. Prentice-Hall Canada, Inc. Toronto c1996, pg. 414

[2-5]J. Cairns and K. Jones, "An Evaluation of the Bond-Splitting Action of Ribbed Bars", *ACI Materials Journal* v. 93 n.1, Jan.-Feb. 1996, pg. 10-19

[2-6]J. Cairns and K. Jones, "The Splitting Forces Generated By Bond", *Magazine of Concrete Research,* v. 47 n. 171, 1995, pg. 153-65.

[2-7]J. Cairns and R. Bin Abdullah, "Bond Strength of Black and Epoxy-Coated Reinforcement- A Theoretical Approach" *ACI Materials Journal* v. 93 n. 4, July-August 1996, pg. 362-9

[2-8] K. Leet, R*einforced Concrete Design,* 2nd Ed. McGraw-Hill Inc, Toronto, 1996, pg. 239

[2-9]Canadian Standards Association *Design of Concrete Structures for Buildings* CAN/A23.3-M84 Rexdale, Ont. 1984

[2-10] "Suggested Development, Splice and Standard Hook Provisions for Deformed Bars in Tension"(ACI 408.1R-90) *ACI Manual of Concrete Practice 1995*, Part 3, ACI, Detroit

[2-11] ENV 1992 - Eurocode 2 Cl. 9

[2-12] Edward G. Nawy *Reinforced Concrete: A Fundamental Approach* 3rd Ed. Prentice-Hall Canada, Inc. Toronto c1996, pg. 415

[2-13] "Standard Test Method for Comparing Concretes on the Basis of Bond Developed with Reinforcing Steel" (ASTM C234-91a) *1994 Annual Book of ASTM Standards*, V 04.02, ASTM, Philadelphia, pg.148-52

[2-14] ENV 1992 - Eurocode 2 Cl. 9

[2-15] J. Cairns and K. Jones, "An Evaluation of the Bond-Splitting Action of Ribbed Bars", *ACI Materials Journal* v. 93 n.1, Jan.-Feb. 1996, pg. 10-19

[2-16] J. Cairns and K. Jones, "The Splitting Forces Generated By Bond", *Magazine of Concrete Research,* v. 47 n. 171, 1995, pg. 153-65.

[2-17] K. Leet, R*einforced Concrete Design,* 2nd Ed. McGraw-Hill Inc, Toronto, 1996, pg. 241

[2-18]S. Ting and A. Nowak, "Effect of Reinforcing Steel Area Loss on Flexural Behaviour of Reinforced Concrete Beams", *ACI Structural Journal* v. 88 n. 3, May-June 1991, pg. 309-14

[2-19]Y. Yuan and M. Marosszeky, "Analysis of Corroded Reinforced Concrete Sections for Repair", *Journal of Structural Engineering* v. 117 n. 7, July 1991, pg. 2018-34

[2-20] J. Phillips, *The Effect of Corrosion on the Structural Performance of New and Repaired One-Way Slabs,* Ph.D. Thesis, University of Toronto, c1993, pg. 143

[2-21] M. Maslehuddin, et al. "Effect of Rusting of Reinforcing Steel on Its Mechanical Properties and Bond with Concrete", *ACI Materials Journal*, v. 87 n.5, Sept.- Oct. 1990, pg. 496-502

[2-22] G.J. Al-Sulaimani, M. Kaleemullah, I. A. Basunbul, and Rasheeduzzafar, "Influence of Corrosion and Cracking on Bond Behaviour and Strength of Reinforced Concrete Members", *ACI Structural Journal*, v. 87 n. 2, Mar.-Apr. 1990, pg. 220-231

[2-23] Abdullah A. Almusallam, Ahmad S. Al-Gahtani, Abdur Rauf Aziz, Fahd H. Dakhil and Rasheeduzzafar, "Effect of Reinforcement Corrosion on Flexural Behaviour of Concrete Slabs", *Journal of Materials in Civil Engineering*, v. 8 n. 3, August 1996, pg. 123 - 7

[2-24] J. Rodriguez, L. M. Ortega, J. Casal and J. M. Diez, "Assessing Structural Conditions of Concrete Structures with Corroded Reinforcement" *Concrete in the Service of Mankind: Concrete Repair, Rehabilitation and Protection,* First Ed. E & FN Spon London, 1996, pg. 65-78

[2-25] J. Rodriguez, L. M. Ortega, J. Casal and J. M. Diez, "Assessing Structural Conditions of Concrete Structures with Corroded Reinforcement" *Concrete in the Service of Mankind: Concrete Repair, Rehabilitation and Protection,* First Ed. E & FN Spon London, 1996, pg. 65-78

3.0 Experimental Procedure

There are two main ways in which corrosion can affect the bond between reinforcing bars and concrete. First, the corrosion products could cause spalling of the concrete cover. This will result in loss of confinement and presumably a reduction in bond strength. Second, there is the direct effect of the corrosion products. How will this change in state of matter affect the concrete - steel interface? A series of experiments was conducted to investigate each of these possible effects.

3.1 The Materials Used

3.1.1 The Reinforcing Steel

The reinforcing steel used was #10M bars corresponding to CSA/G30.18-M92 for a nominal yield strength of 400 MPa. Its actual yield strength was 450 MPa and it had a Young's Modulus of 180 GPa. A diagram of its stress-strain curve is included in Appendix A.

3.1.2 The Concrete

Table 3-1: Mix Designs

	Normal Mix	Silica Fume Mix
w/cm:	0.40	0.40
20 mm Aggregate	1130 kg/m^3	1130 kg/m^3
Sand	670 kg/m^3	670 kg/m^3
Water	155 kg/m^3	155 kg/m^3
Portland Cement	293 kg/m^3	272.5 kg/m^3
Silica Fume	0 kg/m^3	20.5 kg/m^3
Slag	97 kg/m^3	97 kg/m^3
Air Content	5-8 %	5-8 %
Slump	175 ±25 mm	175 ±25 mm

Two types of concrete were used. Both satisfy Class C1 concrete as defined by CAN/CSA A23.1-94. The first, referred to as the Normal Mix, contained Type 10 cement with 25 % slag replacement by mass. The second, referred to as the Silica Fume Mix, contained Type 10SF cement with 25 % slag replacement by mass. The admixtures used were ProAir air entrainer at 30 mL/100 kg cementitious material, 25 XL water reducer at 250 mL/100 kg cementitious material, and RheoBuild 1000, a mid-range plasticizer, as required. The ranges of dosage of RheoBuild 1000 were 200-250 mL/100 kg cementitious material for the Normal Mix and 250-300 mL/100 kg cementitious material for the Silica Fume Mix. These were selected to achieve the desired slump. These two concrete types were chosen to reflect typical concrete qualities used in parking structures. The mix design specifics are indicated in Table 3-1.

A standard curing regime was followed for all concrete specimens. They were moist cured for seven days and then were left in the lab air until they were tested. For the slabs that were corroded, this process was started at seven days of age.

3.2 Structural Testing

3.2.1 Structural Specimen

One standard structural specimen was used for all the structural tests. It was selected for minimum size such that it would fail in flexure. It was attempted to design a specimen that would resemble a section of a slab. The specimen used was 1300 mm long, 350 mm wide and 150 mm deep. It contained 3 #10M bars with a cover of 20 mm. There is a centre-to-centre bar spacing of 125 mm. A diagram of the specimen is provided as Fig. 3-1. The detailed calculations used to design the specimen are included in Appendix B.

Figure 3-1: Specimen Diagram

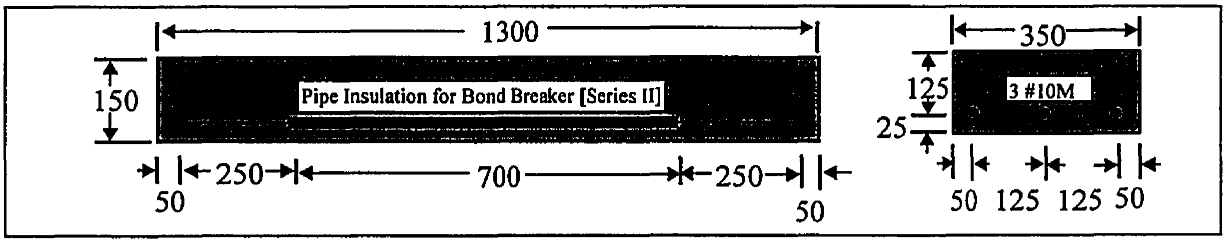

3.2.2 Structural Tests

The specimens were all tested identically. A four point loading test was used. A diagram of the testing set-up is included as Fig. 3-2, with a photograph included as Fig. 3-3. The load and the measurement of 3 LVDTs were continuously recorded as the test was undertaken. One LVDT was used to monitor the midpoint deflection of the slab while the other two were used to measure the curvature over the constant moment region on either side. This was done by hanging a bar from chains attached at the midheight of the slab below the load points. The difference between the deflections of the load points at midheight and of the centre-point at midheight was thus determined. Further information on this curvature measurement is located in Appendix C.

Figure 3-2: Testing Set-Up Schematic

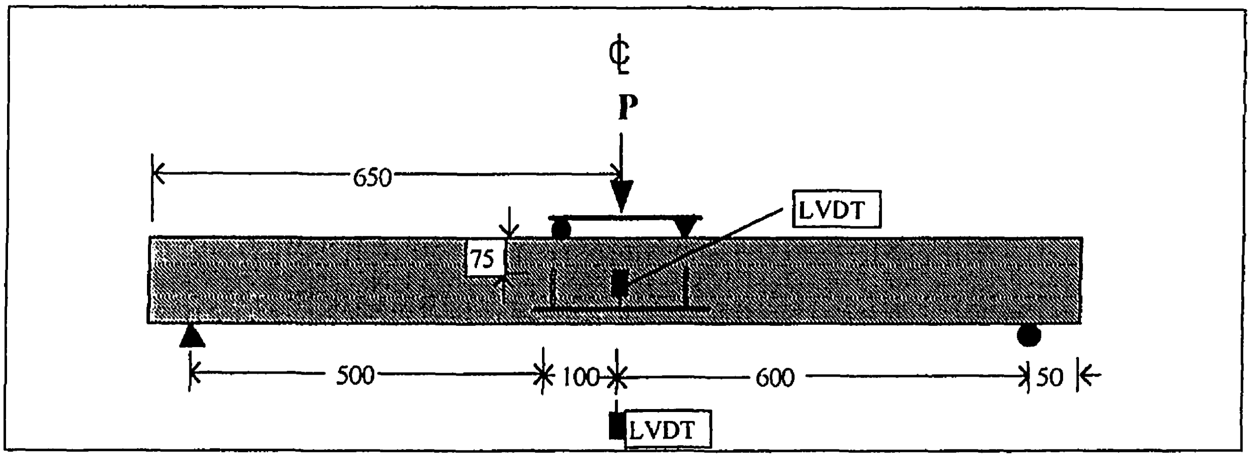

Figure 3-3: Photograph of Testing Set-Up

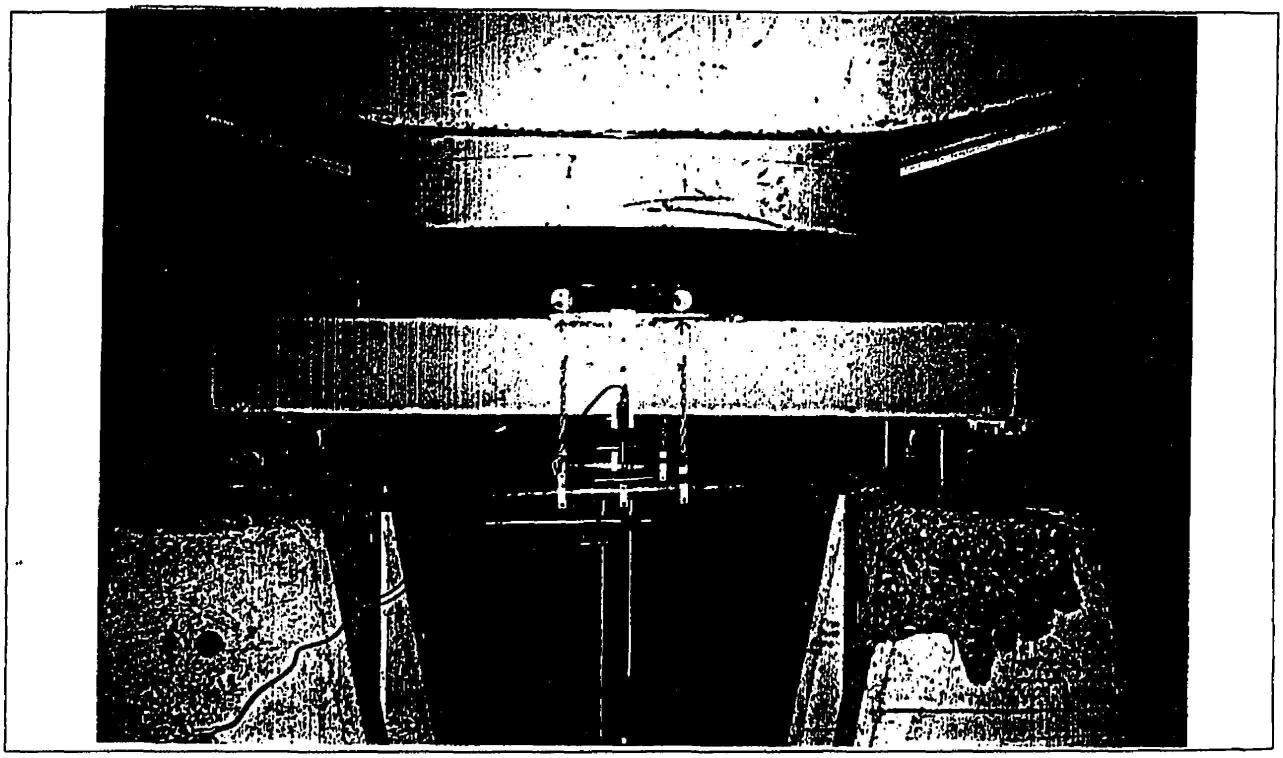

3.3 Material Tests

With each slab, three 100 mm diameter by 200 mm long cylinders were cast. These were used to test certain material properties that were felt to be important for the performance of the slabs under the test conditions. These tests were a compressive strength test, a sorptivity test and a rapid chloride ion penetration test (ASTM C1202). These tests were performed at seven and 28 days of age. Not all tests were performed on all slabs. A schedule was set up so that each series was tested for all properties. At least one cylinder was tested for strength for each slab. An outline of the test program is included as Table 3-2. A description of the material tests follows along with any variations that were used, with justifications.

Table 3-2: Material Testing Schedule

Series	Condition	Strength Test	Rapid Chloride & Resistivity	Sorptivity Test
1, Normal	None	Yes	No	No
	Quarter	Yes	No	No
	Half	Yes	No	No
2, Normal	0	Yes	No	No
	2	Yes	No	Yes
	5	Yes	No	Yes
	8	Yes	Yes	No
	10	Yes	Yes	No
2, Silica	0	Yes	No	No
Fume	2	Yes	No	Yes
	5	Yes	No	Yes
	8	Yes	Yes	No
	10	Yes	Yes	No
3, Normal	10	Yes	Yes	Yes

*** Condition represents either portion of perimeter debonded or expected percentage of bar area corroded, whichever is relevant*

3.3.1 Strength Testing

To determine concrete strength, 100 mm diameter cylinders were tested according to ASTM C39-93a[3-1] with one variation described below. For the slab mixes that only had their strength tested, this was done at seven and twenty-eight days. One cylinder was tested at seven days of age and two were tested at 28 days. For the other slab mixes that were tested for another property, in general only one cylinder was tested for strength at 28 days to confirm that they all had similar properties.

The one variation in testing was the moisture content at 28 days. The normal testing procedure is to ensure that the cylinders are saturated at the time of test. This was followed at seven days as they were just removed from the moist curing room. At 28 days of age, however, the cylinders had been left in lab air for three weeks and thus have dried to a certain extent. It was felt that it was appropriate to test in this moisture condition as the results would then better reflect the conditions at the time of the slabs are tested in four-point loading.

3.3.2 Sorptivity Testing

The sorptivity test measures the rate at which water is drawn into the pore structure of the dry concrete. To do this, disks 100 mm in diameter and 50 mm thick were dried at 50 °C for seven days. They are then removed from the oven and allowed to cool in a sealed container until they reach ambient temperature. The sides are then sealed and one face is immersed in water. The mass of the disk is then taken at intervals for twenty-five minutes. This was done for three disks for each sample. The height of water rise was calculated by dividing the mass gained by the surface area of the disk and the density of water. These values, averaged for the three disks, were plotted versus the square root of time and the slope of the line of best fit is reported as the sorptivity of the sample.

3.3.3 Chloride Ion Penetrability

This test is performed in accordance with ASTM Standard C1202-94: Standard Test Method for Electrical Indication of Concrete's Ability to Resist Chloride Ion Penetration[3-2] or AASHTO T259. This test subjects a 50 mm thick, 100 mm diameter concrete disk to a 60 V potential across the specimen. A sodium chloride reservoir is filled on one side of the disk, while a sodium hydroxide reservoir is filled on the other. This is maintained for 6 hours and the total charge passed is monitored. This charge is used to rate the quality of the concrete according to a scale included with the standard. The more charge passed, the greater the chloride ion penetrability. For further details, please refer to the relevant standard.

This test was also used for an additional purpose. It was used to estimate the resistivity of the concrete. This was done by taking the current at 10 minutes and calculating the resistivity using the equation:

$$\rho = \frac{VA}{IL}$$

where: $\rho \equiv$ the resistivity, in Ω-cm
$V \equiv$ the voltage, in V
$A \equiv$ cross-sectional area, in cm^2
$I \equiv$ current, in A
$L \equiv$ the thickness of the specimen, in cm

The ten minute current was used to calculate the resistivity as this would allow sufficient time for the chloride and hydroxyl ions to have reached an equilibrium state in the pore solution. It would also minimize any effects of polarization that is commonly encountered when dealing with high resistivity materials. It also minimizes any potential thermal effects that may arise. This method of determination may not be as accurate as some other methods using techniques to minimize polarization, for example using alternating current or varying the voltage applied using direct current, but it does give an idea of the expected resistivity. Considering the simplicity of the test and the fact that this is principally being used to characterize to concrete and not for any predictive purposes, it was thought to be sufficient.

3.4 The Experimental Series

These tests were then used to evaluate the effect of corrosion. This was done by preparing three main series of tests, each of which was designed to look at a different effect. The first series examined the effect of spalling on structural performance. The second looked at how corrosion affected bond over a specific length. The third series looked at combined effects of area loss and bond loss and the predictive power of the work. These series consisted of a set of slabs with their accompanying cylinder specimens. The slabs were modified to examine the desired effect and the cylinders were used to establish the material properties of the concrete. As discussed in Section 3.3, not all material tests were performed on all slabs. A schedule was set up to ensure that each series contained at least one slab that was tested for each material property.

3.4.1 Series 1 - Effect of Spalling

Spalling of concrete cover leads to loss of confinement and this could lead to a reduction of bond strength. This was modelled by debonding the bars along the bottom section with pipe insulation. Three standard specimens were tested, each with a different proportion of the bars' perimeter unbonded. One had none of the bar perimeter debonded, to serve as a control, one had one quarter of its bars' perimeters debonded while the final had one half of the bars' perimeters debonded. After casting, the slabs were moist cured for 7 days, then air cured for 21 days before testing.

3.4.2 Series 2 - The Effect of Corrosion Products

To determine the effect of corrosion products on bond strength, ten slabs were cast. Five were of the Normal Mix and five were made with the Silica Fume Mix. All Series 2 slabs had the centre section debonded with closed cell, foam pipe insulation while the ends were left as normal. The uncovered length was chosen so that at no corrosion, the full yield capacity of the rebar would just barely be developed. As the steel used had a definite strain hardening characteristic, it would then be noticeable if the corrosion either increased or decreased the slab capacity as any change in bond capacity would result in a change in possible steel stress and thus moment. The length used, as based upon ACI 408.1R-90,[3-3] was 250 mm. The calculations are included in Appendix B.

All of the slabs were then corroded in the end sections by semi-immersing them in a 3 % NaCl solution and applying a voltage across them. This caused the bars to become anodic. The section protected by the pipe insulation remained uncorroded. A schematic of this set-up is included as Fig. 3-4. One slab of each type was corroded to a different corrosion level as expressed by volumetric mass loss. They were corroded to approximately 2 %, 5 %, 8 % and 10 % corrosion. One was left non-corroded to act as a control. The corrosion was monitored by recording the current that passed and applying Faraday's law to the integrated current. Details of this procedure are included as Appendix D. Corrosion was also confirmed by including a corrosion sample in the slab to be removed after testing. This sample was a pre-weighed length of rebar approximately 100 mm in length that was corroded, then cleaned according to ASTM G1-90[3-4] to remove the rust and finally weighed. The cleaning solution chosen was C.3.3: 200 g sodium hydroxide, 20 g zinc and reagent water to make 1000 mL. For further information, refer to the standard.

Figure 3-4: Corrosion Set-Up

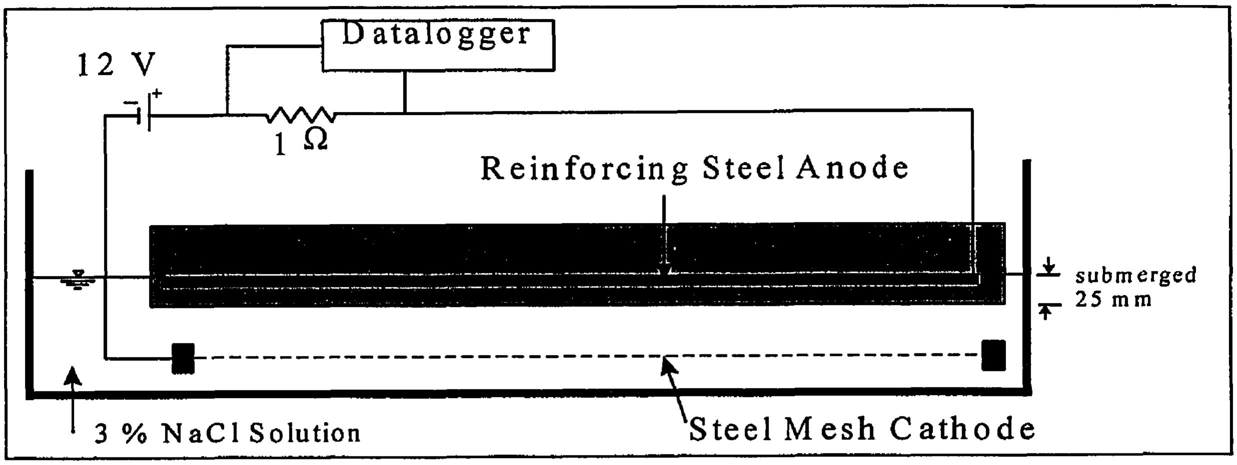

There were two methods used to connect the rebar to the power supply. Initially, the rebars were connected by running a wire from one rebar to the other, but the individual bars were still in parallel to each other. This technique is illustrated as Fig. 3-5(a). This proved to be unsatisfactory as this led to uneven corrosion. The bar where the wire connected to first corroded more, as determined by visual inspection, than the last bar. Thus the technique used to attach the bars was changed. Separate wires were attached to each bar and these were then connected to a common wire. This is illustrated as Fig. 3-5(b). This proved to give more satisfactory results.

Figure 3-5: Alternate Wire Connections

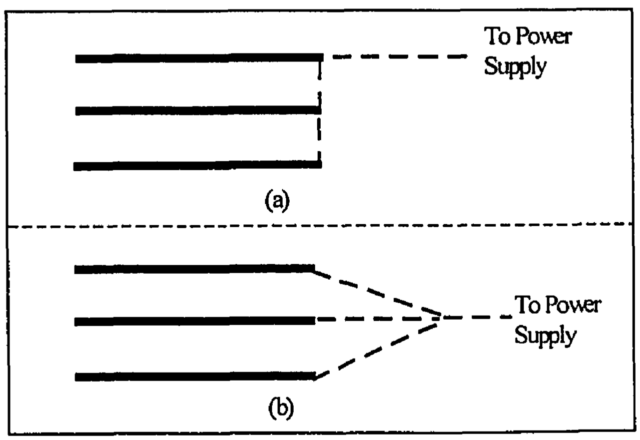

3.4.3 Series 3- Combined Effects

A final slab was then cast to investigate the total effects of corrosion. That is to determine the combined effects of steel section loss and the effect of corrosion products on bond.

This was done by casting a normal slab that did not have any unbonded sections. It was then corroded to a corrosion level of 10 % by applying a current. The ultimate strength was then predicted based upon previous work done in this thesis and that done by J. Phillips[3-5]. It was then tested in flexure in the standard manner.

Thus it was felt that the different effects of corrosion on reinforcing steel - concrete bond would be captured. The results of this experimental investigation are included in the next chapter.

References

[3-1] "Standard Test Method for Compressive Strength of Cylindrical Concrete Specimens" (ASTM C39-93a) *1994 Annual Book of ASTM Standards* V 04.02, ASTM, Philadelphia, pg. 17-21

[3-2] "Standard Test Method for Electrical Indication of Chloride's Ability to Resist Chloride" (ASTM C1202-94) *1994 Annual Book of ASTM Standards* V 04.02, ASTM, Philadelphia, pg. 620-5

[3-3] "Suggested Development, Splice, and Standard Hook Provisions of Deformed Bars in Tension" (ACI 408.1R-90) *ACI Manual of Concrete Practice 1995*, Part 3, ACI, Detroit

[3-4] "Standard Practice for Preparing, Cleaning and Evaluating Corrosion Test Specimens" (ASTM G1-90) *1994 Annual Book of ASTM Standards* V 03.02, Philadelphia, pg. 25-31

[3-5] J. Phillips, *The Effect of Corrosion on the Structural Performance of New and Repaired One-way Slabs,* Ph.D. Thesis, University of Toronto, c1993, pg. 143

4.0 Experimental Results

The results of this experimental program can be divided into three main categories. The first deals with the testing of the material properties of the concrete. The second category relates to the corrosion activity of the slabs and its monitoring and evaluation. The third topic is the structural performance of the slabs. These broad categories will be used to discuss the results in this section.

The results of the structural testing of the third series will not be discussed here, as this is more of a test of the predictive power of the work done to that point. Both the prediction and the results are discussed separately in Chapter 5.

4.1. Material Results

The material results are divided into five main subsections of results. The first one discusses the properties of the fresh concrete tested. The remaining four correspond to the major tests performed: compressive strength, sorptivity, rapid chloride and resistivity. Each of these is discussed separately for the Normal Mix and the Silica Fume Mix. The results in their entirety for the individual slabs are included as Appendix E.

4.1.1. Fresh Concrete Properties

Table 4-1: Fresh Concrete Properties

	Normal Mix	Silica Fume Mix
Avg. Slump	175 mm	112 mm
Slump COV	21.8 %	53 %
Avg. Air Content	6.9 %	6.7 %
Air Content COV	17.4 %	14.0 %
Avg. Plastic Density	2293 kg/m^3	2312 kg/m^3
Plastic Density COV	1.7 %	2.2 %

The fresh concrete properties tested were slump, air content and plastic density. These were used to ensure consistency in concrete properties between the variety of mixes using the same mix design. A report of the various properties for each cast is included as Appendix E, including admixture dosages. Table 4-1 is a summary of the results. The fresh concrete property test results varied little between mixes for the Normal Mix. The air content is within the target range and the plastic density has little variation. The coefficient of variation for the slump is slightly higher than for the other tests, but this is expected due to the nature of the test. Slight variations in workability, the actual factor of interest, can produce large changes in slump; at least at the relevant level of slump.[4-1]

The Silica Fume Mix properties are also summarized in Table 4-1. The results are generally consistent with small coefficients of variation between individual batch results. The exception to this, again, is the slump test. The five values for this test clustered around two points. The first three mixes chronologically had slumps around 150 mm, while the last two had slumps of 50 mm. The mixes had identical mix proportions and the other test results were similar so the mixes were used. This change in slump is attributed to a change in aggregate between these mixes. The aggregate was from the same source and the other physical and chemical properties were identical, but the grading of the aggregate may have slightly changed. The grading affects slump and workability, but other properties of the concrete remain unchanged.[4-2] Extra care was taken with these mixes to ensure good compaction and placement, but no additional measures were required.

4.1.2. Strength Testing

The strength test summary is included as Table 4-2. As expected, the Silica Fume Mix is significantly stronger than the Normal Mix, by approximately 10 MPa. Both the 7 day and 28 day strengths show this change.

Table 4-2: Strength Results

	Normal Mix	Silica Fume Mix
7 Day Strength	23.8 MPa	34.5 MPa
7 Day COV	18.3 %	16.7 %
28 Day Strength	36.4 MPa	42.6 MPa
28 Day COV	14.4 %	13.5 %

4.1.3. Sorptivity Testing

The sorptivity values for the mixes were determined at seven and twenty-eight days. The average values within a mix type are reported in Table 4-3. For the Normal Mix, the values increased slightly between seven and twenty-eight days; while for the Silica Fume Mix, the values decreased slightly. These changes are not considered

Table 4-3: Sorptivity Values

	Normal Mix	Silica Fume Mix
7 Day Sorptivity	0.111 mm/min$^{0.5}$	0.123 mm/min$^{0.5}$
28 Day Sorptivity	0.104 mm/min$^{0.5}$	0.111 mm/min$^{0.5}$

significant, however. The two mixes did have similar values at all ages. Thus, it is concluded that the difference in initial chloride penetration due to sorptivity effects would be negligible between the two different mix types.

4.1.4.Rapid Chloride Testing

Table 4-4: Rapid Chloride Results

	Normal Mix	Silica Fume Mix
7 Day	Moderate	Low
28 Day	Moderate - Low	Very Low

According to the rapid chloride test, the chloride ion penetrability for the normal mix is moderate at seven days of age and moderate to low at twenty-eight days of age. This is typical of the quality of concrete used in parking structures. The Silica Fume Mixes had a low chloride ion penetrability rating at seven days of age, dropping to very low at twenty-eight days of age. This is expected, as the addition of silica fume improves the chloride ion penetration resistance of concrete. The Silica Fume Concrete qualifies as Low-Permeability Concrete as defined by CSA/S413-94 - Parking Structures Code, Cl. 7.3.1.2.[4-3] This requires, among other things, a 28 day coulomb rating of less than 1500 when tested according to ASTM C1202.

4.1.5.Resistivity Measurements

Table 4-5: Resistivity Data

	Normal Mix	Silica Fume Mix
7 Day Resistivity	6245 Ω-cm	13366 Ω-cm
28 Day Resistivity	12339 Ω-cm	50806 Ω-cm

The summary of the resistivity testing of the concrete is in Table 4-5. They follow the results of the rapid chloride testing rather closely. This is expected as they were developed using the rapid chloride testing apparatus. The reasoning for the trends is identical to that previously discussed in Section 4.1.4.

Comparing the results between the two mixes is interesting. The Silica Fume Mix has obtained a similar resistivity at seven days as that obtained by the Normal Mix at twenty-eight days. At twenty-eight days, the resistivity of the Silica Fume Mix is about four times higher. This is a rating that would likely be unachievable for the Normal Mix, no matter its age.

4.2. Corrosion Activity Testing

This section discusses the tests used to determine if corrosion is occurring and to monitor the rate and quantity of corrosion. Included in this section is a discussion of the monitoring of the corrosion current and the determination of corrosion levels using the included rebar test coupon. These aspects will each be discussed individually.

4.2.1.Corrosion Current

The current passing through the slabs was continuously recorded using a Campbell 10X datalogger. A reading was taken every minute. Every half-hour, one number was recorded which was the average of the minute by minute values. Graphs of the output are included as Appendix F. These values were integrated and Faraday's Law applied to determine the mass loss. This was converted to cross-sectional area loss based upon the density of steel. The values achieved are reported in Table 4-6, along with the values from the corrosion samples, discussed in the next section.

Table 4-6: Corrosion Results, Series 2

	Normal, 2 %	Normal, 5 %	Normal, 8 %	Normal, 10 %	Silica Fume, 2 %	Silica Fume, 5 %	Silica Fume, 8 %	Silica Fume, 10 %
Current Estimate	7.6 %	8.9 %	10.3 %	10.3 %	0.4 %	6.4 %	8.1 %	11.8 %
Corrosion Coupon	3.1 %	0.3 %	0.2 %	18.4 %	1.5 %	5.4 %	17.7 %	29.6 %
Connection Method	(a)	(a)	(a)	(b)	(a)	(b)	(b)	(b)

For the Normal Slabs, the corrosion current fluctuated significantly at times, as can be seen from a superficial examination of the graphs. The average current was in the range of 100 mA, but there were current spikes that at times approached at 1000 mA. The current also occasionally decreased to almost zero, though rarely. It did, however, always return to the original value of approximately 100 mA.

The corrosion currents monitored for the slabs made with the Silica Fume Mix were similar in pattern to that for the Normal Mix. Their average value was also about 100 mA.

There were also large variations in current levels, but these were not as high as for the Normal slabs. The maximum value was not more than around 700 mA. The corrosion graph for the Silica Fume slab that was corroded to only 0.4 % electrochemically is different from the others of this series. There is an initial high level of around 75 mA, but this then decreases to a very low current of near 5 mA, that then remains consistent for the duration of the corrosion period.

For two of these slabs, for a 15 day period the datalogger was not registering data as the datalogger's power supply was accidentally disconnected. To represent this time, it was assumed that the average current over this period was 100 mA. This is represented in the graphs and was assumed for calculation of the corrosion loss by electrochemistry.

4.2.2. Corrosion Sample Results

The corrosion test coupons are small, preweighed 10M bars included in the slabs. These were corroded, cleaned and then weighed to determine the level of corrosion that took place in the slabs. The results from this are included in Table 4-6, along with the results from the corrosion current monitoring. Also included in this table is the method that was used to connect the rebar, (a) or (b). (See Section 3.4.2)

For the slabs connected using method (a), 3 out of the 4 resulted in very low levels of corrosion present, compared to that shown by electrochemistry. This may indicate that the connection was not sufficient to ensure that the voltage would be applied to all bars equally. The corrosion test coupons were connected last in order. Another explanation would be that the cover around one bar cracked before the other bars. The current then flowed principally through this bar, causing it to be greatly corroded while the other bars were not. It is unlikely that the crack would first occur over the corrosion sample, due to its small size, and thus the corrosion sample would report a lower level of corrosion than exists. One sample (Silica Fume Mix, 2 % corrosion) had a higher level of corrosion than was predicted electrochemically, but the corrosion currents for this sample were unusual. The final sample of the four agreed rather well.

The slabs connected using method (b) show a different trend. In all of these cases, the corrosion levels by the sample are higher than that reported by corrosion current measurements. They are of the order of one and a half and two times greater. The reason for this may be the reaction that was assumed to occur. The assumed reaction is the one discussed in the Literature

Review, with the iron atom from its 2 valence state reaction with oxygen and hydroxyl ions to form ferrous hydroxide. This may not be the reaction that is occurring. First, iron is a divalent element. There are also many possible reactions that could occur, for example binding with chlorides to produce ferrous chlorides and other, more complex molecules.[4-4] These different reactions were not all considered when developing the original expression for corrosion current evaluation, but may be occurring. This could explain the discrepancy between the two values.

4.2.3. Corrosion Levels

Given the discrepancies between the two methods of determining the corrosion levels, what should be used as the final value for corrosion level? In this section, this dilemma is discussed.

A number was required to be assigned to each slab to represent the amount of steel that was corroded. To do this, the values for each slab from both the corrosion test coupon and the electrochemical current were examined. The method of connection was also considered and from this a number was estimated that would best represent, if not the exact level of actual corrosion, at least the relative level of damage.

For the slabs that were connected using connection type (a), it was felt that these two numbers represented an upper and lower bound of the corrosion damage. Thus the actual damage is reported as the average of these values. The exception is the normal slab that was targeted to be corroded to 2 %, as it was felt that the corrosion sample alone was more representative. This was based on visual examination. For the slabs connected using method (b), it was felt that the integrated current better reflected the level of damage. Thus this number is reported as the level of corrosion. A summary of these results is included as Table 4-7.

Table 4-7: Effective Corrosion Levels, Series 2

Original Name	Normal, 2 %	Normal, 5 %	Normal, 8 %	Normal, 10 %	Silica Fume, 2 %	Silica Fume, 5 %	Silica Fume, 8 %	Silica Fume, 10 %
Corrosion Level	3.1 %	4.6 %	5.3 %	10.3 %	1.0 %	6.4 %	8.1 %	11.8 %

4.3.Structural Test Results

This section will deal with a discussion of the three individual sets of slab results. Each set is discussed individually, examining their load response plots. The bond stresses that were developed are then determined and discussed.

4.3.1. Series 1 - The Effect of Spalling

This series contained three slabs, each of which had a different proportion of its bars' perimeters debonded using closed cell, foam, pipe insulation. The proportions were: none (control), one-quarter and one-half. The bottom portion of the bar towards the tensile surface of the slab was debonded to realistically reflect spalling activity. It might be considered that the one-quarter debonded slab would represent the effects of pop-out, while the half debonded slab would represent delamination. Figure 4-1 illustrates this.

Figure 4-1: Conceptual Spalling Effects

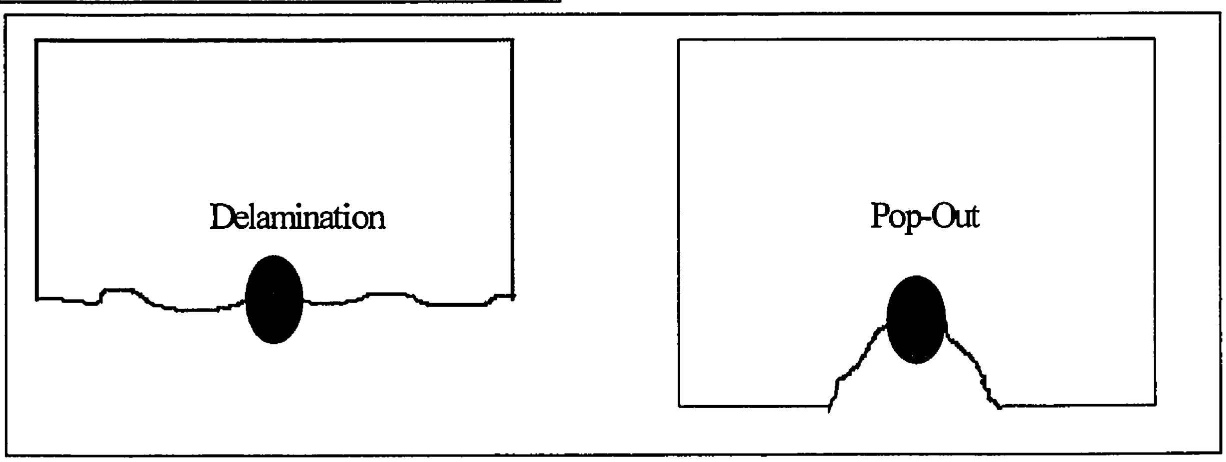

The moment-curvature plot obtained from the structural testing is included here as Fig. 4-2. An examination of this provides some important information. The control slab behaved quite predictably. It contained an initial, very stiff region until the concrete cracked (O-A). The steel then began to load elastically (A-B). While this response is less stiff than the uncracked section, significant stiffness still remains in the slab. Finally the steel begins to yield. This is represented by a significant loss of flexural stiffness (B-C), but as the steel has a substantial strain hardening effect, the slab still accepted more load.

The slab with a quarter of the bars' perimeters debonded had some substantial differences. Initially, it acted the same as the control slab (O-A). This is because the concrete provides most of the load resistance until cracking. After the slab cracks, the quarter-debonded slab was significantly more flexible than the control slab (A-B'). This may be interpreted as the slip required for the bar to achieve equal stress transfer in this situation is more than for the

Figure 4-2: Series 1 Results

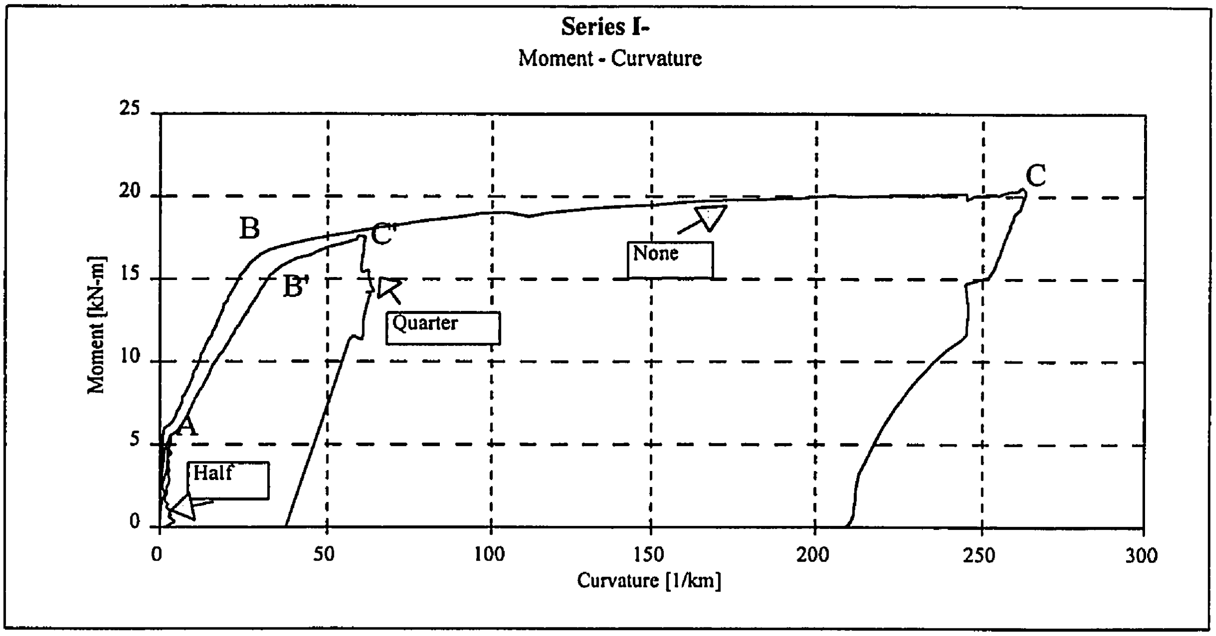

control. The slab does reach a point where the bar appears to begin to yield, however. Another possible explanation of this 'yield plateau' is that the slip has begun to reach a critical point, where increasing stress transfer requires ever increasing amounts of slip. The first explanation of bar yielding is favoured due to the high load at which this is occurring, similar to the yield load for the control slab. The most significant difference between the two load response curves occurs in the third region, after the bars have yielded (B'-C'). For the control specimen, there was a large ductile response. The load was still able to be supported with ever increasing curvature until it was decided to unload the specimen as the curvature LVDTs reached the end of their range. For the one-quarter debonded specimen, this was not the case. There was a short time where the load was still maintained with increasing curvature, but this did not last long. A point was reached where the load could no longer be supported and the slab began to unload itself. This can be clearly seen in the load response diagram. This is interpreted to mean that the bars have reached their ultimate slip and have now become debonded from the concrete. Since the concrete section is already cracked, this means that there is no residual capacity in the beam. It should be noted that this was a rather sudden event and that there was no warning of this failure point approaching, as compared to the normal yielding response.

The slab that contained one-half of its bars' perimeter debonded exhibited even more dramatic results. Until the beam cracked, the test went on as before. When the slab cracked, however, the steel did not begin participating in the resisting the load. The slab did not take any more load and would not support the load previously applied. This is the response that would have been achieved if the slab was unreinforced. The only difference is that the two halves of the slab did not fall but rested upon the steel that spanned between them. This leads to the conclusion that if one half or greater of the bars' perimeter is debonded along the entire slab then effectively no bond will occur between the steel and the concrete. The slabs will then act as if they were unreinforced.

This lack of bond if a bar has greater than half of its perimeter exposed is quite understandable. The bond developed is the component of the bearing stress of the lugs on the concrete that acts along the bar. Also developed, however, is a perpendicular component that in the normal situation is counteracted by the perpendicular component on the opposite side of the bar. This is developed due to the angled face of the lugs. If only a small portion of the perimeter is not confined, then it is possible for the perpendicular components to be equilibrated by the other sections of the perimeter. If the unconfined section reaches to high a proportion of the bars perimeter than the perpendicular components will not be equilibrated. In the case where half of the perimeter is unconfined, then there will be nothing to resist the perpendicular stress components of the bonded perimeter. This will result in the pushing out and sliding of the bar whenever it is loaded. This is due to the effect of the lugs.

4.3.2. Series 2 - The Effect of Corrosion Products

The condition of slabs before testing, the results of the Normal Mix test series, the Silica Fume Mix test series and some general conclusions of what can be inferred from the Moment - Curvature graphs will be discussed.

4.3.2.1. Condition of Slabs Before Testing

All the slabs, except for the Silica Fume Mix slab that was corroded to 2 %, were cracked due to corrosion to some extent before they were tested. The extent of this damage varied, however, from small surface cracks to large sections spalling off the slab. As to be expected, the extent of damage increased with increasing corrosion levels.

The damage was originating from the ends of the bars that were corroded. The middle bar caused a vertical crack through the centre of the slab. It often reached the top face of the slab. The outside bars caused cracks that tended to run from the surface below the bars, through the bars and then they turned to reach the outside face of the concrete. If they extended through this entire section, they caused spalling of the concrete section. The extent of this cracking was only slightly longer than the length of bar that was corroded. There was a definite centre section that remained undamaged by the corrosion attack. A diagram of the typical crack patterns developed as well as common locations of spalling are included as Fig. 4-3.

Figure 4-3: Typical Crack Locations and Areas of Spalling

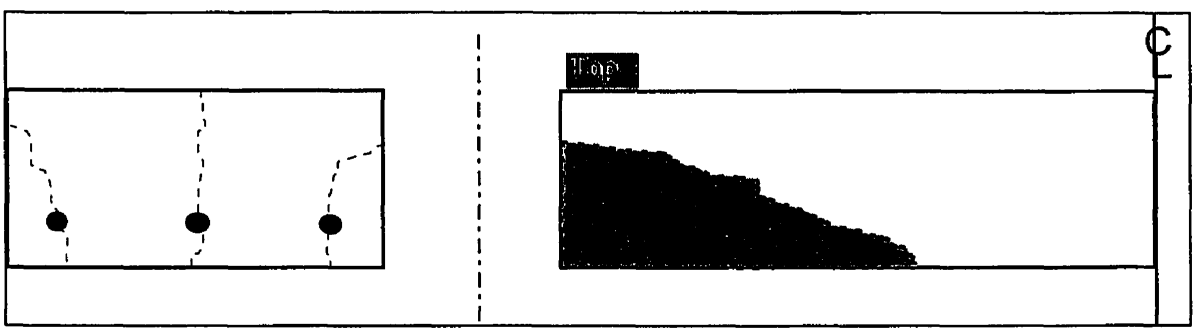

Along with the damage caused by cracking, there were also rust stains forming on the surfaces of the slabs. This staining was mostly concentrated at the area of the cracks. Often, rust 'stalactites' were formed on the bottom of the slab. These were quite easily damaged by the moving of the slabs in preparation for testing, but were seen to consist of a soft, flaky material that was gooey to the touch.

After testing, the condition of the bars in the centre portion covered by pipe insulation was determined. The steel bars were uncorroded as it was assumed indicating that the assumptions were justified.

4.3.2.2. Normal Mix Test Results

In this section, there were two sets of results. These were due to the two different concrete mixtures used for the slabs, the Normal Mix and Silica Fume Mix. These slabs contained steel that was anchored at the ends, but debonded in the middle. The end regions were then corroded to various degrees, while the centre, test region was uncorroded.

During testing, a structural crack developed. Unlike a normal, non-debonded slab where a diffuse crack pattern with a variety of flexural cracks would have developed, there was only one major crack. This is as the centre portion of the steel was unbonded and once the concrete cracks in one location it is then able to relax over the entire unbonded region and no tension is able to be developed in the concrete. The entire tensile strain developed in the steel is relieved at the crack location. The location of this crack was near the centre of the slab in the constant moment region as it is the location of maximum stress and thus first cracking.

The moment-curvature results of the Normal Series are contained here as Fig. 4-4. For all levels of corrosion, there was a very ductile response. The ultimate strengths of the slabs did change as they were corroded, however. It can be seen that the three lower levels of corrosion; 2 %, 5 % and 8 %; were all weaker than the control specimen. Comparing the strengths between these samples, however, does not show any additional trend. They all had similar ultimate capacities. The moment-curvature graphs of the slabs corroded to five and eight percent have a point of interest. In these graphs, there can be seen definite indications of slip. That is, there are areas where, with little change in curvature, there are significant reductions in the moment capacity of the slab. This can be interpreted as where the stress transfer between the steel and the concrete is suddenly reduced so that the stress in the steel decreases. This leads to less moment being required to maintain the same level of curvature. In these cases some residual bond capacity available so that the slab was still able to accept load; the moment capacity did not decrease to zero. In the slab that was corroded to five percent, with increasing curvature, the moment taken reached higher levels than that which lead to the first slip.

Figure 4-4: Series 2 - Normal Mix Results

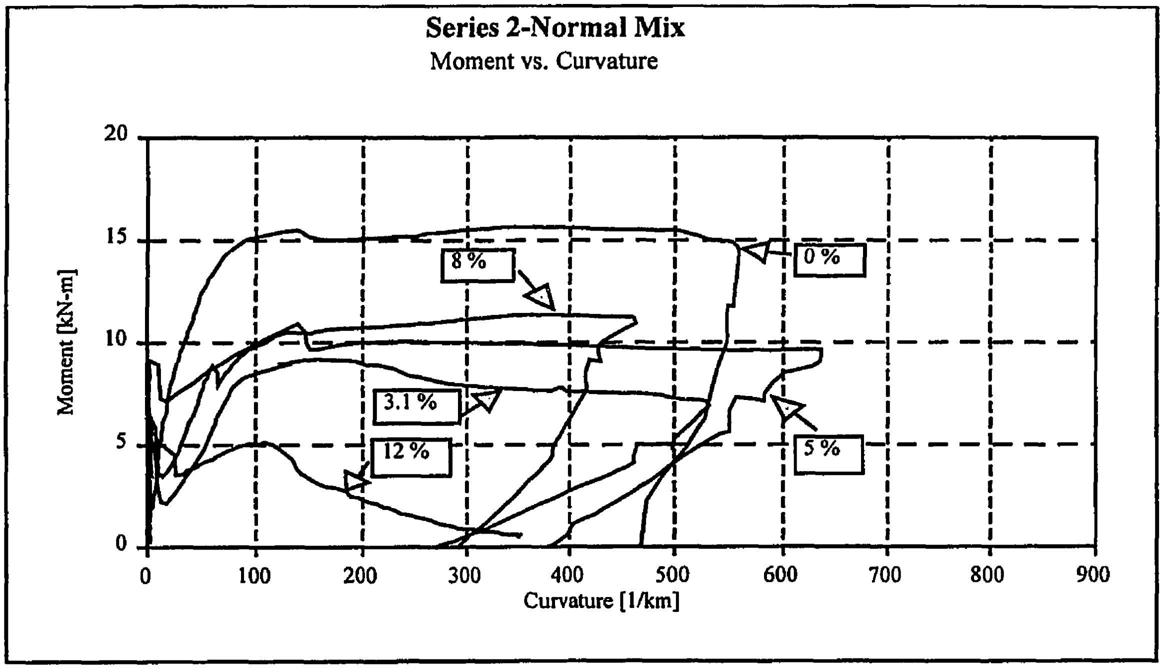

Figure 4-5: Series 2 - Silica Fume Mix Results

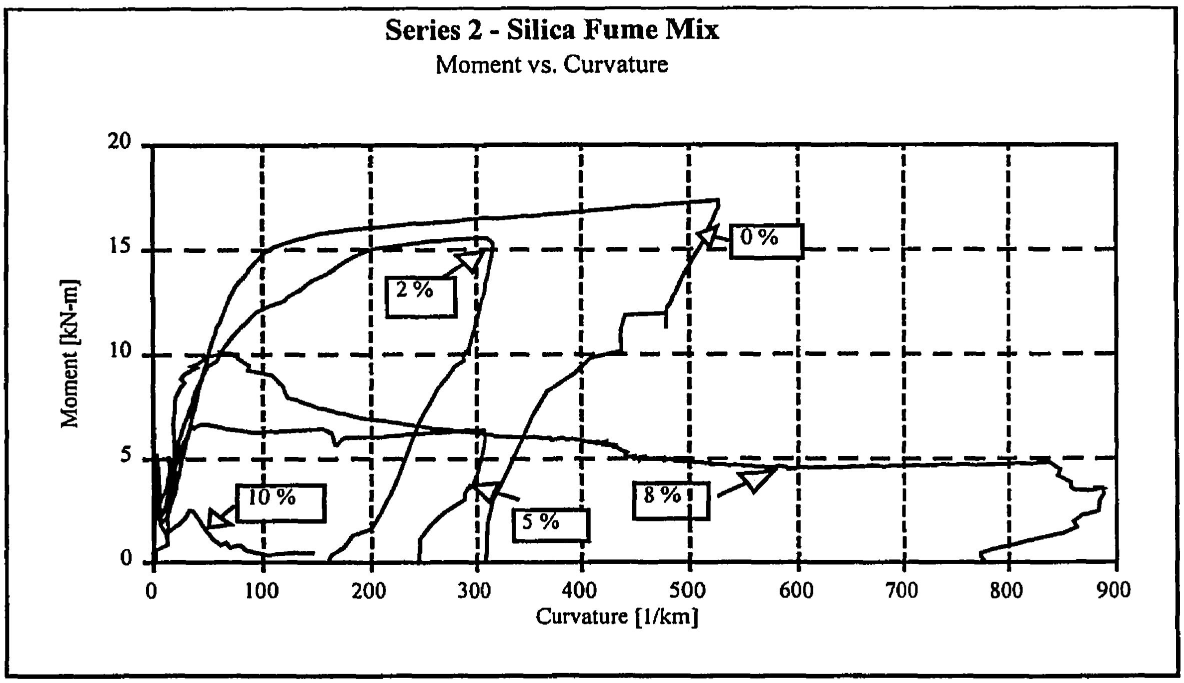

The slab that was corroded to the highest level, 12 %, behaved differently than the other, Normal Mix, corroded slabs. After the slab cracked, the moment capacity reduced dramatically. It showed a great increase in curvature before it accepted more load, that is, when the steel became active. This indicates the greater slip that must be required to activate bond forces. The moment resistance of the slab then increased for some increasing curvature. The moment capacity reached levels similar to that which was reached before the beam cracked, but no higher. It did exhibit a significantly more ductile response that an unreinforced slab that would have had similar capacity.

4.3.2.3.Silica Fume Mix Test Results

The results of the testing of the slabs made with the Silica Fume Mix are contained in Figure 4-5. These graphs plot measured moment-curvature relationships for the specimens. For this set of data, due to problems with the data acquisition, the curvature was not calculated the same way for all five slabs. For the slabs that were corroded to 0 %, 2 % and 8 % steel section loss, there were no difficulties. Their curvatures were calculated using the curvature-meter as usual. For the slabs corroded to 5 % and 10 %, the data from the LVDT's that are part of the curvature-meter were not recorded, so the curvature is based only upon the midpoint deflection. A single crack was developed due to structural testing, just as for the set of slabs cast with the Normal concrete mix.

The control specimen for this set of tests behaved quite predictably, just as for the normal series. It exhibited the same stiff, initial response until cracking, the loss of stiffness post-cracking and the yield plateau. The difference between this and the control for the normal series is that it reached a higher load before yielding. This is because the Silica Fume concrete is stronger than the Normal concrete.

For the Silica Fume Mix slabs that were corroded to 2 % and 5 %, a normal response is achieved in shape. There is a post-cracking increase in load and then a 'yield plateau' where there is a generally constant moment response for ever increasing curvature. These plateaus do not exhibit the gradually increasing load that the control specimen required and the start of this change in response is at a lower load level. Also of interest is a 'jog' in the 5 % corroded specimen in the yield plateau that may indicate some slip in the bars and an adjustment in the response.

The slabs that are corroded to 8 % and 10 % have a different response. After cracking, there is an increase in strength, though for the 10 % slab this does not reach the cracking load. After the load peaks, with increasing curvature there is a decrease in load required. This is exhibited as a negative slope of the post-peak region of the load - response curve. There are also numerous occasions of sudden decrease in moment with little change in curvature. This would indicate occasions of slip of the bars.

4.3.2.4. General Discussion of Test Results

From these, it is obvious that corrosion does have some influence on bond. Further details and evaluation of this influence is discussed in the Section 4.3.3. However, some general trends can be inferred from the moment - curvature diagrams. First, as has been pointed out, there is still a large ductile response. This is encouraging as one of the aims in design is to ensure ductility. The idea is to give adequate warning of impending failure to users of a structure.

Less encouraging is the relative magnitude of the cracking loads and the ultimate load, at least at the higher levels of corrosion achieved. For both sets of tests, the slabs that were corroded to the greatest amount, approximately 10 to 12 %, did not regain their cracking strength in the post-cracking region. Thus if these were structural members that had not cracked due to load but were corroded to this level, and then suddenly loaded past their cracking load, they would then suddenly fail. In these cases the level of corrosion when this dangerous response appeared was approximately 10 %, but this would be a function of the cracking strength of the concrete.

Thus it can be seen that at low levels of corrosion, while there is some possible loss of bond strength, the nature of the response will provide some warning of impending failure. However, at higher levels of corrosion this warning is lost and as such should be evaluated differently and more conservatively when considering structural integrity.

4.3.3. A Discussion of Bond

After testing, the moment and curvature information from Series 2 was taken and used to determine bond strengths. This was done for all the post-cracking points on each response curve using a program written for that purpose. The details of that program are contained in Appendix G. The maximum value of the bond at each corrosion level was then taken and is plotted for both the Normal Mix and Silica Fume Mix. This plot can be seen as Fig. 4-6.

For each set of tests, the linear regression of the bond strength [U,MPa] versus the percentage of steel area lost due to corrosion [x, % by mass] was determined. This gave the equations and r^2 values of:

Normal Mix: $U = 4.71 - 0.250\,x$, $r^2 = 0.6800$

Silica Fume Mix: $U = 5.27 - 0.361\,x$, $r^2 = 0.9112$

Figure 4-6: Bond Strength as a Function of Corrosion Level

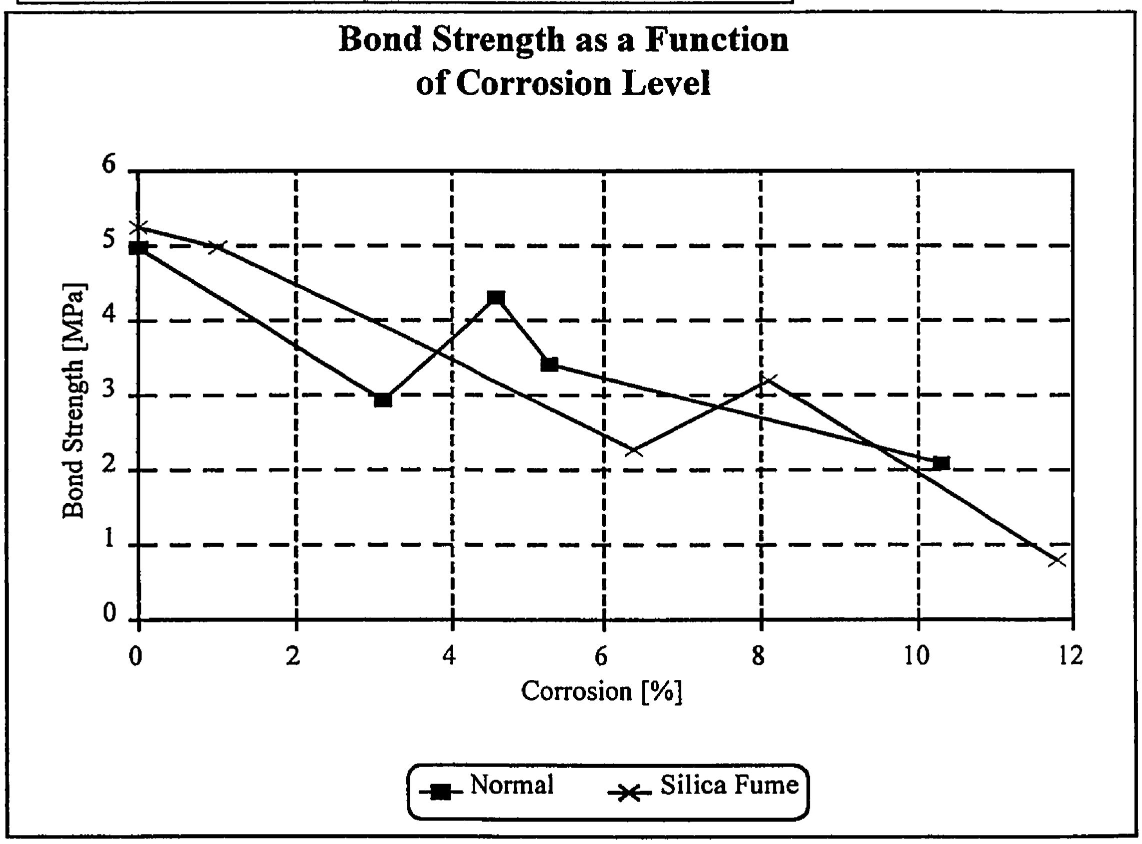

The Silica Fume Mix showed a well-correlated linear relationship, while the results for the Normal Mix were not as clear. The Normal Mix did have a general trend of decreasing bond strength with increasing corrosion levels. The explanation for this lack of clarity in the Normal Mix results may come from the techniques that were used to connect the rebar to the power supply. Out of the four corroded specimens for the Normal Mix results, three were corroded using connection type (a); while for the Silica Fume series three were connected using connection type (b). A discussed previously (Section 3.4.2), connection type (b) gave superior control over the corrosion process and made the corrosion more even between the bars. It was also easier to gauge the amount of corrosion that had occurred. This may explain the difference in correlation coefficients between the two sets of results.

However, it is seen that there is a relationship between the amount of corrosion and the bond strength that exists. It also appears to be linear with a decreasing slope. This agrees with what has been reported before in the literature, for example by Rodriguez, et al.[4-5] As discussed in Chapter 2 - Literature Review, they have developed a linear equation relating bond strength and depth of corrosion penetration based upon a series of tests of bars embedded in cubes.

The loss of bond with increasing corrosion levels is as expected. The corrosion will first damage the concrete due to the expansive pressures it exerts. This will lead to cracking and it is easy to see how this may cause weakening of the anchorage of the reinforcing steel. In addition, the corrosion causes the surface properties of the reinforcing steel to change. It creates a weak layer of corrosion product that will break off under relatively low stress levels. The may lead to lubrication and the prevention of both the development of friction and concrete-steel interlock. At high levels of corrosion, which were probably not reached here, there is also the possibility that the effect of lugs on the reinforcing bars may be eliminated. This would occur if the entire lug was corroded and then would break off at relatively low stresses.

References

[4-1] A.M. Neville, *Properties of Concrete*, 3rd Ed., Longman Scientific and Technical England, 1981, pg. 220

[4-2] A.M. Neville, *Properties of Concrete*, 3rd Ed., Longman Scientific and Technical England, 1981, pg. 210

[4-3] Canadian Standards Association *Parking Structures-Structural Design*, CSA/S413-94, Rexdale, Ont., 1994, Cl. 7.3

[4-4] P. Schiessl, ed. *Corrosion of Steel in Concrete,* Chapman and Hall, Ltd. c1988, pg. 61

[4-5] J. Rodriguez, L. M. Ortega, J. Casal and J. M. Diez, "Assessing Structural Conditions of Concrete Structures with Corroded Reinforcement" *Concrete in the Service of Mankind: Concrete Repair, Rehabilitation and Protection,* First Ed. E & FN Spon London, 1996, pg. 65-78

5.0 Series 3 Evaluation

This section discusses the slab designated as Series 3. The purpose of this slab was not primarily to determine any additional information, but to evaluate what has gone before. Thus, a standard slab was cast from the Normal Mix and corroded to a predetermined level. This level was selected as 10 %. This level was chosen to test the more critical values of the possibilities. Before testing, the information from previous parts of this experimental program was used to predict the capacity, in combination with the work done by J. Phillips.[5-1] How this evaluation was performed and the results of the experimental test are discussed here.

5.1 The Prediction

Two elements were considered explicitly when predicting the failure load and the mode of failure for the slab. These were bond pullout effects and the effect of steel section loss. Shear failure was not considered explicitly as the specimen type used was identical to the ones previously used, where shear was not critical. Corrosion will not affect the shear capacity where there are no stirrups, thus shear capacity need not be checked at this stage.

The corrosion level was determined using the techniques used previously, namely by integrating the current that has passed and by using a corrosion coupon. The integrated current suggested a corrosion level of 18 %, while the corrosion coupon estimated the corrosion level at 11 %. These two values were average to give a representative corrosion level of 14.5 %. This value was used in the work that follows.

To evaluate the beam, a failure envelope was constructed along the length of the beam. This failure envelope consists of two portions. The first is if the beam fails due to steel section loss. This is a constant value along the length of the beam. The second portion is the limit that will cause an anchorage failure. This limit will vary along the length of the beam depending upon the available length for anchorage. The section property evaluation was done considering only the remaining, uncorroded steel, as indicated by J. Phillips.[5-2] The development length calculation was based upon a bond strength of 1.09 MPa, using the formula developed in this report for the Normal Mix. More explicit calculations are included as Appendix H.

After the failure envelope was constructed, the moment diagram for various loads was determined until these two curves intersected. The lowest load at which this occurs is the failure load. Depending upon the location of this first intersection, the failure mode can be determined. If this intersection is in the part of the failure envelope where bond governs, then bond failure will be the failure mode. If it is in the section where steel section loss governs, then the slab will fail by yielding.

The failure envelope was constructed for a corrosion level of 14.5 %, the actual corrosion level determined for the slab tested. Trial and error determined that the lowest load that would cause the curves to intersect is 28.5 kN. This corresponds to a maximum moment of 7.13 kN-m in the centre region. The slab would fail due to a bond failure. A diagram of the failure envelope and the moment diagram at failure is contained herein as Fig. 5-1. It is noteworthy that the capacity envelope does not contain a horizontal portion. That is there is no portion where there is sufficient anchorage to allow the yield strength to be developed, even though it is reduced by the amount of the steel that has been corroded.

Figure 5-1: Prediction

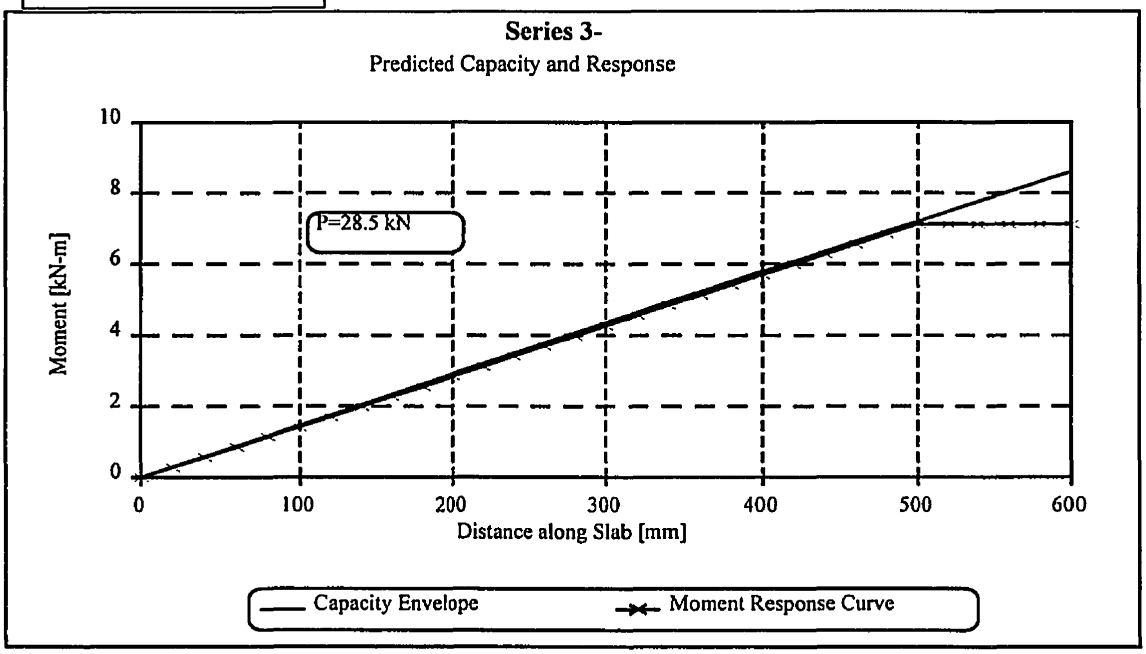

5.2 The Experimental Result

The results of the structural testing are discussed in this section along with the condition of the slab before testing. What is not discussed is the results of the material tests performed. This is as the same concrete mix design that was previously designated as the Normal mix was used. The material test results are a part of the same statistical family that the previous Normal mix results were and were discussed in Chapter 4 with them. The results of this specific set of tests are included in Appendix E.

5.2.1 Condition of Slab Prior to Testing

The test slab had cracking due to corrosion before it was tested. Unlike the slabs from Series 2 that had cracking along the ends and sides, with some reaching to the top face, the cracking in this slab was only visible along the bottom face of the slab. This cracking was primarily in the longitudinal direction and ran the entire length of the slab. There were some minor lateral cracks, however.

There was extensive rust staining along the bottom of the slab as well. This included the formation of the rust 'stalactites' and the deposition of salt ridges along the outside of slab. None of this was visible on the portions on the slab that were not immersed in the salt solution, or were farther from the steel bars.

5.2.2 Structural Testing Results

This specimen was tested in flexure as the other slabs. The moment - curvature response is shown in Figure 5-2. Also shown is the moment - curvature response of the Control specimen for Series 1. It is identical to the slab tested here except it was uncorroded.

The initial portions of both curves are similar (O-A) as for both slabs this is before cracking and as such the condition of the steel does not effect the response. In the control slab, there is a pre-steel yielding portion of the curve that is more flexible (A-B) and this is initially mirrored by the corroded specimen (A-D). The effect of corrosion then begins to be demonstrated. At D, there is evidence of slip occurring and the response is then less stiff than the control (D-E). The load is still increasing, but a greater increase in curvature is required to develop the same increase in supported moment than for the control. At E, the corroded slab exhibits a sudden loss in moment with no change in curvature. This is another point of slip of the bars. In this case, the moment is then regained with little change in curvature and the load continues to increase until point F. The rate of this increase in load is similar to that which was experienced before the slip at point E. After F, their is a dramatic change in the shape of the response curve. The load decreases with increasing curvature. (F-G) The load decreases to a point where it is approximately half of the peak load and then remains steady with increasing curvature. The load remained constant until the slab was unloaded at point G.

Figure 5-2: Series 3 Experimental Results

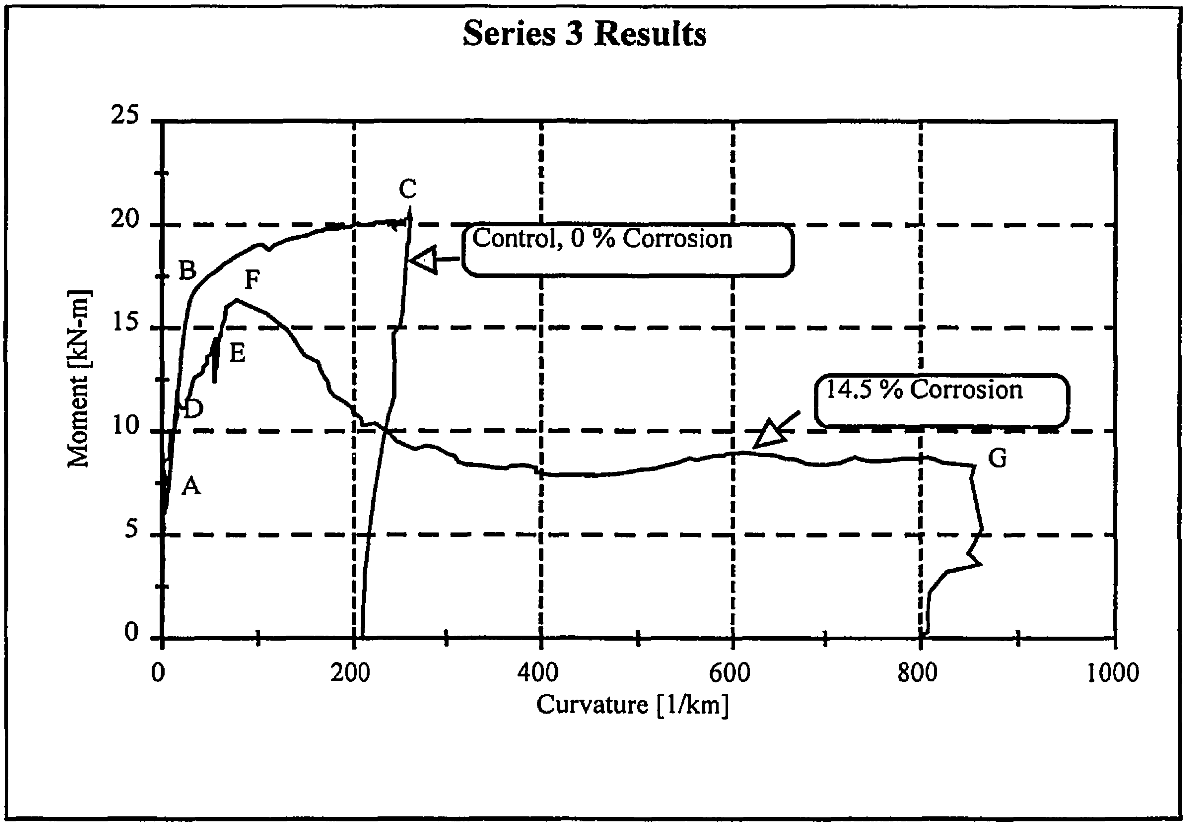

The corroded specimen still exhibited a large ductile response. In Figure 5-2, it appears that the ductility of the corroded response is greater than that of the control specimen. This is not the case. Between these two tests, the range of the curvature-meter LVDT's was changed. The slabs were more flexible than was expected before testing, so a greater range was required for the data. The control test was ended when the curvature-meter reached the end of its range and this gives the appearance of less ductility. The control specimen would still be capable of exhibiting greater ductility than that showed here, at least as much as that demonstrated by the corroded specimen.

The ductile response is unstable for the corroded specimen. It exhibits a negative post-peak modulus and if this situation occurred in practice then rapid failure would have occurred. In a real structure, if the load reached the point F, then the load would not be reduced so the additional response would not be exhibited. The moment at any point on the curve is the maximum capacity at that curvature but this would be insufficient to support the load from the previous point. This would lead to increasing curvature with an inability to support the load until failure is reached. This is much less preferable than the uncorroded response of increasing capacity with increasing curvature.

5.3 Comparing the Prediction and the Response

There were two elements to the prediction; the load at failure and the mode of failure. The predicted load at failure was 28.5 kN and it was predicted to fail in bond. The slab failed at a moment of 16.35 kN-m, which is equivalent to a load of 65.4 kN. It did fail in bond. This can be seen due to the shape of the moment - curvature response curve as discussed in the previous section.

The is a large difference between the predicted failure load and the actual failure load. As the mode of failure was as predicted, the inaccuracies lie in the predicted bond strength. Using the formula developed previously, the predicted bond strength was 1.09 MPa. As the actual failure load was much higher than that predicted, the actual maximum bond strength must be higher. The reason for this is that the corrosion level at which the bond strength was to be predicted was higher than the maximum value used to determine the formula. The maximum experimental value used to develop the relationship was 10.5 %. Thus, to apply this relationship to the level of 14.5 % is an extrapolation. The other, more important, reason is the quality of the relationship developed. While for the Silica Fume mix the relationship had a good correlation coefficient of 0.911, for the Normal mix used in this technique the correlation was only 0.680. Thus it is to be expected that the values predicted would be less accurate.

As a further test, the capacity based upon the results reported by Rodriguez, et al.[5-3] was calculated. This was done by determining the depth of penetration based upon uniform corrosion as the authors did in their paper. The depth of penetration was calculated as 0.416 mm and this resulted in a bond strength of 1.267 MPa. This value was then used in the identical technique to calculate the capacity of the slab. This predicts a capacity of 33.5 kN. A diagram of the moment capacity envelope and bending moment diagram predicted at failure is included as Figure 5-3. While this is a slightly better prediction that that which came from the work done here, it is still much lower than the actual, experimental value.

Finally, the experimentally determined capacity was used to calculate the bond strength truly developed, Fig. 5-4. This was done by using the reverse procedure used to predict the capacity. That is, the bending moment diagram at failure was plotted and the moment capacity envelope was plotted for a number of bond strengths until the two curves intersected, giving failure. This resulted in a bond strength of 2.55 MPa. For this calculation, however, the maximum capacity based upon steel section loss had to be ignored. This was as the capacity based on that prediction was only 13.82 kN-m, which was exceeded experimentally even though the slab failed in bond. This value for the bond strength determined experimentally is much higher than that predicted from the relationships developed earlier, as much as two and a half times.

The bond strengths as predicted by this equation were conservative for this situation and the factor of error was such that it would be considered an appropriate level for the factor of safety. This same degree of error cannot be assumed to always occur, however, and these equations should not be used assuming that this will be the case. A more appropriate technique would be to develop an expression that would predict the true mean value of the bond strength and apply a ration analysis to determine appropriate levels of safety.

Figure 5-3: Prediction Based on Rodriguez, et al.

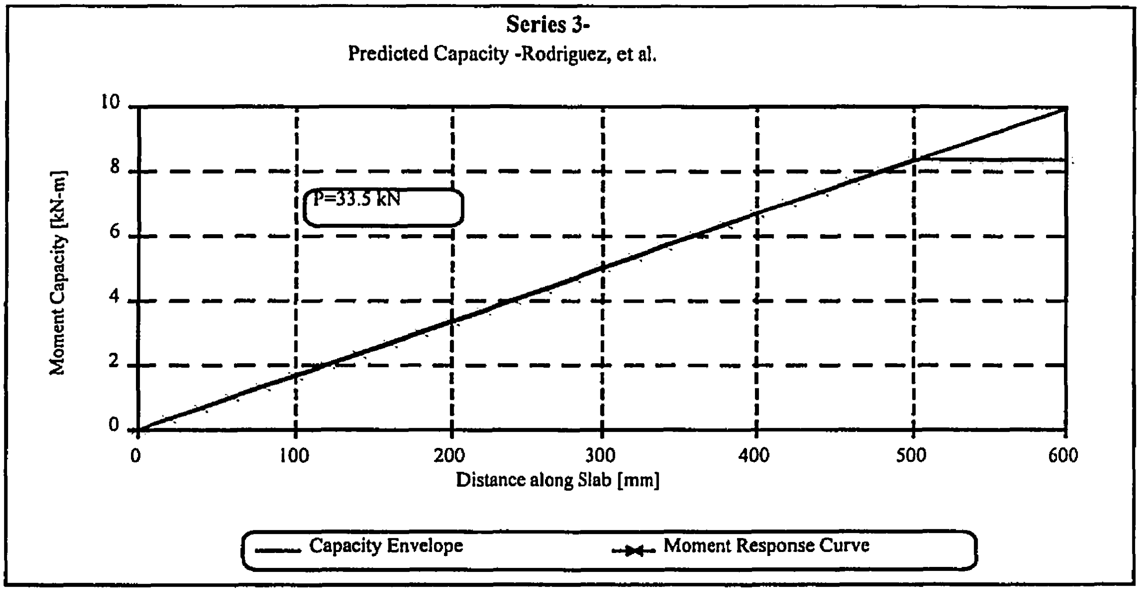

Figure 5-4: Presumed Actual Response

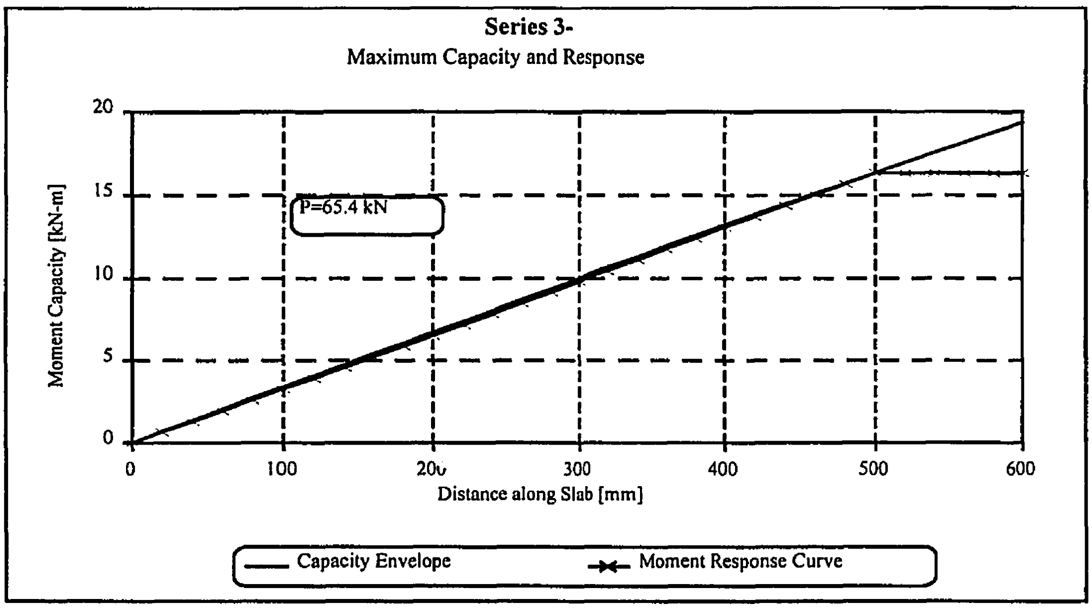

References

[5-1] J. Phillips, *The Effect of Corrosion on the Structural Performance of New and Repaired One-Way Slabs,* Ph.D. Thesis, University of Toronto, c1993, pg. 143

[5-2] J. Phillips, *The Effect of Corrosion on the Structural Performance of New and Repaired One-Way Slabs,* Ph.D. Thesis, University of Toronto, c1993, pg. 143

[5-3] J. Rodriguez, L. M. Ortega, J. Casal and J. M. Diez, "Assessing Structural Conditions of Concrete Structures with Corroded Reinforcement" *Concrete in the Service of Mankind: Concrete Repair, Rehabilitation and Protection,* First Ed. E & FN Spon London, 1996, pg. 65-78

6.0 Conclusions and Recommendations

First, the conclusions that can be drawn for this series of experiments are presented. Then recommendations for further work are discussed.

6.1. Conclusions

1. The apparent corrosion level for the specimens varied depending upon the technique used to measure it; using corrosion coupons or by integrating the corrosion current and applying Faraday's Law. This made it difficult to determine an actual corrosion level for the specimens that would represent the situation produced.
2. The corrosion pattern varied depending upon the technique used to connect the rebar to the power supply. One technique caused different corrosion amounts to occur in the different bars, as determined by visual inspection. The other technique caused more uniform corrosion between the bars.
3. The corrosion current was highly variable both between specimens and at different times in one slab even though the applied voltage remained constant.
4. A bar with approximately one quarter of its perimeter debonded from the concrete over its entire length has the bond strength to develop similar capacity as a standard bar, but will not be as ductile. If half of the bar's perimeter is debonded, though, it will have zero bond strength. The specimen will then act as if it were unreinforced.
5. Cracking and spalling of the concrete in the end regions was exhibited at minimal corrosion levels, e.g. 2-3 %, for the centre debonded and uncorroded specimens.
6. Corrosion damage does not appear to reduce the ductility of reinforced concrete members.
7. Bond strength reduces linearly with increasing corrosion levels, and equations defining this relationship with a variety of success were developed for the concrete tested herein.
8. The relationships developed in this thesis for bond and the method proposed by J. Phillips to deal with section capacity were unable to successfully predict the capacity of a trial slab

corroded to 14.5 % section loss. For this slab, the ultimate capacity was greater than that predicted by the work of J. Phillips considering section loss, though the slab appeared to fail in bond. The predicted capacity based upon bond considerations was less than that predicted by considering section effects. The problem was thought to lie either in the poor fit of the bond prediction expression for the concrete used or due to the difficulty in determining the representative corrosion level. Difficulty may have also arisen as the development length was longer for the Series 3 slab, creating the potential for a different distribution of bond stresses possibly altering the maximum average stress that can be developed. The cracking pattern was also different which may change the behaviour and relationships of corrosion and bond.

6.2. Recommendations

1. In Series 1, where the effect of concrete spalling was simulated, there was a large change in the response between the level of one quarter of the bars' perimeter debonded and one half. More information should be gathered on this changing influence by examining different portions of bars perimeter debonding, for example 30 %, 35 %, 40 %, 45 %. This would require the use of a larger bar so that it is reasonably possible use smaller increments of the proportion of the bar debonded.

2. One of the main difficulties in this work was controlling the amount of corrosion that was developed and characterizing it. This difficulty was partially overcome by change the technique used to connect the rebar to the power supply. This was not a complete remedy, however, and better results may have been obtained if, instead of using three bars, a single bar was used. This would reduce the problems of differential corrosion.

3. The specimens in this study were corroded using an applied voltage. This voltage created a current that was larger than any that would be encountered in the real world. While it is necessary to speed up the corrosion process to study it experimentally, it is suspected that this large current may have effects on the structure of the corrosion products. Instead of being deposited on or near the rebar, the corrosion products may be transported into the body of the concrete or into the salt solution. This would then obviously change the expansive pressures that are exerted as well as the surface characteristics of the reinforcing steel. This may not be

as important when considering section properties, as done by J. Phillips, but would be more important when considering bond influences. It is recommended that a series of tests be performed that would reduce the acceleration of the corrosion process and mimic better the natural situation to evaluate the possibility of this influence. This could possibly be achieved by wet/dry cycling the specimens to cause corrosion without an applied current.

Bibliography

"Suggested Development, Splice and Standard Hook Provisions for Deformed Bars in Tension"(ACI 408.1R-90) *ACI Manual of Concrete Practice 1995*, Part 3, ACI, Detroit

Abdullah A. Almusallam, Ahmad S. Al-Gahtani, Abdur Rauf Aziz, Fahd H. Dakhil and Rasheeduzzafar, "Effect of Reinforcement Corrosion on Flexural Behaviour of Concrete Slabs", *Journal of Materials in Civil Engineering*, v. 8 n. 3, August 1996, pg. 123-7

G.J. Al-Sulaimani, M. Kaleemullah, I. A. Basunbul, and Rasheeduzzafar, "Influence of Corrosion and Cracking on Bond Behaviour and Strength of Reinforced Concrete Members", *ACI Structural Journal*, v. 87 n. 2, Mar.-Apr. 1990, pg. 220-31

"Standard Test Method for Compressive Strength of Cylindrical Concrete Specimens" (ASTM C39-93a) *1994 Annual Book of ASTM Standards* V 04.02, ASTM, Philadelphia, pg. 17-21

"Standard Test Method for Comparing Concretes on the Basis of Bond Developed with Reinforcing Steel" (ASTM C234-91a) *1994 Annual Book of ASTM Standards*, V 04.02, ASTM, Philadelphia, pg.148-52

"Standard Test Method for Half-Cell Potentials of Uncoated Reinforcing Steel in Concrete" (ASTM C876-91) *1994 Annual Book of ASTM Standards* V 04.02, ASTM, Philadelphia, pg. 432-7

"Standard Test Method for Electrical Indication of Chloride's Ability to Resist Chloride" (ASTM C1202-94) *1994 Annual Book of ASTM Standards* V 04.02, ASTM, Philadelphia, pg. 620-5

"Standard Practice for Preparing, Cleaning and Evaluating Corrosion Test Specimens" (ASTM G1-90) *1994 Annual Book of ASTM Standards* V 03.02, Philadelphia, pg. 25-31

J. Cairns and K. Jones, "An Evaluation of the Bond-Splitting Action of Ribbed Bars", *ACI Materials Journal*, v. 93 n.1, Jan.-Feb. 1996, pg. 10-19

J. Cairns and K. Jones, "The Splitting Forces Generated By Bond", *Magazine of Concrete Research*, v. 47 n. 171, 1995, pg. 153-65

J. Cairns and R. Bin Abdullah, "Bond Strength of Black and Epoxy-Coated Reinforcement- A Theoretical Approach", *ACI Materials Journal*, v. 93 n 4, July-August 1996, pg. 362-9

Canadian Standards Association *Design of Concrete Structures for Buildings* CAN/A23.3-M84 Rexdale, Ont., 1984

Canadian Standards Association *Parking Structures-Structural Design*, CSA/S413-94, Rexdale, Ont., 1994

Corrosion Damage to Concrete Structures in Western Asia, United Nations Centre for Human Settlements (Habitat), Nairobi, 1990

ENV 1992 - Eurocode 2

K. Leet, R*einforced Concrete Design*, 2nd Ed. McGraw-Hill Inc., Toronto, 1996

N.P. Mailvaganan, *Repair and Protection of Concrete Structures*, CRC Press c1992

M. Maslehuddin, et al. "Effect of Rusting of Reinforcing Steel on Its Mechanical Properties and Bond with Concrete", *ACI Materials Journal*, v. 87 n.5, Sept.- Oct. 1990, pg. 496-502

Edward G. Nawy *Reinforced Concrete: A Fundamental Approach*, 3rd Ed. Prentice-Hall Canada, Inc. Toronto, c1996

A.M. Neville, *Properties of Concrete*, 3rd Ed., Longman Scientific and Technical England, c1981

P. Pullar-Strecker, *Corrosion Damaged Concrete: Assessment and Repair*, Anchor Brendon Ltd., Tiptree Essex, England, c1987

J. Phillips, *The Effect of Corrosion on the Structural Performance of New and Repaired One-Way Slabs,* Ph.D. Thesis, University of Toronto, c1993

Report of the Advisory Committee on the Deterioration, Repair and Maintenance of Parking Garages, Ministry of Housing, Ontario Buildings Branch, July 1988

J. Rodriguez, L. M. Ortega, J. Casal and J. M. Diez, "Assessing Structural Conditions of Concrete Structures with Corroded Reinforcement" *Concrete in the Service of Mankind: Concrete Repair, Rehabilitation and Protection,* First Ed. E & FN Spon London, 1996

P. Schiessl, ed. *Corrosion of Steel in Concrete,* Chapman and Hall, Ltd. c1988

A. Smith, E. Hinton and R. Lewis, *Civil Engineering Systems: Analysis and Design* 1st ed., John Wiley and Sons, Toronto, c1983

S. Ting and A. Nowak, "Effect of Reinforcing Steel Area Loss on Flexural Behaviour of Reinforced Concrete Beams", *ACI Structural Journal*, v. 88 n. 3, May-June 1991, pg. 309-14

R. A. Treece, and J. O. Jirsa, "Bond Strength of Epoxy Coated Reinforcing Bars", *ACI Materials Journal,* v86 n2 March-April 1989 p. 167-174

Y. Yuan and M. Marosszeky, "Analysis of Corroded Reinforced Concrete Sections for Repair", *Journal of Structural Engineering*, v. 117 n. 7, July 1991, pg. 2018-34

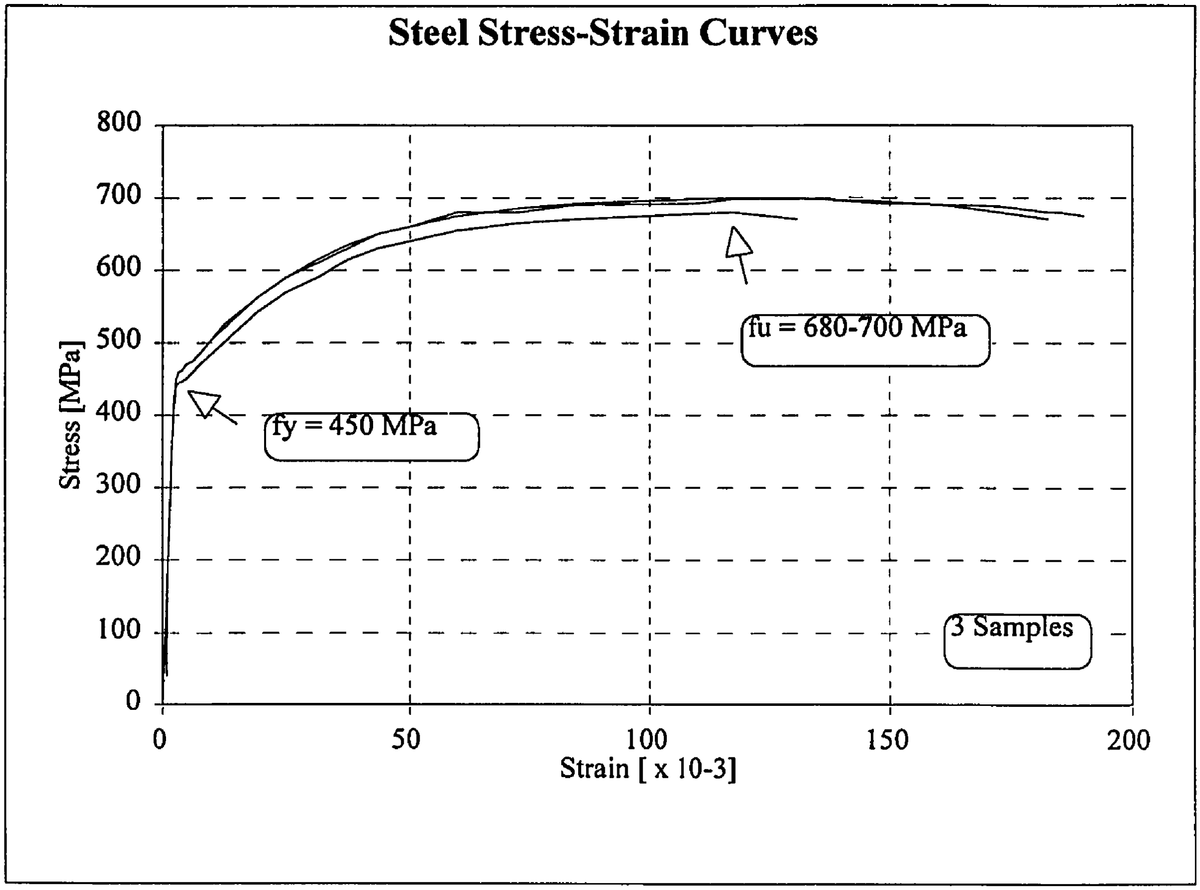
Steel Stress-Strain Curves
800
700
600
500
400
300
200
100
0
Stress [MPa]
fu = 680-700 MPa
fy = 450 MPa
3 Samples
0
50
100
150
200
Strain [x 10-3]

Structural Design Calculations

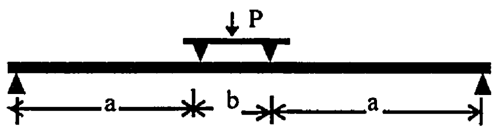

Aims: 1. Failure mode in moment rather than shear.

2. Resembles a section of a slab. (wider than it is deep, no stirrups)
3. Minimize size.
4. At least three bars to provide some internal averaging of effects.

For initial designs, use a concrete strength of 35 MPa and a steel yield point of 450 MPa.

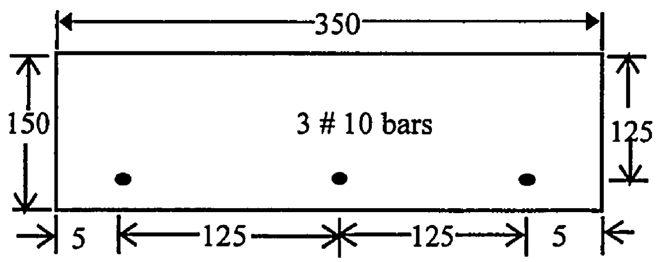

This is a diagram of the final cross-section arrived at.

Follows is a calculation of its shear and moment capacities.

Moment Capacity

$T = C$

$A_s f_y = 0.85 f'_c b a$

$(300\ mm^2)(450\ MPa) = 0.85\ (35\ MPa)(350\ mm)\ a$

$a = 13\ mm$

$M = T\ (d - a/2)$

$= (300\ mm^2)\ (450\ MPa)(125\ mm - (13\ mm)/2)$

$= 16.0\ kN\text{-}m$

Shear Capacity

$V_c = 0.2\ (\sqrt{f'_c})\ b_w\ d$

$= 0.2\ (\sqrt{35}\ MPa)\ (350\ mm)\ (125\ mm)$

$= 51.8\ kN$

A length had to be chosen so that the beam would fail in moment long before it failed in shear.

It was decided that the limiting factor would be that it would reach no more than 65 % of its shear capacity when it fails in moment.

The testing set-up would be simply supported with a constant moment region.

$M_{max} = (P/2)*a$

$V_{max} = P/2$

Therefore, $M_{max} / V_{max} = a$

Also, M_{max} = 16.0 kN-m and V_{max} = 0.65 (51.8 kN) = 33.7 kN

Thus, a = 0.475 m

Thus the distance from the support to the loading point shall be 500 mm.

The distance b was selected as the minimum that would be reasonably sure to provide a sufficient constant moment region.

In this case, it was felt that 200 mm would be sufficient.

To provide for cover on the ends, 50 mm were added on either side.

This gives a total specimen length of 1300 mm.

Thus, the dimensions of the test specimen were 1300 mm x 350 mm x 150 mm. Three #10M rebars were used with a bottom cover of 25 mm to the centre of the bars (or 20 mm clear cover). Fifty millimetres cover was provided at the ends and at either side.

Development Length Calculations (As per ACI 408.1R-90)

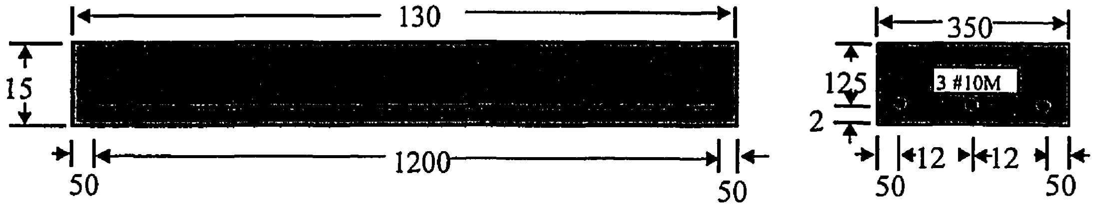

$A_b = 100\ mm^2 = 0.155\ in^2$ (Area of a single bar)

$d_b = 10\ mm = 0.787\ in$ (bar diameter)

$f_y = 450\ MPa = 65\ 220\ psi$ (yield stress of steel)

$f'_c = 35\ MPa = 5070\ psi$ (concrete compressive strength)

$\Phi = 1.0$ (factor of safety)

$C_c = 25\ mm = 1.0\ in$ (concrete cover)

$K = 0.5\ d_b + C_c = 1.197$ (confinement factor)

$l_{db} = 5500 A_b / (\Phi K \sqrt{f'_c}) = 10.01\ in = 250\ mm$

Therefore the development length chosen was 250 mm.

(Note that ACI is in pound-inch units and thus a conversion was required from metric and back again.)

Curvature-meter Evaluation

The curvature-meter is the technique used to evaluate the deformation tendencies of the various slabs. It consists of a bar hung from two points on the neutral axis at either end of the constant moment region of the beam. As the neutral axis changes during the test for reinforced concrete, the mid height was used. Then, using a LVDT, the deflection between the midpoint of the span at the neutral axis and the bar is measured. This information can then be used to calculate the curvature. This calculation assumes an elastic response, which is not the case for concrete after it has cracked. It was still useful, however, as it allowed a comparison between slabs of their relative deformation. The development of the relevant formulas is described in the following.

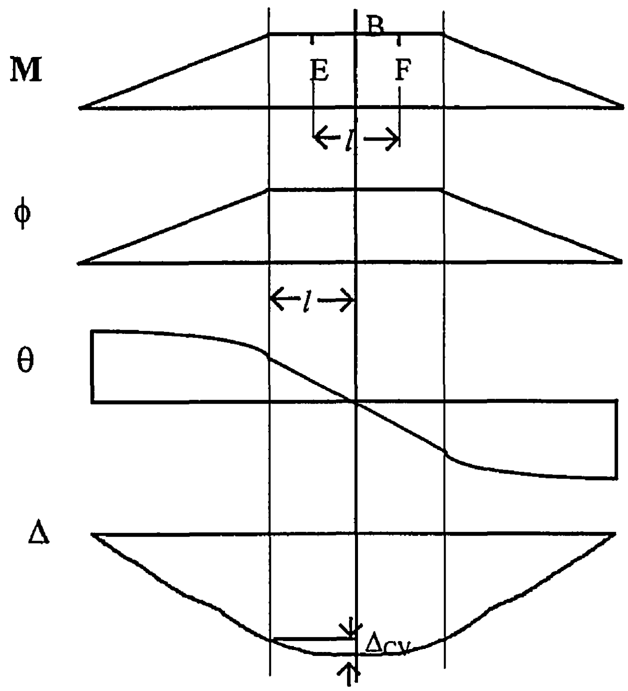

Consider the diagrams to the left. These are typical moment, curvature, slope and deflection diagrams for a member loaded in four point bending, assuming that the beam behaves elastically. Using these, we will first compute the average slope between A and B. It is :

$$\theta_{AV,AB} = \frac{-\Delta_{CV}}{l}$$

Note that the negative of this is the average slope of section BC. Also note that the average slope in these sections corresponds to the slope at the midpoints of these sections as the slope varies linearly for this region. The midpoints have been designated E and F. Note that the distance between E and F is also l. Now it is necessary to calculate the curvature in the constant moment region. This will correspond exactly to the average curvature between E and F as the curvature is constant. Thus:

$$\phi_{CMR} = \phi_{EF,AV} = \frac{\frac{\Delta}{l} - (-\frac{\Delta}{l})}{l} = 2\frac{\Delta}{l^2}$$

This formula has been used to determine the curvature of the slabs.

Corrosion Current Calculations

The current was continually recorded as described in the Experimental Procedures. This value was then converted into percent lost based upon the following procedure.

By Faraday's Law, $n = \frac{C}{F}$

where: n is the number of equivalents reacting,
C is the charge passed and
F is Faraday's constant, 96487 C/equiv.

Now, $C = It$

where: I is the current passing and
t is the length of time.

Also, $n = mz$

where: m is the number of mols,
n is the number of equivalents and
z is the charge on an ion.

Thus, $m = \frac{It}{Fz}$.

Now, we desire mass loss.

But, $w = mA^{tm}$

where: w is the mass loss, and
A^{tm} is the atomic mass.

Thus, $w = \frac{ItA^{tm}}{Fz}$

To convert this to volumetric percent loss, first the volume loss needs to be determined.

$V_{loss} = \frac{w}{r}$

where: ρ is the density of the steel.

The original volume of the corroded steel is $A_s * l_{corr}$

where: A_s is the area of steel and
l_{corr} is the total length of steel that is to be corroded.

Thus, $\% \text{ lost} = \frac{w}{\rho A_s l_{corr}} x100\%$ or $\frac{ItA^{tm}}{FzA_s l_{corr} \rho} x100\%$

Now it is possible to convert this for the situations that will be encountered in this experimental program. There will be two slightly different situations. For series 2, the corroded length will be just the ends of the rebars, while for series 3, the corroded length will be the entire bar.

Series 2

A^{tm} = 55.85 g/mol (as mostly iron)

F= 96487 C/equiv.

z = 2 equiv/mol

$A_s = 100\ mm^2$

l_{corr} = 6*250 mm + 100 mm = 1600 mm

$\rho = 7850\ kg/m^3 = 7850 \times 10^{-6}\ g/mm^3$

Thus %lost = 23.04×10^{-6} It

where: I is in Amperes and
t is in seconds.

Series 3

A^{tm} = 55.85 g/mol (as mostly iron)

F= 96487 C/equiv

z = 2 equiv/mol

$A_s = 100\ mm^2$

l_{corr} = 3*1200 mm + 100 mm = 3700 mm

$\rho = 7850\ kg/m^3 = 7850 \times 10^{-6}\ g/mm^3$

Thus, % lost = 9.964×10^{-6} It

where: I is in Amperes and
t is in seconds.

Fresh Concrete Properties of Mixes

Series 1 - Control Slab:

Slump: 180 mm
Air Content: 9 %
Plastic Density: 2305 kg/m^3
Admixture Dosages:
ProAir: 45 mL/100 kg cementitious
25 XL: 250 mL/100 kg cementitious
RheoBuild1000: 500 mL/100 kg cementitious

Series 1 - Half Covered:

Slump: 180 mm
Air Content: 8 %
Plastic Density: 2246 kg/m^3
Admixture Dosages:
ProAir: 35 mL/100 kg cementitious
25 XL: 260 mL/100 kg cementitious
RheoBuild 1000: 310 mL/100 kg cementitious

Series 1 - Quarter Covered:

Slump: 200 mm
Air Content: 5 %
Plastic Density: 2260 kg/m^3
Admixture Dosages:
ProAir: 30 mL/100 kg cementitious
25 XL: 250 mL/100 kg cementitious
RheoBuild1000: 300 mL/100 kg cementitious

Series 2 - Normal, Control:

Slump: 110 mm
Air Content: 6.5 %
Plastic Density: 2336 kg/m^3
Admixture Dosages:
ProAir: 30 mL/100 kg cementitious
25 XL: 250 mL/100 kg cementitious
RheoBuild1000: 300 mL/100 kg cementitious

Series 2 - Normal, 2 % Corrosion:

Slump: 210 mm
Air Content: 6 %
Plastic Density: 2274kg/m^3
Admixture Dosages:
ProAir: 30 mL/100 kg cementitious
25 XL: 250 mL/100 kg cementitious
RheoBuild1000: 275mL/100 kg cementitious

Series 2 - Normal, 5 % Corrosion:

Slump: 210 mm
Air Content: 6.5 %
Plastic Density: 2336 kg/m^3
Admixture Dosages:
ProAir: 30 mL/100 kg cementitious
25 XL: 250 mL/100 kg cementitious
RheoBuild1000: 250 mL/100 kg cementitious

Series 2 - Normal, 8 % Corrosion:

Slump: 210 mm
Air Content: 8 %
Plastic Density: 2246 kg/m^3
Admixture Dosages:
ProAir: 30 mL/100 kg cementitious
25 XL: 250 mL/100 kg cementitious
RheoBuild1000: 225 mL/100 kg cementitious

Series 2 - Normal, 10 % Corrosion:

Slump: 160 mm
Air Content: 7 %
Plastic Density: 2306 kg/m^3
Admixture Dosages:
ProAir: 30 mL/100 kg cementitious
25 XL: 250 mL/100 kg cementitious
RheoBuild1000: 200 mL/100 kg cementitious

Series 2 - Silica, Control:

Slump: 125 mm
Air Content: 7 %
Plastic Density: 2316 kg/m^3
Admixture Dosages:
ProAir: 30 mL/100 kg cementitious
25 XL: 250 mL/100 kg cementitious
RheoBuild1000: 350 mL/100 kg cementitious

Series 2 - Silica, 2 % Corrosion:

Slump: 160 mm
Air Content: 8 %
Plastic Density: 2246 kg/m^3
Admixture Dosages:
ProAir: 30 mL/100 kg cementitious
25 XL: 250 mL/100 kg cementitious
RheoBuild1000: 350 mL/100 kg cementitious

Series 2 - Silica, 5 % Corrosion:

Slump: 50 mm
Air Content: 5.5 %
Plastic Density: 2359 kg/m^3
Admixture Dosages:
ProAir: 30 mL/100 kg cementitious
25 XL: 250 mL/100 kg cementitious
RheoBuild1000: 300 mL/100 kg cementitious

Series 2 - Silica, 8 % Corrosion:

Slump: 175 mm
Air Content: 7 %
Plastic Density: 2274 kg/m^3
Admixture Dosages:
ProAir: 30 mL/100 kg cementitious
25 XL: 250 mL/100 kg cementitious
RheoBuild1000: 300 mL/100 kg cementitious

Series 2 - Silica, 10 % Corrosion:

Slump: 50 mm
Air Content: 6 %
Plastic Density: 2362 kg/m^3
Admixture Dosages:
ProAir: 30 mL/100 kg cementitious
25 XL: 250 mL/100 kg cementitious
RheoBuild1000: 300 mL/100 kg cementitious

Series 3 - 10 % Corrosion:

Slump: 130 mm
Air Content: 6.5 %
Plastic Density: 2359 kg/m^3
Admixture Dosages:
ProAir: 30 mL/100 kg cementitious
25 XL: 250 mL/100 kg cementitious
RheoBuild1000:200 mL/100 kg cementitious

Material Results Summary

Specimen	Strength [MPa]		Rapid Chloride		Resistivity [Ω-cm]		Sorptivity [mm/min$^{0.5}$]	
	7 Day	28 Day	7 Day	28 Day	7 Day	28 Day	7 Day	28 Day
1-N-0	25.7	38.6	-	-	-	-	-	-
1-N-1/4	21.6	31.5	-	-	-	-	-	-
1-N-1/2	19.4	31.9	-	-	-	-	-	-
2-N-0	30.5	42.9	-	-	-	-	-	-
2-N-2	-	32.2	-	-	-	-	0.0814	0.1189
2-N-5	-	38.6	-	-	-	-	0.0974	0.1202
2-N-8	-	30.4	Mod.	Mod.	6894	11578	-	-
2-N-10	-	32.1	Mod.	Low	7466	15736	-	-
2-S-0	26.9	47.9	-	-	-	-	-	-
2-S-2	-	40.9	-	-	-	-	0.1178	0.1119
2-S-5	39.0	37.1	Low	V. Low	14279	49162	-	-
2-S-8	-	41.2	-	-	-	-	0.1283	0.1102
2-S-10	33.1	49.6	Low	V. Low	12453	52450	-	-
3-N-10	22.0	37.0	High	Mod.	4374	9704	0.1550	0.0728

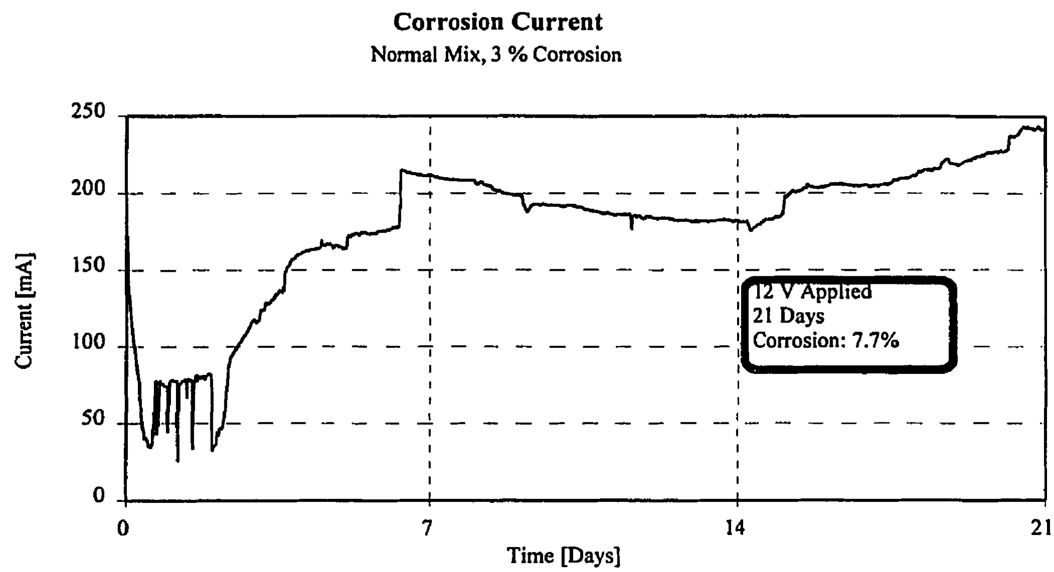
Corrosion Current
Normal Mix, 3 % Corrosion
250
200
150
100
50
0
Current [mA]
12 V Applied
21 Days
Corrosion: 7.7%
0
7
14
21
Time [Days]

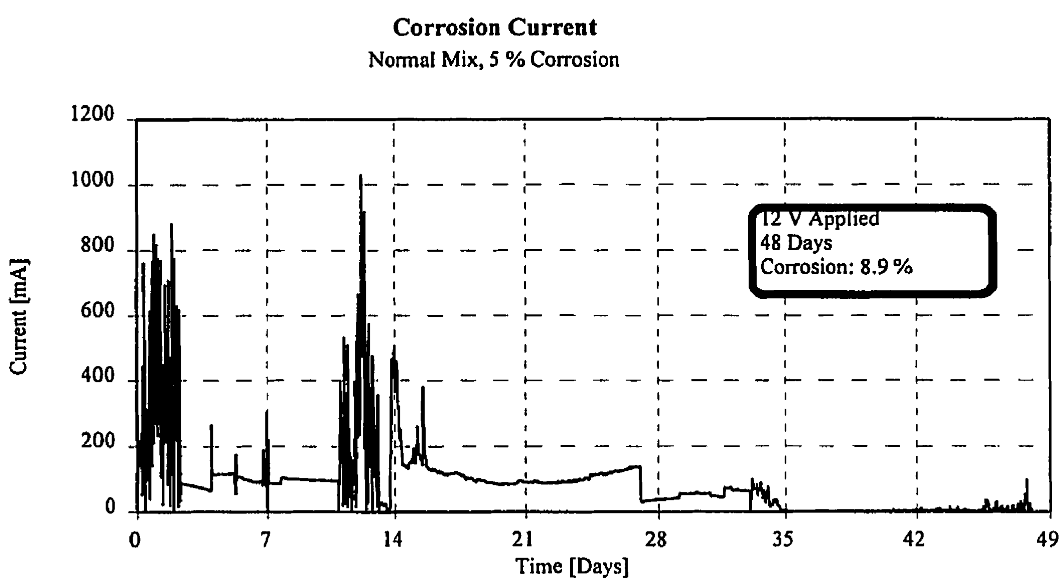
Corrosion Current
Normal Mix, 5 % Corrosion
1200
1000
800
600
400
200
0
Current [mA]
12 V Applied
48 Days
Corrosion: 8.9 %
0
7
14
21
28
35
42
49
Time [Days]

Corrosion Current
Normal Mix, 8 % Corrosion

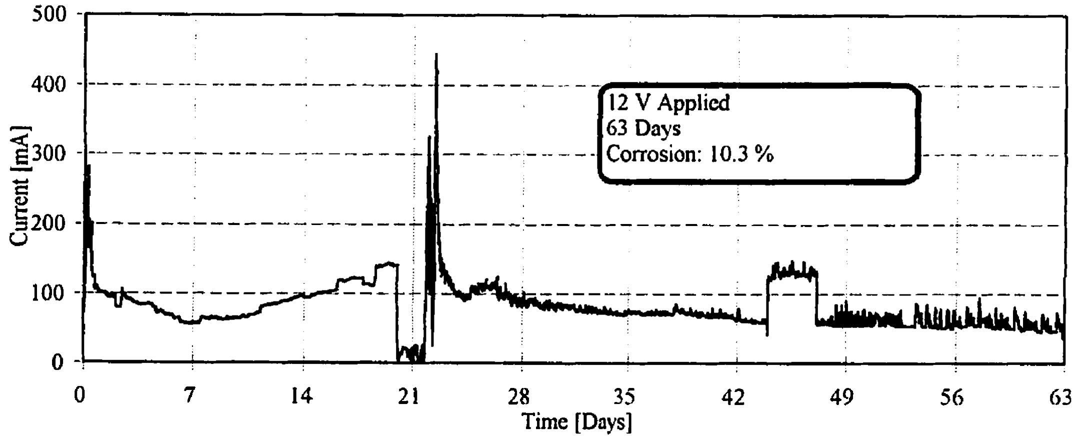

Corrosion Current
Normal Mix, 10 % Corrosion

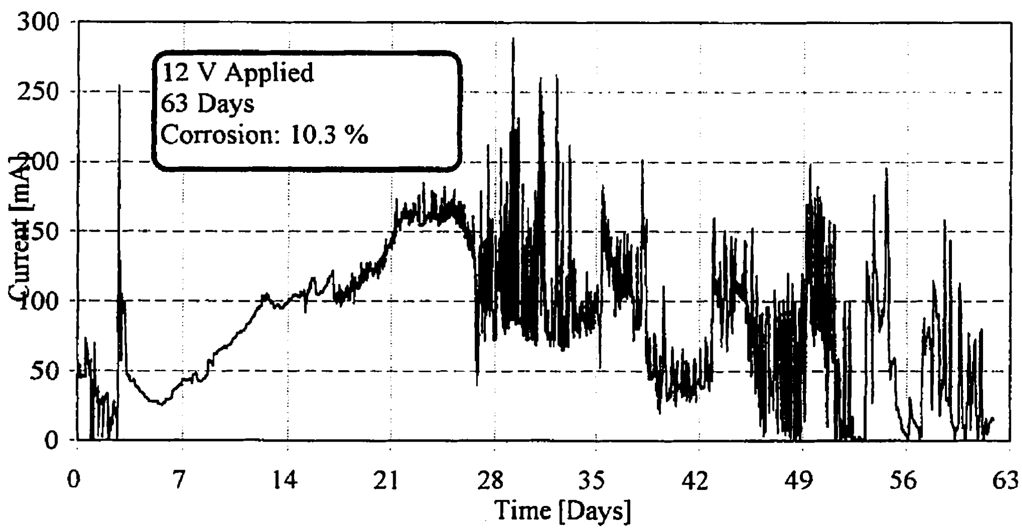

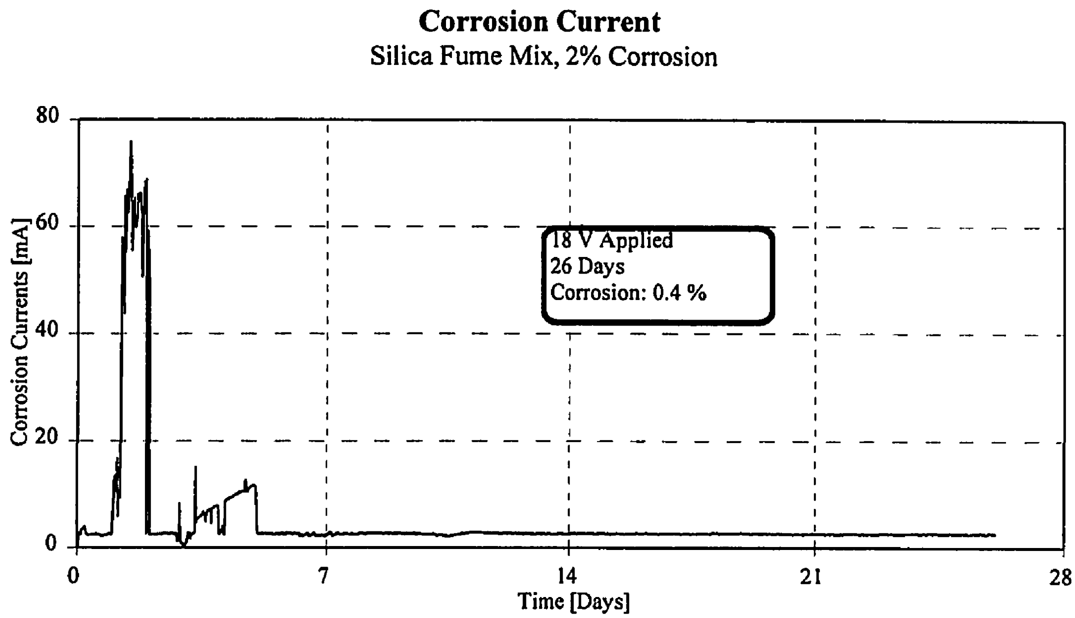
Corrosion Current
Silica Fume Mix, 2% Corrosion
18 V Applied
26 Days
Corrosion: 0.4 %
Corrosion Currents [mA]
0
20
40
60
80
0
7
14
21
28
Time [Days]

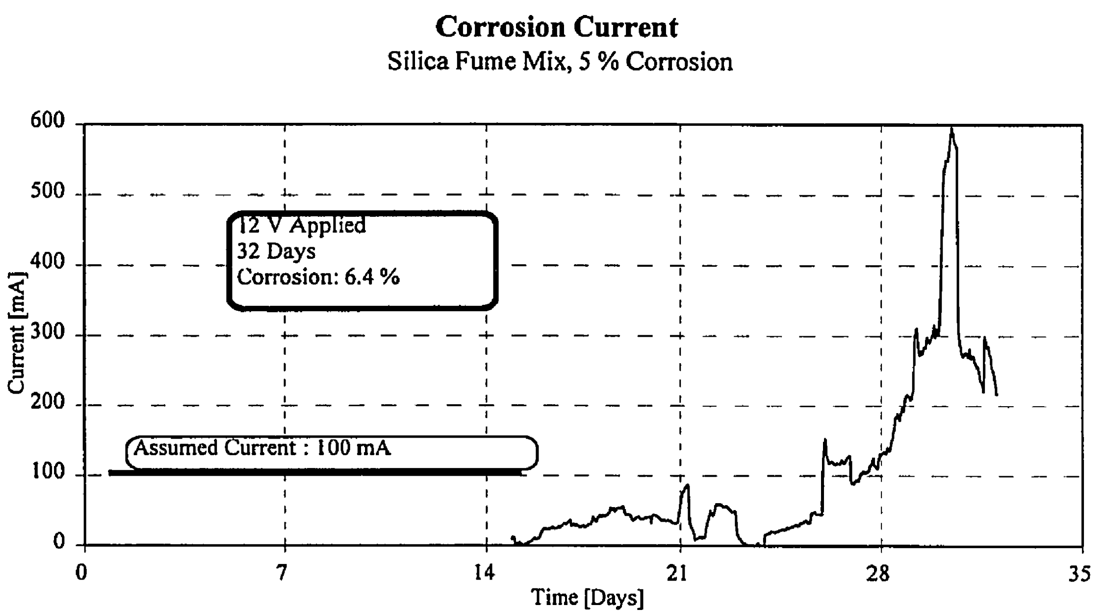
Corrosion Current
Silica Fume Mix, 5 % Corrosion
12 V Applied
32 Days
Corrosion: 6.4 %
Assumed Current : 100 mA
Current [mA]
0
100
200
300
400
500
600
0
7
14
21
28
35
Time [Days]

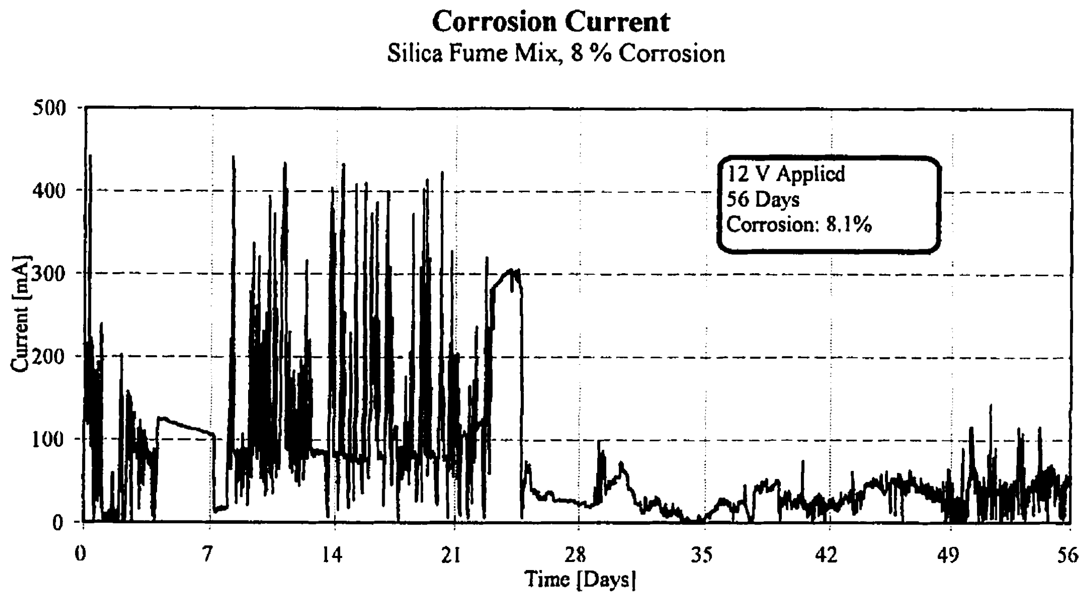
Corrosion Current
Silica Fume Mix, 8 % Corrosion
12 V Applied
56 Days
Corrosion: 8.1%
Current [mA]
Time [Days]
500
400
300
200
100
0
0
7
14
21
28
35
42
49
56

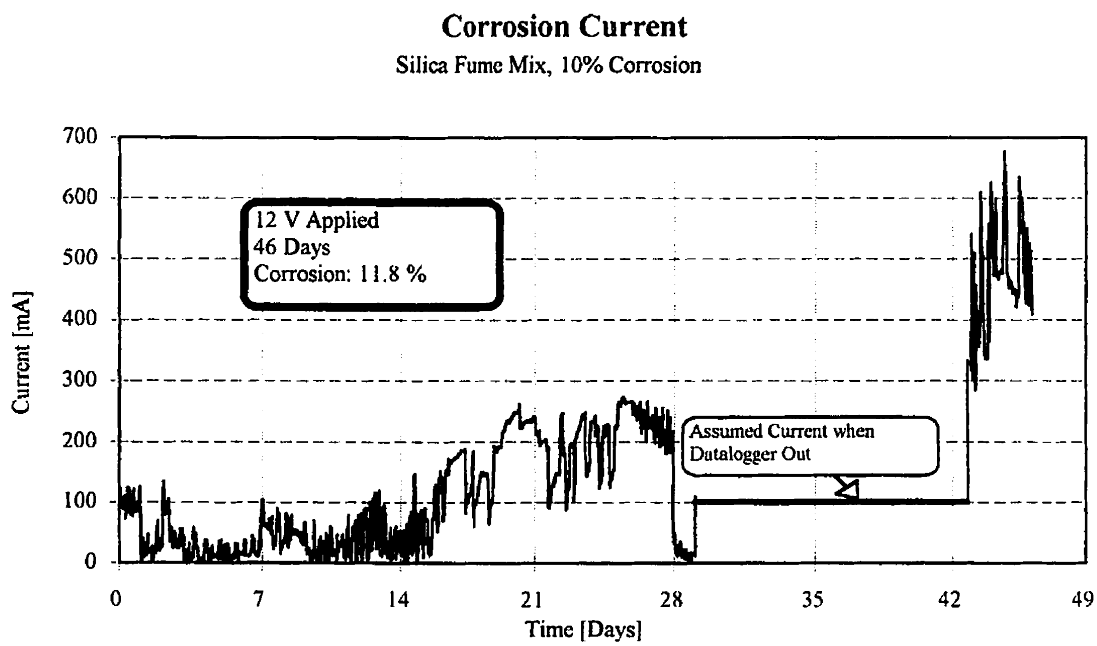
Corrosion Current
Silica Fume Mix, 10% Corrosion
12 V Applied
46 Days
Corrosion: 11.8 %
Assumed Current when Datalogger Out
Current [mA]
Time [Days]
700
600
500
400
300
200
100
0
0
7
14
21
28
35
42
49

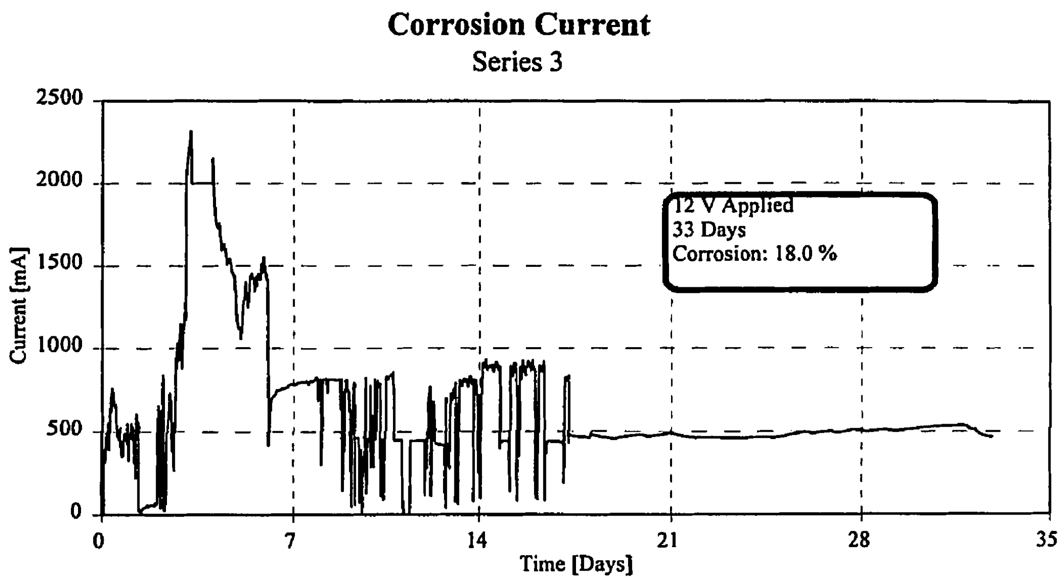
Corrosion Current
Series 3
2500
2000
1500
1000
500
0
Current [mA]
12 V Applied
33 Days
Corrosion: 18.0 %
0
7
14
21
28
35
Time [Days]

Bond Evaluation

To evaluate the strength of the bond in the Series 2 slabs, it was first necessary to determine the stress in the bars. This was using the measured moments and curvatures for all points in the moment curvature diagram after the slabs cracked using a computer program written in FORTRAN 77 for this purpose. A copy of this program is below. It contains a root-finding subroutine written by A. Smith, E. Hinton and R. Lewis, *Civil Engineering Systems: Analysis & Design*, John Wiley & Sons, Toronto, c1983

```
************************************************************************
      PROGRAM STEELFORCE
*   K. Stanish, May 27, 1997
*   This program was created to determine the force in the steel of a reinforced
*   concrete prismatic beam of rectangular cross-section, given the moment
*   and the curvature. It is designed for one layer of steel only.
*   This uses a bisection root finding technique from SMITH, HINTON and LEWIS.
      REAL CSTART,CEND,DX,EPS,PHI,MACT,D,B,AS,FC
      REAL EPSC,ALPHA,BETA,FS
      INTEGER NW, NUM, J
      CHARACTER*13 INFILE, OUTFILE
      EXTERNAL FUN
      COMMON PHI,MACT, D,B,AS,FC,EPSC,ALPHA,BETA
      NW=0
      PRINT*, 'Enter the name of the input file:(IN APOS.)'
      READ*, INFILE
      PRINT*, 'Enter the name of the output file:(IN APOS.)'
      READ*, OUTFILE
      OPEN(UNIT=11, FILE=INFILE, FORM='FORMATTED', STATUS='OLD')
      OPEN(UNIT=12, FILE=OUTFILE, FORM='FORMATTED', STATUS='NEW')
      REWIND(UNIT=11)
      CALL INITIAL(D,B,FC,EPSC,AS,EPS,NUM)
      WRITE (12,25)
      DO 23 J=1,NUM
          CALL SITUATION(MACT,PHI,CSTART,DX)
          CALL BISECT(FUN,CSTART,DX,EPS,NW,CEND)
          FS=(B*BETA*ALPHA*FC*CEND)/AS
          WRITE (12,24) MACT,PHI,CEND,FS
23    CONTINUE
24    FORMAT (1X,F6.2,5X,E10.3,5X,F5.1,5X,F11.2,5X,F11.2)
25    FORMAT (2X,'MACT',8X,'PHI',12X,'C',15X,'FS1',15X,'FS2')
26    FORMAT (1X,F6.2,5X,E10.3,5X,F5.1,5X,F11.2,5X,'YIELD')
      CLOSE (UNIT=11)
      CLOSE (UNIT=12)
      END
************************************************************
      SUBROUTINE INITIAL(D,B,FC,EPSC,AS,EPS,NUM)
      REAL D,B,FC,EPSC,AS,EPS
      INTEGER NUM
      READ (11,*) D,B,FC,EPSC,AS,EPS,NUM
```

```
      RETURN
      END
************************************************************
      SUBROUTINE SITUATION(MACT,PHI,CSTART,DX)
      REAL MACT, PHI, CSTART, DX
      READ (11,*) MACT,PHI,CSTART,DX
      RETURN
      END
************************************************************
      SUBROUTINE FUN(C,MRT)
      COMMON PHI, MACT, D,B,AS,FC,EPSC, ALPHA,BETA
      REAL EPST,PHI,MACT,D,B,AS,FC,EPSC,C,MRT,QUOT,ALPHA,BETA,MCAL
      EPST=PHI*C
      QUOT=EPST/EPSC
      BETA=(4-QUOT)/(6-2*QUOT)
      ALPHA=(QUOT-QUOT*QUOT/3)/BETA
      MCAL=B*FC*BETA*C*ALPHA*(D-BETA*C/2)/1000000
      MRT=MCAL-MACT
      RETURN
      END
************************************************************
     SUBROUTINE BISECT(FUN,XSTART,DX,EPS,NW,XROOT)
************************************************************
* The routine determines by the method of interval halving the root
* of an equation of a single variable.
*   FUN    = name of subroutine supplied by the user
*            to define the equation.
*            For example:
*            SUBROUTINE EQUN(X,F)
*            F=X*X-6.0*X+4.0
*            RETURN
*            END
*   XSTART = Start of coarse search range
*   DX     = Initial increment for coarse search
*   EPS    = Minimum acceptable interval of uncertainty
*            for convergence
*   NW     = Output channel for intermediate printout.
*            Set NW=0 to suppress all printout.
*   XROOT  = Computed value of root
* A coarse search is carried out to find the initial interval of
* uncertainty. If no root is found within 10000*DX the search is
* abandoned.
* Note that two roots close to together may be missed by the coarse
* search.
* A distinction is made between roots and possible discontinuities
* and a warning is printed.
* The name of the actual subroutine corresponding to FUN must appear
* in an external statement in the driving program.
************************************************************
     X1=XSTART
     XROOT=XSTART
     DX1=DX
C  START COARSE SEARCH
     CALL FUN(X1,F1)
```

```
      IF(NW.GT.0) WRITE(NW,50)X1,F1
      FAC=1.0
    5 CONTINUE
      X2=X1+DX1
      CALL FUN(X2,F2)
      IF(NW.GT.0) WRITE(NW,50)X2,F2
C TEST FOR CHANGE OF SIGN INFUNCTION
      IF(F1*F2.LT.0.0) GOTO 20
C NO CHANGE OF SIGN
      FAC=2.0*FAC
      DX1=FAC*DX
      F1=F2
      X1=X2
C SET LIMIT ON EXTENT OF SEARCH
      IF(FAC.LT.10000.0) GOTO 5
      IF(NW.GT.0)WRITE(NW,10)XSTART,X2
   10 FORMAT(24H IN BISECT NO ROOT FOUND,
     +      8H BETWEEN,F12.3,4H AND,F12.3)
      STOP
   20 CONTINUE
C INTERVAL OF UNCERTAINTY DEFINED BY X1,X2
C NOW FIND SLOPE OF FUNCTION IN THIS INTERVAL
      SIGN=1.0
      IF(F2.LT.0.0) SIGN=-1.0
C SET VARIABLE TO TEST FOR DISCONTINUITY
      FM1=F1
      FM=F1
C MAIN ITERATION LOOP STARTS HERE
   30 CONTINUE
      NDISC=0
      XM=0.5*(X1+X2)
      IF(SIGN*FM.LT.SIGN*FM1) NDISC=1
      CALL FUN(XM,FM)
C OUTPUT ITERATION VALUES IF REQUIRED
      IF(NW.GT.0) WRITE(NW,50)XM,FM
   50 FORMAT(10H IN BISECT,2F16.4)
      IF(SIGN*FM.LT.0.0) GOTO 60
      GOTO 70
   60 CONTINUE
      X1=XM
      GOTO 80
   70 CONTINUE
      X2=XM
   80 CONTINUE
C TEST FOR CONVERGENCE
      IF(ABS(X2-X1).GT.EPS) GOTO 30
      XROOT=XM
      IF(NDISC.EQ.0) RETURN
      IF(NW.GT.0) WRITE(NW,90)
   90 FORMAT(39H IN BISECT POSSIBLE DISCONTINUITY FOUND)
      RETURN
      END
```

After the stress in the steel was determined for all points in the post-cracking region of the moment-curvature response, the bond stress that had arisen were determined. This was done by dividing the force in a bar by the surface area of the bar that is in contact with the concrete at each end. The maximum value was then determined and that was reported as the bond capacity of the corroded bars.

Series 3 Predictions

Material Properties: f'_c = 37.0 MPa f_y = 450 MPa
b = 350 mm d = 125 mm
A_s = 300 mm^2 (before corrosion)
14.5 % corrosion loss

Section Calculations:

This is calculated as if the steel was reduced by the percent that it was corroded by. Thus, consider as if the slab had a steel area of 0.855(300 mm^2) or 256.5 mm^2.

$$T = C$$
$$A_s f_y = 0.85\ f'_c\ b\ a$$
$$(256.5\ \text{mm}^2)(450\ \text{MPa}) = 0.85\ (37.0\ \text{MPa})(350\ \text{mm})\ a$$
$$a = 10.5\ \text{mm}$$

$$M = T\ (d - a/2)$$
$$= (246\ \text{mm}^2)\ (450\ \text{MPa})(125\ \text{mm} - (10.5\ \text{mm})/2)$$
$$= 13.82\ \text{kN-m}$$

The shear properties of the section remain unchanged from the normal section and thus will not be a factor.

Bond Effects:

The bond strength will also possibly limit the design. The anchorage capacity of the bar will vary along the length of the slab, and is thus derived here as a function of the longitudinal position.

u= 4.71-0.250 (14.5) = 1.09 MPa (from previous work)

Thus, $F_s = upl(x) \leq f_y A_s$

The limit is already calculated as the section property. This is concerned with the first situation.

As before, C = T

$$0.85\, f'_c\, b\, a = F_s$$

$$a = \frac{F_s}{0.85 f'_c b} = \frac{upl(x)}{0.85 f'_c b}$$

$$\text{Now, } M_f = F_s(d - \frac{a}{2}) = upl(x)\left(d - \frac{upl(x)}{1.7 f'_c b}\right)$$

Thus, we can plot the failure envelope, realizing that l(x)=x if x is the distance from the support, which is also the location the bars start.

Moment Diagram:

Also required is the moment diagram as a function of x. There are two sections to this moment diagram, when x < 500 mm and when 500 mm<x<600 mm. If we note symmetry, then it is simple to determine by inspection that:

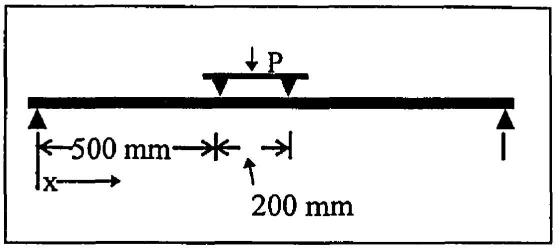

$$M(x) = P/2\ x; \quad x \le 500 \text{ mm}$$

$$= P/4\ ; \quad 500 \text{ mm} \le x \le 600 \text{ mm}.$$

This information was then plotted for different values of P until the two curves intersect. The lowest load at which this occurs is the failure load. Depending upon which mode governs at the point of intersection of the curves, the failure mode can be determined. For this situation, the intersection of the curves occurs when P = 28.5 kN. The location of intersection is in the region where bond strength.

Series 1
-
Control

Load (kN)	Moment (kN-m)	M.P. Displ. (mm)	E. Curv. LVDT (mm)	W. Curv. LVDT (mm)	Curv. LVDT Avg. (mm)	Curvature (1/km)
1.71	0.43	0.007	0.001	0.002	0.002	-0.30
2.79	0.70	0.033	0.001	0.002	0.000	-0.06
3.83	0.96	0.048	0.001	0.002	0.002	-0.37
4.92	1.23	0.069	0.001	0.002	0.001	-0.18
6.04	1.51	0.083	0.000	0.001	-0.001	0.25
7.11	1.78	0.103	-0.000	0.001	0.001	-0.21
8.18	2.05	0.122	-0.001	0.001	-0.000	0.03
9.19	2.30	0.139	-0.000	-0.001	0.001	-0.15
10.29	2.57	0.159	-0.001	0.000	-0.001	0.18
11.32	2.83	0.177	-0.002	0.001	-0.001	0.26
12.37	3.09	0.197	-0.002	-0.001	-0.002	0.35
13.45	3.36	0.219	-0.003	-0.001	-0.002	0.39
14.45	3.61	0.254	-0.003	-0.001	-0.002	0.48
15.53	3.88	0.253	-0.003	-0.002	-0.001	0.29
16.61	4.15	0.279	-0.003	-0.001	-0.003	0.61
17.62	4.41	0.294	-0.004	-0.002	-0.004	0.73
18.67	4.67	0.318	-0.004	-0.002	-0.004	0.76
20.75	5.19	0.358	-0.006	-0.004	-0.005	0.94
21.86	5.46	0.383	-0.006	-0.003	-0.004	0.81
22.90	5.72	0.409	-0.007	-0.005	-0.006	1.23
23.89	5.97	0.433	-0.008	-0.006	-0.006	1.16
24.98	6.24	0.567	-0.018	-0.018	-0.017	3.41
25.89	6.47	0.627	-0.020	-0.023	-0.022	4.40
26.87	6.72	0.688	-0.023	-0.027	-0.025	4.98
27.97	6.99	0.776	-0.025	-0.030	-0.027	5.41
29.06	7.27	0.957	-0.030	-0.032	-0.032	6.30
30.13	7.53	1.015	-0.033	-0.034	-0.034	6.79
31.14	7.79	1.089	-0.037	-0.036	-0.034	6.84
32.24	8.06	1.164	-0.040	-0.039	-0.039	7.85
33.28	8.32	1.232	-0.043	-0.041	-0.042	8.35
34.35	8.59	1.299	-0.046	-0.044	-0.045	9.06
35.39	8.85	1.474	-0.050	-0.047	-0.048	9.60
36.38	9.09	1.516	-0.052	-0.048	-0.051	10.15
37.47	9.37	1.590	-0.055	-0.051	-0.052	10.36
38.51	9.63	1.668	-0.058	-0.053	-0.056	11.21
39.52	9.88	1.770	-0.062	-0.056	-0.059	11.80
40.57	10.14	1.856	-0.065	-0.058	-0.062	12.35
41.66	10.41	1.951	-0.068	-0.060	-0.063	12.55
42.70	10.68	2.037	-0.072	-0.063	-0.067	13.49
43.80	10.95	2.117	-0.075	-0.065	-0.070	14.09
44.81	11.20	2.198	-0.079	-0.069	-0.073	14.65
45.82	11.46	2.283	-0.082	-0.070	-0.077	15.31
46.41	11.60	2.408	-0.089	-0.073	-0.080	15.94
47.42	11.86	2.445	-0.089	-0.074	-0.081	16.29

48.47	12.12	2.503	-0.092	-0.076	-0.085	16.99
49.56	12.39	2.571	-0.095	-0.078	-0.087	17.32
50.63	12.66	2.644	-0.099	-0.080	-0.089	17.89
51.64	12.91	2.705	-0.101	-0.079	-0.092	18.44
52.66	13.16	2.795	-0.105	-0.085	-0.095	19.01
53.70	13.42	2.888	-0.109	-0.086	-0.096	19.11
54.71	13.68	2.979	-0.113	-0.088	-0.102	20.32
55.78	13.94	3.076	-0.117	-0.092	-0.103	20.59
56.77	14.19	3.171	-0.120	-0.093	-0.108	21.64
57.86	14.46	3.297	-0.127	-0.096	-0.111	22.24
58.90	14.73	3.414	-0.131	-0.098	-0.115	22.93
59.91	14.98	3.524	-0.137	-0.101	-0.119	23.79
60.93	15.23	3.623	-0.142	-0.102	-0.122	24.35
61.92	15.48	3.740	-0.146	-0.106	-0.127	25.37
62.93	15.73	3.858	-0.154	-0.109	-0.131	26.24
63.92	15.98	4.004	-0.162	-0.114	-0.136	27.11
65.01	16.25	4.138	-0.169	-0.117	-0.143	28.62
66.03	16.51	4.342	-0.182	-0.123	-0.152	30.44
67.01	16.75	4.555	-0.195	-0.132	-0.164	32.80
68.03	17.01	4.923	-0.221	-0.146	-0.184	36.73
68.77	17.19	5.323	-0.248	-0.157	-0.204	40.78
69.42	17.35	5.725	-0.273	-0.167	-0.221	44.24
70.03	17.51	6.125	-0.298	-0.183	-0.241	48.16
70.64	17.66	6.512	-0.326	-0.198	-0.261	52.20
71.20	17.80	6.913	-0.353	-0.210	-0.284	56.76
71.92	17.98	7.303	-0.380	-0.229	-0.307	61.36
72.51	18.13	7.702	-0.413	-0.245	-0.328	65.55
73.02	18.25	8.100	-0.443	-0.262	-0.353	70.54
73.66	18.41	8.500	-0.474	-0.281	-0.377	75.42
74.25	18.56	8.900	-0.504	-0.299	-0.401	80.16
74.73	18.68	9.280	-0.538	-0.317	-0.426	85.11
75.21	18.80	9.680	-0.568	-0.335	-0.453	90.61
75.87	18.97	10.080	-0.603	-0.356	-0.480	96.01
76.22	19.06	10.600	-0.659	-0.388	-0.521	104.25
75.21	18.80	10.880	-0.698	-0.415	-0.556	111.25
76.09	19.02	11.280	-0.718	-0.453	-0.588	117.50
76.57	19.14	11.680	-0.750	-0.484	-0.617	123.37
77.05	19.26	12.080	-0.788	-0.513	-0.651	130.13
77.40	19.35	12.480	-0.823	-0.545	-0.684	136.75
77.72	19.43	12.870	-0.864	-0.578	-0.723	144.50
78.04	19.51	13.270	-0.907	-0.611	-0.760	152.00
78.60	19.65	13.680	-0.945	-0.640	-0.793	158.50
78.81	19.70	14.080	-0.975	-0.665	-0.820	164.00
79.08	19.77	14.480	-1.003	-0.694	-0.848	169.50
79.18	19.80	14.870	-1.035	-0.713	-0.875	175.00
79.16	19.79	15.260	-1.067	-0.734	-0.902	180.37

79.40	19.85	15.680	-1.098	-0.753	-0.928	185.50
79.53	19.88	16.080	-1.130	-0.773	-0.952	190.37
79.66	19.92	16.500	-1.170	-0.793	-0.983	196.62
80.33	20.08	17.120	-1.225	-0.822	-1.023	204.50
79.96	19.99	17.520	-1.258	-0.840	-1.050	210.00
80.04	20.01	17.920	-1.288	-0.858	-1.073	214.63
80.25	20.06	18.330	-1.314	-0.879	-1.096	219.13
80.38	20.10	18.720	-1.336	-0.898	-1.118	223.50
80.36	20.09	19.120	-1.347	-0.915	-1.133	226.50
80.36	20.09	19.520	-1.362	-0.932	-1.148	229.50
80.38	20.10	19.920	-1.373	-0.943	-1.158	231.50
80.28	20.07	20.320	-1.383	-0.953	-1.170	234.00
80.49	20.12	20.750	-1.395	-0.965	-1.181	236.12
80.54	20.14	21.160	-1.413	-0.975	-1.195	239.00
80.65	20.16	21.600	-1.427	-0.984	-1.206	241.12
80.68	20.17	21.990	-1.439	-0.993	-1.217	243.37
80.70	20.18	22.390	-1.448	-1.000	-1.225	245.00
79.58	19.90	22.640	-1.450	-0.998	-1.226	245.12
79.16	19.79	23.050	-1.450	-0.998	-1.225	245.00
79.26	19.82	23.460	-1.451	-0.998	-1.225	245.00
79.56	19.89	23.880	-1.455	-0.998	-1.227	245.37
79.45	19.86	24.280	-1.461	-0.995	-1.230	246.00
79.50	19.88	24.680	-1.466	-0.993	-1.230	246.00
79.69	19.92	25.070	-1.471	-0.989	-1.233	246.50
79.77	19.94	25.260	-1.475	-0.990	-1.233	246.50
80.14	20.04	25.650	-1.483	-0.989	-1.236	247.25
80.30	20.08	26.060	-1.490	-0.990	-1.242	248.37
80.25	20.06	26.460	-1.499	-0.990	-1.246	249.25
80.33	20.08	26.870	-1.508	-0.992	-1.250	250.00
80.49	20.12	27.240	-1.517	-0.995	-1.258	251.50
80.38	20.10	27.640	-1.524	-0.995	-1.259	251.87
80.46	20.12	28.050	-1.533	-0.998	-1.267	253.37
80.54	20.14	28.440	-1.540	-1.000	-1.269	253.75
80.33	20.08	28.860	-1.545	-1.000	-1.274	254.87
80.70	20.18	29.260	-1.555	-1.003	-1.279	255.87
80.97	20.24	29.650	-1.564	-1.008	-1.287	257.37
81.16	20.29	29.920	-1.571	-1.012	-1.292	258.38
81.18	20.30	30.040	-1.573	-1.013	-1.294	258.88
81.21	20.30	30.380	-1.587	-1.020	-1.303	260.50
82.28	20.57	30.640	-1.592	-1.023	-1.308	261.50
81.16	20.29	30.910	-1.601	-1.027	-1.314	262.88
80.12	20.03	30.940	-1.598	-1.025	-1.313	262.50
79.02	19.76	30.960	-1.596	-1.023	-1.309	261.87
77.98	19.50	30.930	-1.594	-1.020	-1.308	261.50
76.89	19.22	30.850	-1.590	-1.018	-1.306	261.13
75.71	18.93	30.720	-1.582	-1.013	-1.298	259.50

74.38	18.59	30.670	-1.581	-1.010	-1.296	259.13
73.31	18.33	30.600	-1.578	-1.008	-1.293	258.50
72.19	18.05	30.560	-1.575	-1.006	-1.291	258.25
71.10	17.77	30.520	-1.571	-1.003	-1.288	257.62
69.98	17.49	30.440	-1.568	-1.001	-1.285	257.00
68.96	17.24	30.400	-1.566	-0.999	-1.283	256.50
67.84	16.96	30.320	-1.562	-0.998	-1.280	256.00
66.80	16.70	30.280	-1.559	-0.995	-1.278	255.50
65.73	16.43	30.240	-1.557	-0.993	-1.276	255.12
64.67	16.17	30.150	-1.553	-0.990	-1.272	254.38
63.54	15.89	30.120	-1.548	-0.988	-1.270	254.00
62.50	15.63	30.040	-1.546	-0.985	-1.268	253.50
61.49	15.37	30.000	-1.543	-0.983	-1.264	252.75
60.48	15.12	29.920	-1.538	-0.980	-1.259	251.87
58.85	14.71	29.140	-1.488	-0.959	-1.224	244.75
53.96	13.49	28.960	-1.489	-0.966	-1.228	245.50
50.87	12.72	28.960	-1.486	-0.965	-1.227	245.37
48.92	12.23	28.960	-1.487	-0.968	-1.226	245.25
47.74	11.94	28.960	-1.488	-0.965	-1.226	245.12
46.60	11.65	28.960	-1.485	-0.965	-1.226	245.12
45.21	11.30	28.680	-1.481	-0.953	-1.217	243.37
42.91	10.73	28.290	-1.458	-0.935	-1.196	239.12
39.47	9.87	27.900	-1.424	-0.925	-1.173	234.62
34.67	8.67	27.300	-1.388	-0.901	-1.146	229.25
28.77	7.19	26.680	-1.353	-0.889	-1.118	223.50
23.06	5.76	26.090	-1.320	-0.875	-1.096	219.13
17.80	4.45	25.540	-1.298	-0.864	-1.079	215.75
12.89	3.22	24.920	-1.279	-0.853	-1.064	212.88
8.92	2.23	24.520	-1.274	-0.845	-1.059	211.87
6.10	1.52	24.440	-1.275	-0.841	-1.058	211.62
4.43	1.11	24.370	-1.273	-0.840	-1.057	211.37
3.13	0.78	24.300	-1.273	-0.840	-1.056	211.25
1.90	0.48	24.150	-1.270	-0.837	-1.054	210.75
0.75	0.19	23.860	-1.266	-0.833	-1.051	210.12
-0.26	-0.07	23.480	-1.263	-0.821	-1.043	208.50
-0.38	-0.10	23.360	-1.257	-0.820	-1.040	208.00

Series 1 Quarter Debonded

Load (kN)	Moment (kN-m)	M.P. Displ. (mm)	E. Curv. LVDT (mm)	W. Curv. LVDT (mm)	Curv. LVDT Avg. (mm)	Curvature (1/km)
0.13	0.03	0.000	-0.002	0.005	0.002	-0.46
1.23	0.31	0.070	-0.004	0.004	0.001	-0.11
2.46	0.62	0.110	-0.004	0.001	-0.001	0.29
3.65	0.91	0.110	-0.003	0.003	-0.000	0.03
4.76	1.19	0.150	-0.003	0.003	-0.000	0.03

5.94	1.48	0.160	-0.005	0.003	-0.001	0.16
6.97	1.74	0.190	-0.002	0.002	-0.001	0.24
8.05	2.01	0.220	-0.006	-0.001	-0.002	0.30
9.08	2.27	0.240	-0.005	0.002	0.000	-0.01
10.24	2.56	0.270	-0.005	0.001	-0.003	0.50
11.39	2.85	0.290	-0.007	0.001	-0.003	0.60
12.42	3.10	0.320	-0.007	0.000	-0.004	0.73
13.53	3.38	0.350	-0.008	0.002	-0.004	0.89
14.58	3.65	0.390	-0.008	-0.001	-0.005	0.94
15.67	3.92	0.420	-0.009	-0.002	-0.006	1.11
16.76	4.19	0.430	-0.011	-0.003	-0.006	1.24
17.87	4.47	0.470	-0.012	-0.005	-0.007	1.39
18.89	4.72	0.510	-0.009	-0.006	-0.008	1.65
19.90	4.97	0.550	-0.014	-0.009	-0.010	2.03
21.01	5.25	0.630	-0.017	-0.010	-0.013	2.59
22.10	5.52	0.690	-0.023	-0.012	-0.016	3.23
23.19	5.80	0.870	-0.025	-0.029	-0.027	5.44
24.23	6.06	0.960	-0.028	-0.037	-0.031	6.29
25.27	6.32	1.040	-0.031	-0.043	-0.037	7.32
26.31	6.58	1.110	-0.032	-0.048	-0.040	7.92
27.46	6.87	1.190	-0.035	-0.052	-0.043	8.64
28.50	7.13	1.290	-0.036	-0.057	-0.047	9.33
29.60	7.40	1.360	-0.038	-0.062	-0.050	9.99
30.77	7.69	1.450	-0.042	-0.066	-0.054	10.72
31.95	7.99	1.550	-0.045	-0.070	-0.057	11.43
33.04	8.26	1.630	-0.046	-0.072	-0.061	12.24
34.13	8.53	1.710	-0.052	-0.077	-0.067	13.33
35.12	8.78	1.800	-0.057	-0.081	-0.069	13.79
36.22	9.05	1.910	-0.059	-0.083	-0.072	14.49
37.20	9.30	1.990	-0.063	-0.088	-0.076	15.16
38.22	9.55	2.070	-0.066	-0.091	-0.079	15.72
39.28	9.82	2.160	-0.070	-0.096	-0.082	16.30
40.35	10.09	2.270	-0.073	-0.099	-0.085	17.06
41.50	10.37	2.370	-0.075	-0.104	-0.090	17.94
42.57	10.64	2.500	-0.081	-0.110	-0.095	19.00
43.69	10.92	2.590	-0.081	-0.115	-0.099	19.78
44.73	11.18	2.680	-0.086	-0.121	-0.103	20.65
45.82	11.46	2.830	-0.089	-0.123	-0.107	21.36
46.81	11.70	2.980	-0.094	-0.128	-0.111	22.25
47.90	11.98	3.100	-0.097	-0.133	-0.114	22.84
48.97	12.24	3.190	-0.101	-0.137	-0.120	23.99
49.99	12.50	3.310	-0.106	-0.141	-0.124	24.70
51.03	12.76	3.430	-0.107	-0.145	-0.127	25.47
52.20	13.05	3.550	-0.113	-0.149	-0.131	26.29
53.24	13.31	3.670	-0.117	-0.152	-0.135	26.91
54.28	13.57	3.780	-0.120	-0.156	-0.139	27.85

55.38	13.84	3.910	-0.128	-0.163	-0.143	28.62
56.37	14.09	4.020	-0.131	-0.163	-0.147	29.39
57.46	14.36	4.150	-0.135	-0.166	-0.151	30.23
58.53	14.63	4.270	-0.140	-0.170	-0.155	31.08
59.73	14.93	4.420	-0.146	-0.174	-0.160	32.05
60.90	15.23	4.590	-0.153	-0.178	-0.166	33.12
61.89	15.47	4.750	-0.161	-0.183	-0.172	34.49
62.96	15.74	4.950	-0.168	-0.192	-0.180	36.09
64.08	16.02	5.180	-0.180	-0.204	-0.192	38.40
65.09	16.27	5.460	-0.193	-0.217	-0.206	41.10
65.76	16.44	5.860	-0.213	-0.239	-0.225	45.01
66.75	16.69	6.110	-0.223	-0.251	-0.237	47.41
67.81	16.95	6.480	-0.243	-0.263	-0.253	50.58
68.69	17.17	6.870	-0.270	-0.279	-0.275	55.09
69.60	17.40	7.270	-0.296	-0.293	-0.296	59.14
70.51	17.63	7.700	-0.320	-0.274	-0.297	59.49
70.16	17.54	8.100	-0.332	-0.284	-0.308	61.68
69.10	17.27	8.130	-0.330	-0.282	-0.306	61.27
67.84	16.96	8.190	-0.328	-0.282	-0.305	61.08
66.59	16.65	8.250	-0.327	-0.282	-0.305	61.08
65.57	16.39	8.310	-0.324	-0.283	-0.304	60.76
64.48	16.12	8.390	-0.322	-0.284	-0.304	60.70
63.30	15.83	8.530	-0.320	-0.283	-0.302	60.36
62.21	15.55	8.670	-0.317	-0.285	-0.302	60.39
61.70	15.43	9.070	-0.319	-0.292	-0.305	60.98
62.10	15.53	9.500	-0.316	-0.303	-0.311	62.14
61.97	15.49	9.910	-0.312	-0.313	-0.314	62.74
60.77	15.19	10.030	-0.297	-0.327	-0.313	62.58
59.30	14.83	10.060	-0.294	-0.337	-0.316	63.16
58.18	14.54	10.110	-0.295	-0.342	-0.318	63.52
57.09	14.27	10.190	-0.292	-0.355	-0.323	64.51
56.77	14.19	10.630	-0.267	-0.351	-0.310	61.94
56.63	14.16	11.030	-0.233	-0.399	-0.317	63.35
55.35	13.84	11.310	-0.225	-0.402	-0.313	62.61
52.55	13.14	11.630	-0.216	-0.401	-0.309	61.76
49.88	12.47	11.690	-0.214	-0.395	-0.304	60.89
47.96	11.99	11.750	-0.213	-0.395	-0.305	60.96
46.73	11.68	11.750	-0.212	-0.396	-0.305	60.91
45.50	11.38	11.810	-0.211	-0.396	-0.304	60.79
45.56	11.39	12.210	-0.201	-0.397	-0.299	59.84
46.28	11.57	12.620	-0.182	-0.399	-0.291	58.26
45.24	11.31	12.710	-0.169	-0.399	-0.284	56.87
-0.11	-0.03	7.990	-0.078	-0.298	-0.188	37.58

Series 1 - Half

Load (kN)	Moment (kN-m)	M.P. Displ. (mm)	E. Curv. LVDT (mm)	W. Curv. LVDT (mm)	Curv. LVDT Avg. (mm)	Curvature (1/km)
0.04	0.01	0.000	-0.003	-0.000	0.000	0.00
1.14	0.28	0.030	-0.001	0.001	-0.000	0.05
2.23	0.56	0.050	-0.002	-0.000	-0.001	0.12
3.33	0.83	0.080	-0.003	-0.002	-0.002	0.30
4.33	1.08	0.110	-0.003	-0.003	-0.003	0.51
5.42	1.36	0.120	-0.004	-0.003	-0.003	0.59
6.43	1.61	0.140	-0.001	-0.003	-0.003	0.66
7.45	1.86	0.160	-0.006	-0.003	-0.007	1.31
8.48	2.12	0.200	-0.006	-0.003	-0.007	1.31
9.47	2.37	0.240	-0.008	-0.004	-0.005	0.91
10.43	2.61	0.240	-0.006	-0.005	-0.005	1.07
11.45	2.86	0.280	-0.007	-0.007	-0.006	1.14
15.71	3.93	0.410	-0.012	-0.010	-0.014	2.88
16.77	4.19	0.480	-0.015	-0.008	-0.012	2.36
17.84	4.46	0.520	-0.016	-0.007	-0.018	3.51
18.87	4.72	0.600	-0.017	-0.013	-0.014	2.70
19.93	4.98	0.660	-0.020	-0.011	-0.017	3.45
20.96	5.24	0.720	-0.022	-0.010	-0.016	3.16
22.04	5.51	0.810	-0.022	-0.009	-0.016	3.29
20.92	5.23	1.000	-0.024	-0.006	-0.017	3.41
19.81	4.95	1.030	-0.025	-0.005	-0.016	3.16
18.70	4.68	1.080	-0.022	-0.005	-0.012	2.37
17.57	4.39	1.140	-0.022	-0.004	-0.013	2.53
16.31	4.08	1.160	-0.022	-0.004	-0.013	2.55
15.01	3.75	1.200	-0.019	-0.002	-0.011	2.16
13.85	3.46	1.200	-0.017	-0.003	-0.015	3.02
12.65	3.16	1.210	-0.019	-0.003	-0.012	2.40
11.57	2.89	1.240	-0.018	-0.002	-0.015	2.94
10.39	2.60	1.280	-0.016	-0.003	-0.014	2.73
9.35	2.34	1.520	-0.016	-0.002	-0.009	1.86
8.24	2.06	1.920	-0.015	-0.001	-0.012	2.30
7.11	1.78	2.390	-0.015	-0.000	-0.008	1.54
6.32	1.58	2.810	-0.014	-0.000	-0.008	1.51
5.50	1.37	3.270	-0.018	-0.000	-0.013	2.59
4.89	1.22	3.690	-0.017	-0.000	-0.010	2.00
4.41	1.10	4.120	-0.014	-0.008	-0.012	2.48
3.61	0.90	4.600	-0.024	-0.007	-0.018	3.55
3.55	0.89	5.060	-0.024	-0.007	-0.015	3.06
3.29	0.82	5.520	-0.023	-0.008	-0.016	3.10
3.07	0.77	5.940	-0.025	-0.007	-0.014	2.88
2.84	0.71	6.390	-0.022	-0.012	-0.020	3.99
2.87	0.72	6.850	-0.018	-0.012	-0.016	3.11
2.83	0.71	7.320	-0.017	-0.012	-0.016	3.14

Series 2- Normal Mix, Control

Load (kN)	Moment (kN-m)	M.P. Displ. (mm)	E. Curv. LVDT (mm)	W. Curv. LVDT (mm)	Curv. LVDT Avg. (mm)	Curvature (1/km)
-0.14	-0.04	0.00	0.009	0.008	0.004	-0.89
1.30	0.32	0.12	0.007	0.002	0.001	-0.28
3.04	0.76	0.17	0.006	0.001	0.003	-0.51
5.30	1.32	0.23	0.005	0.002	0.001	-0.20
8.41	2.10	0.31	0.003	0.000	0.002	-0.31
11.79	2.95	0.36	0.002	-0.001	0.000	-0.04
14.20	3.55	0.37	0.001	-0.002	-0.007	1.31
15.43	3.86	0.35	0.001	-0.001	-0.005	0.90
16.69	4.17	0.38	-0.002	-0.002	-0.001	0.29
15.61	3.90	0.42	-0.005	-0.007	-0.006	1.25
14.30	3.57	0.45	-0.001	-0.010	-0.009	1.77
12.92	3.23	0.47	-0.001	-0.017	-0.009	1.79
11.53	2.88	0.50	-0.001	-0.013	-0.012	2.48
10.22	2.55	0.52	-0.001	-0.014	-0.008	1.52
9.07	2.27	0.53	-0.000	-0.015	-0.008	1.61
7.95	1.99	0.53	0.000	-0.016	-0.015	3.05
6.96	1.74	0.53	0.000	-0.015	-0.008	1.52
8.11	2.03	0.92	0.001	-0.041	-0.027	5.37
9.32	2.33	1.13	0.002	-0.058	-0.028	5.66
10.76	2.69	1.32	0.005	-0.074	-0.035	7.04
12.25	3.06	1.49	0.008	-0.087	-0.040	7.92
13.53	3.38	1.55	0.010	-0.094	-0.047	9.36
14.74	3.68	1.56	0.010	-0.094	-0.047	9.43
15.82	3.95	1.57	0.011	-0.092	-0.045	8.97
16.93	4.23	1.67	0.011	-0.104	-0.046	9.18
17.89	4.47	1.77	0.015	-0.115	-0.054	10.70
18.95	4.74	1.86	0.018	-0.123	-0.052	10.43
20.07	5.02	1.99	0.022	-0.134	-0.056	11.21
21.17	5.29	2.09	0.024	-0.144	-0.066	13.29
22.28	5.57	2.20	0.027	-0.155	-0.064	12.79
23.35	5.84	2.31	0.029	-0.166	-0.072	14.45
24.47	6.12	2.41	0.031	-0.177	-0.074	14.76
25.57	6.39	2.50	0.032	-0.187	-0.080	15.95
26.63	6.66	2.61	0.037	-0.199	-0.089	17.70
27.70	6.93	2.71	0.036	-0.212	-0.093	18.50
28.74	7.19	2.80	0.037	-0.221	-0.092	18.44
29.78	7.45	2.89	0.040	-0.233	-0.097	19.39
30.80	7.70	3.00	0.042	-0.247	-0.103	20.62
31.89	7.97	3.09	0.047	-0.260	-0.109	21.75
32.93	8.23	3.18	0.045	-0.275	-0.118	23.61
33.97	8.49	3.29	0.045	-0.284	-0.123	24.65
34.93	8.73	3.39	0.045	-0.299	-0.130	25.94
35.95	8.99	3.48	0.045	-0.313	-0.139	27.73
36.99	9.25	3.57	0.042	-0.320	-0.145	29.05
37.98	9.49	3.64	0.039	-0.334	-0.150	29.98
39.02	9.75	3.74	0.033	-0.350	-0.162	32.40

40.01	10.00	3.85	0.029	-0.360	-0.171	34.20
41.15	10.29	3.98	0.020	-0.376	-0.185	36.95
42.11	10.53	4.13	0.013	-0.390	-0.188	37.67
43.26	10.82	4.28	0.013	-0.411	-0.200	40.02
44.36	11.09	4.45	0.016	-0.431	-0.213	42.53
45.34	11.34	4.61	0.023	-0.454	-0.216	43.10
46.28	11.57	4.77	0.033	-0.473	-0.226	45.10
47.29	11.82	4.93	0.033	-0.493	-0.230	45.94
48.31	12.08	5.01	0.029	-0.500	-0.238	47.58
49.35	12.34	5.13	0.018	-0.513	-0.246	49.15
50.41	12.60	5.25	0.009	-0.528	-0.262	52.48
51.40	12.85	5.41	0.000	-0.539	-0.275	54.95
52.52	13.13	5.57	-0.010	-0.558	-0.285	57.01
53.64	13.41	5.77	-0.020	-0.579	-0.304	60.85
54.66	13.66	5.96	-0.031	-0.598	-0.319	63.89
55.70	13.92	6.17	-0.041	-0.620	-0.334	66.83
56.77	14.19	6.38	-0.054	-0.644	-0.352	70.43
57.81	14.45	6.69	-0.072	-0.680	-0.380	75.98
58.90	14.73	6.98	-0.096	-0.714	-0.410	82.09
59.97	14.99	7.41	-0.132	-0.756	-0.450	89.95
60.66	15.17	7.85	-0.175	-0.806	-0.495	99.03
60.98	15.25	8.29	-0.223	-0.852	-0.538	107.50
61.28	15.32	8.73	-0.243	-0.899	-0.574	114.87
61.68	15.42	9.16	-0.290	-0.939	-0.617	123.37
61.81	15.45	9.58	-0.333	-0.980	-0.658	131.50
61.97	15.49	10.01	-0.368	-1.015	-0.693	138.50
61.52	15.38	10.45	-0.397	-1.036	-0.717	143.38
60.82	15.21	10.89	-0.430	-1.055	-0.743	148.63
60.39	15.10	11.30	-0.464	-1.095	-0.781	156.25
60.21	15.05	11.73	-0.505	-1.125	-0.817	163.37
60.10	15.03	12.15	-0.534	-1.154	-0.848	169.62
60.05	15.01	12.59	-0.574	-1.191	-0.883	176.50
60.15	15.04	13.01	-0.611	-1.228	-0.921	184.12
60.18	15.05	13.45	-0.650	-1.263	-0.958	191.50
60.34	15.09	13.89	-0.677	-1.309	-0.987	197.37
60.37	15.09	14.29	-0.712	-1.353	-1.033	206.50
60.45	15.11	14.73	-0.746	-1.396	-1.075	215.00
60.61	15.15	15.13	-0.787	-1.439	-1.113	222.62
60.69	15.17	15.56	-0.822	-1.480	-1.153	230.50
60.77	15.19	15.97	-0.875	-1.503	-1.191	238.25
60.69	15.17	16.41	-0.933	-1.518	-1.228	245.50
60.72	15.18	16.86	-0.980	-1.530	-1.258	251.50
61.01	15.25	17.30	-1.023	-1.525	-1.276	255.25
61.17	15.29	17.73	-1.060	-1.512	-1.289	257.75
61.41	15.35	18.17	-1.083	-1.522	-1.306	261.13
61.46	15.37	18.61	-1.118	-1.535	-1.328	265.50
61.46	15.37	19.07	-1.151	-1.548	-1.351	270.12
61.52	15.38	19.50	-1.178	-1.561	-1.373	274.50
61.60	15.40	19.97	-1.210	-1.575	-1.394	278.87
61.70	15.43	20.41	-1.240	-1.588	-1.415	283.00

61.78	15.45	20.85	-1.268	-1.598	-1.435	287.00
61.89	15.47	21.29	-1.297	-1.610	-1.453	290.62
62.00	15.50	21.76	-1.328	-1.623	-1.477	295.37
62.08	15.52	22.17	-1.358	-1.633	-1.497	299.37
62.08	15.52	22.62	-1.390	-1.644	-1.519	303.75
62.02	15.51	23.08	-1.414	-1.653	-1.535	307.00
62.18	15.55	23.49	-1.445	-1.661	-1.555	311.00
62.29	15.57	23.93	-1.478	-1.670	-1.576	315.13
62.26	15.57	24.37	-1.510	-1.681	-1.598	319.50
62.40	15.60	24.81	-1.542	-1.690	-1.618	323.50
62.48	15.62	25.21	-1.575	-1.700	-1.640	328.00
62.42	15.61	25.62	-1.605	-1.710	-1.660	332.00
62.64	15.66	26.07	-1.639	-1.720	-1.683	336.50
62.53	15.63	26.49	-1.672	-1.730	-1.704	340.75
62.61	15.65	26.89	-1.705	-1.739	-1.725	345.00
62.58	15.65	27.29	-1.746	-1.748	-1.749	349.75
62.56	15.64	27.74	-1.780	-1.758	-1.769	353.87
62.56	15.64	28.19	-1.815	-1.768	-1.793	358.50
62.53	15.63	28.62	-1.848	-1.778	-1.815	363.00
62.56	15.64	29.05	-1.880	-1.791	-1.836	367.25
62.61	15.65	29.48	-1.913	-1.805	-1.863	372.50
62.53	15.63	29.93	-1.945	-1.819	-1.883	376.62
62.58	15.65	30.33	-1.981	-1.833	-1.908	381.50
62.50	15.63	30.77	-2.011	-1.845	-1.930	386.00
62.61	15.65	31.21	-2.043	-1.860	-1.953	390.62
62.42	15.61	31.61	-2.071	-1.874	-1.975	395.00
62.45	15.61	32.05	-2.103	-1.890	-1.999	399.87
62.02	15.51	36.98	-2.428	-2.075	-2.254	450.87
62.05	15.51	37.43	-2.458	-2.094	-2.278	455.63
62.08	15.52	37.87	-2.490	-2.113	-2.304	460.87
62.05	15.51	38.32	-2.522	-2.133	-2.330	466.00
62.00	15.50	38.76	-2.555	-2.150	-2.355	471.00
62.05	15.51	39.21	-2.588	-2.169	-2.385	477.00
61.92	15.48	39.66	-2.631	-2.190	-2.413	482.50
61.94	15.49	40.11	-2.665	-2.213	-2.441	488.12
61.97	15.49	40.57	-2.701	-2.234	-2.470	494.00
61.92	15.48	41.02	-2.747	-2.258	-2.509	501.87
60.82	15.21	41.47	-2.959	-2.242	-2.605	521.00
60.13	15.03	41.90	-3.074	-2.228	-2.654	530.87
59.91	14.98	42.36	-3.181	-2.206	-2.698	539.50
59.81	14.95	42.81	-3.196	-2.211	-2.706	541.12
59.83	14.96	43.24	-3.200	-2.228	-2.716	543.25
59.89	14.97	43.70	-3.200	-2.255	-2.730	546.00
59.81	14.95	44.14	-3.203	-2.284	-2.746	549.25
59.46	14.87	44.57	-3.201	-2.330	-2.768	553.62
58.71	14.68	45.02	-3.200	-2.370	-2.788	557.50
57.62	14.40	45.10	-3.201	-2.378	-2.793	558.50
56.47	14.12	45.11	-3.201	-2.380	-2.793	558.62
55.24	13.81	44.97	-3.201	-2.375	-2.790	558.00

54.15	13.54	44.83	-3.201	-2.368	-2.786	557.25
52.98	13.24	44.71	-3.201	-2.361	-2.783	556.63
51.80	12.95	44.59	-3.202	-2.355	-2.781	556.13
50.60	12.65	44.46	-3.201	-2.348	-2.778	555.50
49.51	12.38	44.35	-3.201	-2.343	-2.775	555.00
48.39	12.10	44.25	-3.198	-2.336	-2.770	554.00
47.10	11.78	44.24	-3.201	-2.335	-2.770	554.00
47.16	11.79	43.11	-3.201	-2.273	-2.739	547.87
44.30	11.08	43.15	-3.201	-2.272	-2.739	547.75
42.57	10.64	43.14	-3.201	-2.272	-2.739	547.75
41.34	10.33	43.14	-3.202	-2.271	-2.739	547.87
40.27	10.07	43.14	-3.200	-2.272	-2.739	547.75
39.12	9.78	42.32	-3.201	-2.255	-2.730	546.00
35.92	8.98	40.93	-3.201	-2.195	-2.699	539.87
30.69	7.67	39.46	-3.201	-2.131	-2.667	533.38
25.35	6.34	38.09	-3.197	-2.074	-2.636	527.13
19.46	4.86	36.58	-3.113	-2.011	-2.554	510.75
14.01	3.50	35.09	-2.956	-1.950	-2.444	488.87
9.14	2.28	33.72	-2.815	-1.914	-2.365	473.00
5.61	1.40	33.55	-2.792	-1.918	-2.355	471.00
3.32	0.83	33.49	-2.782	-1.917	-2.351	470.12
2.00	0.50	33.44	-2.777	-1.915	-2.348	469.50
0.74	0.18	33.39	-2.771	-1.913	-2.344	468.87
-0.37	-0.09	33.21	-2.750	-1.905	-2.330	466.00

Series 2 - Normal Mix, 2 % Corrosion

Load (kN)	Moment (kN-m)	M.P. Displ. (mm)	E. Curv. LVDT (mm)	W. Curv. LVDT (mm)	Curv. LVDT Avg. (mm)	Curvature (1/km)
0.10	0.03	0.00	-0.001	0.002	0.000	-0.03
1.18	0.29	0.05	-0.001	0.002	0.000	-0.06
2.24	0.56	0.10	-0.002	0.002	0.000	-0.05
3.31	0.83	0.14	-0.003	0.001	0.001	-0.16
2.08	0.52	0.28	-0.009	-0.000	-0.006	1.12
0.98	0.24	0.28	-0.007	0.000	-0.004	0.84
2.11	0.53	0.31	-0.007	-0.001	-0.004	0.78
3.21	0.80	0.35	-0.007	-0.002	-0.004	0.89
4.28	1.07	0.38	-0.008	-0.002	-0.005	1.04
5.35	1.34	0.42	-0.008	-0.002	-0.005	1.04
6.43	1.61	0.43	-0.009	-0.002	-0.007	1.43
7.53	1.88	0.46	-0.009	-0.003	-0.006	1.20
8.61	2.15	0.49	-0.009	-0.004	-0.007	1.31
9.71	2.43	0.53	-0.010	-0.003	-0.007	1.36
10.80	2.70	0.55	-0.010	-0.004	-0.007	1.36
11.85	2.96	0.59	-0.010	-0.004	-0.007	1.48
12.94	3.24	0.63	-0.010	-0.005	-0.009	1.70
14.04	3.51	0.65	-0.010	-0.005	-0.009	1.75

15.17	3.79	0.70	-0.011	-0.005	-0.009	1.75
16.27	4.07	0.71	-0.011	-0.006	-0.009	1.73
17.36	4.34	0.75	-0.011	-0.006	-0.009	1.76
18.47	4.62	0.77	-0.012	-0.007	-0.010	1.99
19.56	4.89	0.80	-0.013	-0.007	-0.010	2.05
20.66	5.16	0.82	-0.014	-0.008	-0.011	2.18
21.75	5.44	0.88	-0.015	-0.009	-0.013	2.50
20.02	5.00	1.00	-0.030	-0.028	-0.031	6.14
15.80	3.95	1.05	-0.039	-0.039	-0.039	7.86
13.05	3.26	1.08	-0.044	-0.046	-0.045	9.01
11.31	2.83	1.12	-0.049	-0.052	-0.051	10.19
10.04	2.51	1.16	-0.054	-0.059	-0.056	11.24
8.90	2.23	1.21	-0.061	-0.068	-0.065	13.06
8.67	2.17	1.42	-0.082	-0.095	-0.089	17.75
9.57	2.39	1.61	-0.097	-0.119	-0.108	21.50
10.64	2.66	1.80	-0.117	-0.138	-0.128	25.61
11.74	2.93	1.97	-0.137	-0.156	-0.147	29.44
12.82	3.21	2.13	-0.151	-0.176	-0.164	32.84
13.92	3.48	2.30	-0.165	-0.194	-0.180	36.01
15.03	3.76	2.47	-0.181	-0.214	-0.198	39.59
16.10	4.03	2.63	-0.195	-0.233	-0.215	42.93
17.20	4.30	2.81	-0.209	-0.252	-0.231	46.18
18.30	4.57	2.97	-0.225	-0.268	-0.247	49.41
19.38	4.85	3.13	-0.238	-0.286	-0.263	52.58
23.25	5.81	3.76	-0.261	-0.344	-0.303	60.51
24.37	6.09	3.93	-0.267	-0.365	-0.316	63.21
25.46	6.37	4.13	-0.272	-0.365	-0.319	63.84
26.47	6.62	4.33	-0.278	-0.388	-0.333	66.58
27.54	6.89	4.52	-0.284	-0.407	-0.347	69.44
28.56	7.14	4.71	-0.291	-0.428	-0.360	72.06
29.49	7.37	4.89	-0.298	-0.449	-0.375	75.06
30.26	7.57	5.09	-0.307	-0.453	-0.381	76.10
31.22	7.81	5.29	-0.318	-0.474	-0.396	79.25
31.92	7.98	5.50	-0.326	-0.494	-0.411	82.19
32.64	8.16	5.70	-0.339	-0.518	-0.429	85.85
33.15	8.29	5.89	-0.353	-0.541	-0.447	89.44
33.49	8.37	6.11	-0.366	-0.563	-0.465	92.94
33.73	8.43	6.31	-0.383	-0.583	-0.484	96.84
34.03	8.51	6.52	-0.396	-0.607	-0.503	100.50
34.32	8.58	6.73	-0.411	-0.634	-0.523	104.50
34.48	8.62	6.93	-0.430	-0.656	-0.545	109.00
34.75	8.69	7.14	-0.453	-0.675	-0.565	113.00
34.96	8.74	7.35	-0.466	-0.698	-0.583	116.50
35.23	8.81	7.57	-0.481	-0.718	-0.601	120.25
35.50	8.87	7.77	-0.495	-0.734	-0.616	123.25
35.60	8.90	7.97	-0.513	-0.753	-0.632	126.37
35.76	8.94	8.17	-0.528	-0.773	-0.650	130.00
35.90	8.97	8.38	-0.477	-0.793	-0.635	127.00
36.00	9.00	8.58	-0.487	-0.811	-0.649	129.88

36.22	9.05	8.77	-0.500	-0.828	-0.665	133.00
36.32	9.08	8.97	-0.518	-0.848	-0.683	136.50
36.46	9.11	9.19	-0.535	-0.868	-0.703	140.50
36.62	9.15	9.40	-0.568	-0.890	-0.729	145.75
36.70	9.17	9.58	-0.598	-0.905	-0.753	150.50
36.83	9.21	9.80	-0.628	-0.932	-0.780	156.00
36.80	9.20	10.01	-0.655	-0.950	-0.803	160.50
36.75	9.19	10.21	-0.675	-0.968	-0.823	164.50
36.70	9.17	10.42	-0.700	-0.988	-0.846	169.12
36.64	9.16	10.63	-0.738	-1.013	-0.878	175.50
36.62	9.15	10.83	-0.750	-1.033	-0.894	178.75
36.54	9.13	11.05	-0.779	-1.055	-0.918	183.50
36.51	9.13	11.28	-0.805	-1.080	-0.943	188.62
36.35	9.09	11.48	-0.830	-1.108	-0.970	194.00
36.19	9.05	11.69	-0.850	-1.113	-0.983	196.50
35.66	8.91	11.90	-0.855	-1.178	-1.018	203.50
35.74	8.93	12.11	-0.876	-1.210	-1.045	209.00
35.66	8.91	12.31	-0.910	-1.236	-1.075	215.00
35.50	8.87	12.51	-0.938	-1.261	-1.102	220.37
35.12	8.78	12.73	-0.970	-1.283	-1.128	225.50
34.93	8.73	12.93	-1.000	-1.305	-1.153	230.62
34.27	8.57	13.15	-1.035	-1.336	-1.188	237.50
33.68	8.42	13.35	-1.065	-1.368	-1.218	243.50
33.44	8.36	13.57	-1.100	-1.400	-1.253	250.50
33.31	8.33	13.77	-1.119	-1.430	-1.275	255.00
33.12	8.28	13.97	-1.141	-1.451	-1.298	259.50
32.93	8.23	14.18	-1.165	-1.473	-1.320	264.00
32.67	8.17	14.37	-1.188	-1.493	-1.343	268.50
32.40	8.10	14.54	-1.220	-1.507	-1.365	273.00
32.35	8.09	14.75	-1.235	-1.515	-1.378	275.50
32.21	8.05	14.96	-1.265	-1.518	-1.393	278.50
32.13	8.03	15.18	-1.295	-1.502	-1.400	280.00
31.92	7.98	15.39	-1.328	-1.533	-1.431	286.25
31.84	7.96	15.59	-1.353	-1.553	-1.455	291.00
31.79	7.95	15.77	-1.368	-1.573	-1.472	294.38
31.65	7.91	15.98	-1.378	-1.598	-1.489	297.87
31.55	7.89	16.19	-1.393	-1.613	-1.504	300.87
31.55	7.89	16.44	-1.428	-1.635	-1.533	306.50
31.44	7.86	16.66	-1.463	-1.664	-1.565	313.00
31.33	7.83	16.88	-1.486	-1.688	-1.590	318.00
31.28	7.82	17.08	-1.515	-1.713	-1.618	323.50
31.17	7.79	17.30	-1.558	-1.741	-1.650	330.00
31.09	7.77	17.51	-1.593	-1.775	-1.686	337.25
31.04	7.76	17.72	-1.620	-1.792	-1.708	341.50
30.98	7.75	17.94	-1.643	-1.813	-1.729	345.88
30.88	7.72	18.16	-1.670	-1.845	-1.760	352.00
30.85	7.71	18.38	-1.704	-1.873	-1.790	358.00
30.80	7.70	18.57	-1.728	-1.888	-1.810	362.00
30.72	7.68	18.73	-1.761	-1.909	-1.838	367.50

30.69	7.67	18.94	-1.789	-1.930	-1.862	372.37
30.69	7.67	19.21	-1.820	-1.950	-1.888	377.50
30.61	7.65	19.48	-1.843	-1.981	-1.913	382.62
31.14	7.79	19.69	-1.876	-2.015	-1.948	389.50
31.12	7.78	19.91	-1.913	-2.023	-1.968	393.62
30.56	7.64	20.13	-1.923	-2.048	-1.986	397.25
30.42	7.61	20.34	-1.935	-2.070	-2.005	401.00
30.40	7.60	20.56	-1.951	-2.105	-2.030	406.00
30.37	7.59	20.76	-1.968	-2.138	-2.055	411.00
30.45	7.61	20.97	-1.993	-2.170	-2.084	416.87
30.32	7.58	21.17	-2.025	-2.208	-2.119	423.75
30.29	7.57	21.37	-2.045	-2.243	-2.148	429.50
30.21	7.55	21.57	-2.082	-2.288	-2.187	437.38
30.16	7.54	21.77	-2.111	-2.333	-2.225	445.00
30.10	7.53	21.98	-2.133	-2.360	-2.250	450.00
30.10	7.53	22.18	-2.163	-2.402	-2.283	456.62
30.05	7.51	22.39	-2.189	-2.446	-2.319	463.87
30.00	7.50	22.60	-2.208	-2.480	-2.348	469.50
30.00	7.50	22.81	-2.233	-2.514	-2.376	475.25
29.89	7.47	23.03	-2.262	-2.549	-2.408	481.50
29.73	7.43	23.27	-2.295	-2.578	-2.440	488.00
29.41	7.35	23.49	-2.328	-2.595	-2.463	492.50
29.04	7.26	23.71	-2.366	-2.635	-2.504	500.75
28.85	7.21	23.92	-2.397	-2.675	-2.538	507.50
28.77	7.19	24.13	-2.428	-2.713	-2.573	514.63
28.72	7.18	24.36	-2.458	-2.752	-2.607	521.38
28.69	7.17	24.58	-2.486	-2.788	-2.641	528.12
27.65	6.91	24.69	-2.493	-2.818	-2.656	531.25
26.58	6.65	24.48	-2.453	-2.793	-2.625	525.00
25.49	6.37	24.32	-2.433	-2.773	-2.605	521.00
24.39	6.10	24.15	-2.404	-2.750	-2.580	516.00
23.27	5.82	23.95	-2.378	-2.725	-2.554	510.87
22.20	5.55	23.76	-2.345	-2.702	-2.525	505.00
21.08	5.27	23.56	-2.317	-2.679	-2.500	500.00
19.05	4.76	23.49	-2.304	-2.670	-2.490	498.00
20.22	5.05	23.48	-2.304	-2.669	-2.489	497.75
19.95	4.99	22.20	-2.151	-2.502	-2.324	464.75
17.62	4.40	22.00	-2.128	-2.480	-2.306	461.25
16.47	4.12	22.00	-2.129	-2.479	-2.308	461.50
15.62	3.91	21.76	-2.096	-2.448	-2.270	454.00
14.97	3.74	21.50	-2.051	-2.410	-2.230	446.00
14.24	3.56	21.19	-2.023	-2.368	-2.194	438.75
13.47	3.37	20.87	-1.970	-2.325	-2.149	429.87
12.65	3.16	20.55	-1.925	-2.283	-2.103	420.50
11.82	2.96	20.21	-1.870	-2.234	-2.053	410.50
10.97	2.74	19.85	-1.819	-2.191	-2.004	400.75

10.13	2.53	19.51	-1.761	-2.148	-1.954	390.75
9.28	2.32	19.15	-1.721	-2.100	-1.910	382.00
8.48	2.12	18.79	-1.669	-2.058	-1.863	372.50
7.66	1.91	18.45	-1.624	-2.018	-1.822	364.37
6.85	1.71	18.09	-1.580	-1.978	-1.778	355.50
6.07	1.52	17.73	-1.536	-1.933	-1.734	346.75
5.29	1.32	17.36	-1.488	-1.894	-1.692	338.37
4.56	1.14	17.01	-1.445	-1.853	-1.649	329.75
3.80	0.95	16.65	-1.408	-1.811	-1.608	321.62
3.13	0.78	16.30	-1.359	-1.768	-1.563	312.63
2.41	0.60	15.91	-1.307	-1.728	-1.516	303.12
1.76	0.44	15.56	-1.263	-1.688	-1.475	295.00
1.20	0.30	15.22	-1.223	-1.658	-1.439	287.88
0.74	0.18	14.87	-1.172	-1.627	-1.398	279.63
0.33	0.08	14.57	-1.135	-1.600	-1.368	273.50
-0.05	-0.01	14.39	-1.123	-1.580	-1.353	270.50
-0.03	-0.01	14.33	-1.130	-1.578	-1.355	271.00

Series 2 - Normal Mix, 5 % Corrosion

Load (kN)	Moment (kN-m)	M.P. Displ. (mm)	E. Curv. LVDT (mm)	W. Curv. LVDT (mm)	Curv. LVDT Avg. (mm)	Curvature (1/km)
-0.03	-0.01	0.00	0.001	0.001	0.001	-0.15
0.96	0.24	0.02	0.001	0.003	0.001	-0.12
1.93	0.48	0.04	0.000	0.000	0.001	-0.10
2.25	0.56	0.07	0.002	0.002	-0.000	0.04
3.36	0.84	0.10	0.002	0.001	0.001	-0.21
4.38	1.09	0.11	0.002	0.001	0.001	-0.18
5.43	1.36	0.13	0.001	-0.001	-0.002	0.33
6.46	1.62	0.15	0.001	-0.004	-0.002	0.45
7.48	1.87	0.18	0.001	-0.001	-0.000	0.05
8.50	2.12	0.20	0.000	-0.001	-0.001	0.12
9.49	2.37	0.22	-0.000	-0.001	-0.001	0.19
10.49	2.62	0.24	-0.000	-0.002	-0.001	0.21
11.48	2.87	0.26	-0.001	-0.002	-0.002	0.33
12.48	3.12	0.28	-0.001	-0.002	-0.002	0.39
13.53	3.38	0.31	-0.001	-0.002	-0.002	0.45
14.55	3.64	0.33	-0.002	-0.006	-0.009	1.81
15.54	3.89	0.34	-0.003	-0.003	-0.003	0.61
16.59	4.15	0.37	-0.003	-0.008	-0.006	1.20
17.68	4.42	0.42	-0.003	-0.004	-0.004	0.73
18.71	4.68	0.45	-0.004	-0.005	-0.005	0.91
19.73	4.93	0.48	-0.004	-0.006	-0.007	1.37
20.76	5.19	0.53	-0.004	-0.008	-0.011	2.16
19.37	4.84	0.67	-0.005	-0.004	-0.007	1.37
18.00	4.50	0.67	-0.003	-0.003	-0.006	1.21
16.83	4.21	0.68	-0.003	-0.003	-0.007	1.30
15.72	3.93	0.70	-0.003	-0.006	-0.006	1.11

16.79	4.20	0.90	-0.003	-0.003	-0.003	0.69
17.84	4.46	0.97	-0.003	-0.003	-0.003	0.65
18.93	4.73	1.05	-0.003	-0.006	-0.006	1.27
19.99	5.00	1.13	-0.005	-0.004	-0.004	0.74
21.06	5.27	1.22	-0.004	-0.004	-0.004	0.80
22.12	5.53	1.30	-0.005	-0.008	-0.007	1.39
23.06	5.76	1.39	-0.005	-0.008	-0.008	1.64
21.91	5.48	1.36	-0.007	-0.010	-0.008	1.55
22.98	5.74	1.43	-0.005	-0.004	-0.005	0.91
24.13	6.03	1.51	-0.005	-0.008	-0.009	1.71
25.14	6.29	1.58	-0.008	-0.006	-0.005	1.04
26.15	6.54	1.67	-0.007	-0.009	-0.009	1.89
27.20	6.80	1.74	-0.008	-0.007	-0.006	1.11
28.24	7.06	1.82	-0.008	-0.007	-0.006	1.11
29.25	7.31	1.91	-0.008	-0.008	-0.007	1.32
30.32	7.58	1.99	-0.007	-0.008	-0.007	1.36
31.36	7.84	2.08	-0.007	-0.010	-0.011	2.14
32.37	8.09	2.17	-0.010	-0.009	-0.008	1.51
33.47	8.37	2.27	-0.008	-0.012	-0.014	2.81
34.48	8.62	2.38	-0.009	-0.015	-0.012	2.45
35.55	8.89	2.44	-0.009	-0.009	-0.008	1.69
36.56	9.14	2.55	-0.010	-0.014	-0.014	2.70
35.76	8.94	2.77	-0.046	-0.053	-0.053	10.50
33.28	8.32	2.77	-0.049	-0.056	-0.056	11.10
31.60	7.90	2.79	-0.054	-0.059	-0.057	11.33
30.26	7.57	2.82	-0.055	-0.057	-0.060	12.09
29.20	7.30	2.84	-0.060	-0.062	-0.061	12.16
28.69	7.17	3.04	-0.086	-0.093	-0.090	18.05
29.52	7.38	3.26	-0.107	-0.125	-0.117	23.30
30.42	7.61	3.47	-0.133	-0.161	-0.148	29.50
31.31	7.83	3.67	-0.162	-0.201	-0.180	36.09
32.27	8.07	3.88	-0.195	-0.233	-0.216	43.24
33.23	8.31	4.09	-0.224	-0.261	-0.243	48.58
34.24	8.56	4.29	-0.256	-0.294	-0.274	54.81
35.12	8.78	4.49	-0.283	-0.334	-0.310	62.08
36.03	9.01	4.70	-0.325	-0.363	-0.345	68.90
37.07	9.27	4.91	-0.364	-0.400	-0.384	76.83
37.95	9.49	5.11	-0.401	-0.434	-0.421	84.13
38.86	9.71	5.32	-0.440	-0.489	-0.464	92.89
39.71	9.93	5.53	-0.475	-0.521	-0.497	99.40
40.46	10.11	5.74	-0.511	-0.556	-0.534	106.88
41.31	10.33	5.95	-0.563	-0.593	-0.579	115.87
42.17	10.54	6.15	-0.603	-0.632	-0.619	123.87
42.89	10.72	6.36	-0.638	-0.668	-0.654	130.88
43.66	10.92	6.58	-0.686	-0.708	-0.698	139.50
42.14	10.54	6.71	-0.722	-0.738	-0.730	146.00

40.97	10.24	6.73	-0.725	-0.744	-0.736	147.12
39.79	9.95	6.75	-0.730	-0.746	-0.739	147.87
38.78	9.69	6.85	-0.748	-0.763	-0.755	151.00
38.78	9.69	7.05	-0.780	-0.800	-0.790	158.00
39.15	9.79	7.26	-0.818	-0.840	-0.829	165.75
39.42	9.85	7.47	-0.855	-0.880	-0.869	173.75
39.74	9.93	7.69	-0.893	-0.921	-0.908	181.50
39.87	9.97	7.90	-0.933	-0.998	-0.967	193.38
40.06	10.01	8.11	-0.973	-1.038	-1.006	201.12
40.11	10.03	8.32	-1.008	-1.078	-1.044	208.75
40.25	10.06	8.51	-1.047	-1.115	-1.083	216.50
40.27	10.07	8.73	-1.085	-1.158	-1.122	224.37
40.22	10.05	8.93	-1.125	-1.198	-1.163	232.62
40.30	10.07	9.15	-1.168	-1.241	-1.205	241.00
40.22	10.05	9.34	-1.205	-1.277	-1.242	248.37
40.22	10.05	9.55	-1.245	-1.315	-1.281	256.12
40.17	10.04	9.76	-1.284	-1.355	-1.321	264.12
40.19	10.05	9.97	-1.326	-1.390	-1.360	272.00
40.11	10.03	10.17	-1.368	-1.433	-1.403	280.50
40.11	10.03	10.37	-1.413	-1.472	-1.444	288.87
40.09	10.02	10.58	-1.453	-1.510	-1.483	296.50
39.98	9.99	10.79	-1.496	-1.555	-1.527	305.37
39.98	9.99	10.99	-1.530	-1.593	-1.564	312.75
39.90	9.97	11.20	-1.570	-1.632	-1.603	320.50
39.85	9.96	11.42	-1.614	-1.673	-1.647	329.38
39.87	9.97	11.64	-1.658	-1.718	-1.690	338.00
39.77	9.94	11.84	-1.698	-1.758	-1.730	346.00
39.85	9.96	12.05	-1.736	-1.796	-1.769	353.87
39.77	9.94	12.25	-1.776	-1.835	-1.808	361.50
39.74	9.93	12.46	-1.820	-1.874	-1.848	369.62
39.66	9.91	12.67	-1.862	-1.915	-1.890	378.00
39.66	9.91	12.87	-1.893	-1.914	-1.905	381.00
39.55	9.89	13.08	-1.933	-1.955	-1.945	389.00
39.52	9.88	13.28	-1.974	-1.993	-1.985	397.00
39.47	9.87	13.49	-2.013	-2.038	-2.026	405.25
39.31	9.83	13.68	-2.060	-2.075	-2.070	414.00
39.31	9.83	13.89	-2.101	-2.112	-2.110	422.00
39.31	9.83	14.09	-2.140	-2.153	-2.149	429.75
39.20	9.80	14.30	-2.180	-2.193	-2.189	437.87
39.15	9.79	14.51	-2.224	-2.235	-2.233	446.62
39.10	9.77	14.72	-2.269	-2.262	-2.268	453.50
38.96	9.74	14.93	-2.313	-2.285	-2.301	460.13
38.91	9.73	15.14	-2.355	-2.325	-2.343	468.50
38.88	9.72	15.36	-2.395	-2.366	-2.384	476.75
38.86	9.71	15.58	-2.443	-2.409	-2.428	485.50
38.86	9.71	15.79	-2.486	-2.450	-2.471	494.25
38.72	9.68	15.99	-2.528	-2.493	-2.513	502.50

38.64	9.66	16.21	-2.569	-2.528	-2.550	510.00
38.67	9.67	16.41	-2.598	-2.566	-2.588	517.62
38.64	9.66	16.61	-2.634	-2.606	-2.623	524.62
38.54	9.63	17.18	-2.741	-2.683	-2.716	543.13
38.46	9.61	17.38	-2.779	-2.725	-2.755	551.00
38.46	9.61	17.84	-2.872	-2.809	-2.837	567.38
38.54	9.63	18.05	-2.908	-2.848	-2.881	576.25
38.51	9.63	18.25	-2.948	-2.885	-2.921	584.25
38.46	9.61	18.46	-2.990	-2.925	-2.963	592.50
38.56	9.64	18.67	-3.028	-2.963	-3.001	600.12
38.48	9.62	18.87	-3.066	-2.936	-3.008	601.63
38.59	9.65	19.07	-3.103	-2.970	-3.015	603.00
38.59	9.65	19.28	-3.142	-3.007	-3.180	636.00
37.47	9.37	19.31	-3.153	-3.013	-3.180	636.00
36.38	9.09	19.13	-3.128	-2.983	-3.176	635.13
35.33	8.83	18.98	-3.103	-2.958	-3.142	628.38
34.21	8.55	18.84	-3.078	-2.933	-3.012	602.37
33.17	8.29	18.68	-3.053	-2.905	-2.983	596.50
32.11	8.03	18.50	-3.023	-2.875	-2.953	590.50
31.06	7.77	18.35	-3.005	-2.853	-2.933	586.50
30.10	7.53	18.23	-2.986	-2.835	-2.914	582.75
28.69	7.17	18.20	-2.983	-2.830	-2.911	582.12
29.33	7.33	17.45	-2.871	-2.724	-2.784	556.87
26.61	6.65	16.85	-2.808	-2.684	-2.749	549.75
24.85	6.21	16.87	-2.809	-2.687	-2.750	550.00
23.57	5.89	16.87	-2.808	-2.694	-2.753	550.50
22.58	5.64	16.90	-2.808	-2.689	-2.753	550.50
22.10	5.52	16.62	-2.766	-2.649	-2.706	541.25
21.14	5.28	16.34	-2.721	-2.605	-2.663	532.62
20.08	5.02	16.08	-2.679	-2.569	-2.624	524.88
18.92	4.73	15.81	-2.640	-2.528	-2.583	516.62
17.79	4.45	15.55	-2.599	-2.488	-2.543	508.50
16.61	4.15	15.29	-2.554	-2.453	-2.503	500.62
15.48	3.87	15.02	-2.513	-2.421	-2.465	493.00
14.37	3.59	14.78	-2.476	-2.386	-2.430	486.00
13.16	3.29	14.51	-2.429	-2.345	-2.388	477.50
11.95	2.99	14.25	-2.387	-2.307	-2.346	469.12
10.78	2.69	13.97	-2.340	-2.266	-2.303	460.50
9.67	2.42	13.72	-2.286	-2.228	-2.254	450.87
8.62	2.15	13.46	-2.239	-2.188	-2.213	442.50
7.57	1.89	13.20	-2.187	-2.145	-2.165	433.00
6.50	1.63	12.91	-2.133	-2.119	-2.124	424.88
5.54	1.39	12.64	-2.076	-2.081	-2.075	415.00
4.60	1.15	12.36	-2.013	-2.035	-2.023	404.50
3.37	0.84	12.22	-1.983	-2.020	-2.003	400.50
2.35	0.59	12.14	-1.965	-2.011	-1.991	398.13
1.47	0.37	11.92	-1.933	-1.988	-1.960	392.00
0.64	0.16	11.72	-1.899	-1.959	-1.932	386.37

Series 2 - Normal Mix, 8% Corrosion

Load (kN)	Moment (kN-m)	M.P. Displ. (mm)	E. Curv. LVDT (mm)	W. Curv. LVDT (mm)	Curv. LVDT Avg. (mm)	Curvature (1/km)
-0.05	-0.01	0.00	-0.000	-0.001	-0.003	0.51
-0.07	-0.02	0.00	-0.001	-0.001	-0.005	1.05
-0.02	-0.01	-0.01	-0.003	0.002	0.002	-0.36
1.32	0.33	0.06	-0.001	-0.004	-0.003	0.55
2.53	0.63	0.07	0.000	-0.001	-0.002	0.41
2.32	0.58	0.04	-0.003	-0.005	-0.003	0.69
1.35	0.34	0.03	0.001	-0.004	-0.007	1.34
2.41	0.60	0.09	0.012	-0.030	-0.008	1.61
3.43	0.86	0.11	0.011	-0.031	-0.008	1.69
4.43	1.11	0.13	0.011	-0.032	-0.009	1.75
5.42	1.36	0.15	0.011	-0.032	-0.009	1.87
6.43	1.61	0.18	0.010	-0.036	-0.014	2.79
7.49	1.87	0.20	0.011	-0.032	-0.011	2.12
8.54	2.14	0.24	0.011	-0.032	-0.010	2.09
9.55	2.39	0.26	0.009	-0.034	-0.011	2.23
10.61	2.65	0.29	0.012	-0.037	-0.015	3.08
11.61	2.90	0.31	0.010	-0.036	-0.016	3.19
12.66	3.16	0.34	0.009	-0.036	-0.013	2.52
13.65	3.41	0.36	0.009	-0.037	-0.013	2.61
14.73	3.68	0.37	0.010	-0.040	-0.021	4.22
15.78	3.95	0.41	0.008	-0.042	-0.021	4.19
16.78	4.20	0.43	0.007	-0.039	-0.015	2.94
17.91	4.48	0.46	0.006	-0.041	-0.018	3.52
18.96	4.74	0.48	0.004	-0.038	-0.016	3.12
19.95	4.99	0.51	0.004	-0.042	-0.021	4.10
21.01	5.25	0.53	0.006	-0.040	-0.021	4.16
22.07	5.52	0.56	0.004	-0.043	-0.017	3.40
23.14	5.78	0.58	0.005	-0.046	-0.023	4.58
24.15	6.04	0.62	0.004	-0.044	-0.023	4.53
25.14	6.29	0.64	0.002	-0.044	-0.020	3.91
23.35	5.84	0.82	-0.029	-0.054	-0.040	8.01
20.36	5.09	0.84	-0.031	-0.055	-0.043	8.55
18.40	4.60	0.84	-0.033	-0.053	-0.043	8.65
17.03	4.26	0.86	-0.035	-0.056	-0.045	8.96
15.91	3.98	0.87	-0.037	-0.062	-0.050	10.03
14.75	3.69	0.87	-0.044	-0.058	-0.048	9.61
13.92	3.48	1.08	-0.069	-0.071	-0.069	13.84
14.74	3.68	1.28	-0.094	-0.087	-0.089	17.80
15.81	3.95	1.45	-0.111	-0.104	-0.109	21.83
16.80	4.20	1.60	-0.125	-0.112	-0.119	23.74
17.85	4.46	1.73	-0.140	-0.129	-0.133	26.68
18.92	4.73	1.87	-0.148	-0.140	-0.146	29.18
19.99	5.00	2.01	-0.160	-0.148	-0.154	30.76
21.02	5.25	2.16	-0.170	-0.160	-0.165	33.01
22.10	5.52	2.28	-0.181	-0.173	-0.176	35.13

23.14	5.78	2.42	-0.179	-0.185	-0.184	36.84
24.15	6.04	2.56	-0.188	-0.196	-0.190	38.08
25.22	6.31	2.71	-0.195	-0.212	-0.205	40.98
26.21	6.55	2.84	-0.203	-0.222	-0.213	42.66
27.22	6.81	2.96	-0.212	-0.234	-0.222	44.46
28.24	7.06	3.10	-0.217	-0.242	-0.235	46.96
29.25	7.31	3.24	-0.215	-0.259	-0.238	47.67
30.32	7.58	3.38	-0.224	-0.266	-0.246	49.26
31.36	7.84	3.54	-0.228	-0.280	-0.258	51.64
32.40	8.10	3.70	-0.237	-0.287	-0.262	52.34
33.44	8.36	3.87	-0.249	-0.302	-0.280	55.90
34.45	8.61	4.03	-0.255	-0.317	-0.286	57.29
35.52	8.88	4.22	-0.267	-0.335	-0.301	60.24
34.16	8.54	4.33	-0.289	-0.357	-0.323	64.60
32.96	8.24	4.34	-0.287	-0.352	-0.323	64.60
31.89	7.97	4.38	-0.288	-0.359	-0.326	65.17
32.99	8.25	4.58	-0.305	-0.381	-0.344	68.76
34.03	8.51	4.75	-0.313	-0.402	-0.359	71.84
34.85	8.71	4.95	-0.328	-0.425	-0.381	76.20
35.66	8.91	5.15	-0.339	-0.451	-0.395	79.08
36.51	9.13	5.37	-0.355	-0.463	-0.411	82.25
37.31	9.33	5.57	-0.371	-0.483	-0.428	85.62
38.00	9.50	5.76	-0.384	-0.509	-0.450	89.92
38.56	9.64	5.96	-0.382	-0.541	-0.463	92.65
39.12	9.78	6.17	-0.395	-0.585	-0.491	98.20
39.71	9.93	6.38	-0.412	-0.632	-0.522	104.37
40.09	10.02	6.58	-0.423	-0.674	-0.551	110.12
40.59	10.15	6.78	-0.433	-0.696	-0.565	113.00
40.97	10.24	6.98	-0.445	-0.717	-0.580	116.00
41.15	10.29	7.19	-0.457	-0.708	-0.583	116.50
41.31	10.33	7.39	-0.470	-0.721	-0.595	119.00
41.55	10.39	7.61	-0.474	-0.733	-0.605	121.00
41.63	10.41	7.81	-0.483	-0.748	-0.615	123.00
41.79	10.45	8.02	-0.489	-0.763	-0.626	125.25
41.93	10.48	8.23	-0.498	-0.778	-0.639	127.75
42.06	10.52	8.43	-0.505	-0.795	-0.650	130.00
42.01	10.50	8.64	-0.515	-0.797	-0.655	131.00
42.09	10.52	8.84	-0.525	-0.814	-0.671	134.12
41.98	10.50	9.04	-0.535	-0.830	-0.683	136.50
41.93	10.48	9.25	-0.536	-0.846	-0.693	138.50
41.90	10.48	9.46	-0.545	-0.853	-0.698	139.62
41.90	10.48	9.68	-0.546	-0.871	-0.710	142.00
41.87	10.47	9.88	-0.557	-0.885	-0.721	144.12
41.95	10.49	10.10	-0.560	-0.900	-0.730	146.00
41.90	10.48	10.32	-0.569	-0.914	-0.741	148.25
41.87	10.47	10.53	-0.570	-0.924	-0.748	149.62
41.85	10.46	10.74	-0.578	-0.935	-0.758	151.62
41.90	10.48	10.94	-0.578	-0.951	-0.765	153.00

42.14	10.54	11.15	-0.585	-0.972	-0.779	155.75
42.35	10.59	11.35	-0.604	-1.005	-0.804	160.87
42.57	10.64	11.56	-0.618	-1.040	-0.829	165.87
42.59	10.65	11.77	-0.640	-1.075	-0.859	171.75
42.70	10.68	11.97	-0.658	-1.105	-0.883	176.50
42.83	10.71	12.18	-0.675	-1.139	-0.908	181.62
42.81	10.70	12.38	-0.695	-1.167	-0.933	186.50
42.86	10.72	12.58	-0.718	-1.198	-0.958	191.62
42.94	10.74	12.80	-0.743	-1.223	-0.985	197.00
42.99	10.75	13.00	-0.763	-1.254	-1.010	202.00
43.07	10.77	13.21	-0.780	-1.278	-1.030	206.00
43.10	10.78	13.42	-0.797	-1.305	-1.053	210.62
43.10	10.78	13.62	-0.815	-1.332	-1.075	215.00
43.10	10.78	13.82	-0.833	-1.358	-1.097	219.37
43.21	10.80	14.04	-0.828	-1.383	-1.106	221.12
43.21	10.80	14.24	-0.845	-1.408	-1.128	225.50
43.29	10.82	14.46	-0.858	-1.435	-1.148	229.50
43.31	10.83	14.67	-0.876	-1.438	-1.158	231.50
43.34	10.84	14.87	-0.896	-1.454	-1.175	235.00
43.42	10.86	15.09	-0.908	-1.475	-1.192	238.37
43.42	10.86	15.29	-0.925	-1.499	-1.213	242.50
43.50	10.88	15.50	-0.943	-1.520	-1.233	246.50
43.55	10.89	15.71	-0.948	-1.538	-1.245	249.00
43.69	10.92	15.91	-0.967	-1.564	-1.266	253.12
43.80	10.95	16.10	-0.987	-1.590	-1.289	257.87
43.74	10.94	16.31	-1.003	-1.613	-1.309	261.75
43.82	10.96	16.52	-1.020	-1.639	-1.330	266.00
43.93	10.98	16.73	-1.043	-1.645	-1.345	269.00
43.96	10.99	16.95	-1.060	-1.670	-1.368	273.50
44.09	11.02	17.16	-1.078	-1.694	-1.387	277.37
44.20	11.05	17.36	-1.097	-1.720	-1.410	282.00
44.22	11.06	17.58	-1.115	-1.746	-1.432	286.37
44.44	11.11	17.79	-1.135	-1.774	-1.456	291.12
44.52	11.13	18.00	-1.155	-1.804	-1.480	296.00
44.52	11.13	18.21	-1.173	-1.833	-1.504	300.87
44.68	11.17	18.41	-1.196	-1.859	-1.530	306.00
44.73	11.18	18.62	-1.223	-1.884	-1.554	310.87
44.81	11.20	18.83	-1.231	-1.884	-1.559	311.75
44.81	11.20	19.03	-1.255	-1.907	-1.583	316.62
44.94	11.24	19.24	-1.275	-1.938	-1.608	321.50
45.05	11.26	19.44	-1.298	-1.963	-1.633	326.50
45.02	11.26	19.64	-1.315	-1.988	-1.653	330.62
45.16	11.29	19.85	-1.336	-2.003	-1.672	334.37
45.18	11.30	20.06	-1.355	-2.029	-1.694	338.87
45.21	11.30	20.27	-1.378	-2.046	-1.714	342.87
45.37	11.34	20.47	-1.402	-2.073	-1.739	347.87
45.29	11.32	20.68	-1.428	-2.098	-1.763	352.62
45.37	11.34	20.88	-1.450	-2.115	-1.785	357.00

45.37	11.34	21.10	-1.475	-2.142	-1.810	362.00
45.40	11.35	21.30	-1.498	-2.170	-1.836	367.12
45.34	11.34	21.51	-1.520	-2.196	-1.860	372.00
45.40	11.35	21.72	-1.533	-2.215	-1.875	375.00
45.42	11.36	21.93	-1.555	-2.243	-1.900	380.00
45.42	11.36	22.13	-1.581	-2.273	-1.929	385.75
45.37	11.34	22.34	-1.608	-2.303	-1.958	391.50
45.29	11.32	22.54	-1.633	-2.298	-1.965	393.00
45.21	11.30	22.75	-1.653	-2.328	-1.991	398.25
45.21	11.30	22.95	-1.654	-2.353	-2.007	401.37
45.29	11.32	23.16	-1.673	-2.383	-2.030	406.00
45.26	11.32	23.37	-1.695	-2.413	-2.057	411.37
45.24	11.31	23.57	-1.716	-2.420	-2.070	414.00
45.26	11.32	23.79	-1.735	-2.443	-2.093	418.50
45.18	11.30	23.99	-1.755	-2.475	-2.118	423.50
45.18	11.30	24.20	-1.773	-2.503	-2.140	428.00
45.10	11.28	24.40	-1.790	-2.510	-2.152	430.37
45.10	11.28	24.61	-1.806	-2.535	-2.173	434.50
45.13	11.28	24.82	-1.823	-2.566	-2.197	439.37
45.02	11.26	25.02	-1.836	-2.582	-2.211	442.25
44.97	11.24	25.23	-1.853	-2.613	-2.235	447.00
45.02	11.26	25.43	-1.865	-2.641	-2.256	451.25
44.92	11.23	25.64	-1.878	-2.672	-2.278	455.50
44.92	11.23	25.84	-1.893	-2.701	-2.301	460.12
44.73	11.18	26.05	-1.905	-2.709	-2.310	462.00
43.66	10.92	26.24	-1.903	-2.729	-2.318	463.62
42.54	10.64	26.14	-1.850	-2.669	-2.260	452.00
41.42	10.35	26.09	-1.799	-2.618	-2.209	441.87
40.30	10.07	26.07	-1.753	-2.567	-2.160	432.00
39.23	9.81	26.00	-1.731	-2.544	-2.140	428.00
38.11	9.53	25.85	-1.730	-2.546	-2.141	428.12
36.40	9.10	25.74	-1.735	-2.558	-2.148	429.62
36.72	9.18	24.97	-1.683	-2.524	-2.098	419.50
34.08	8.52	24.68	-1.663	-2.486	-2.081	416.12
32.53	8.13	24.67	-1.665	-2.493	-2.083	416.50
31.33	7.83	24.68	-1.665	-2.509	-2.086	417.25
30.34	7.59	24.67	-1.663	-2.499	-2.083	416.62
29.57	7.39	24.46	-1.648	-2.485	-2.068	413.62
28.40	7.10	24.26	-1.633	-2.470	-2.053	410.50
27.41	6.85	24.06	-1.616	-2.454	-2.035	407.00
26.26	6.57	23.86	-1.600	-2.438	-2.021	404.12
25.09	6.27	23.64	-1.584	-2.420	-2.003	400.50
24.07	6.02	23.43	-1.567	-2.404	-1.986	397.12
23.03	5.76	23.22	-1.553	-2.389	-1.972	394.37
22.02	5.50	23.00	-1.538	-2.375	-1.958	391.50
20.95	5.24	22.78	-1.518	-2.360	-1.941	388.12
19.83	4.96	22.57	-1.499	-2.345	-1.924	384.75
18.85	4.71	22.35	-1.490	-2.341	-1.918	383.62

17.86	4.47	22.14	-1.479	-2.350	-1.918	383.50
16.85	4.21	21.92	-1.465	-2.337	-1.903	380.50
16.10	4.03	21.70	-1.448	-2.314	-1.883	376.50
14.97	3.74	21.46	-1.423	-2.297	-1.860	372.00
13.84	3.46	21.23	-1.400	-2.266	-1.833	366.50
12.64	3.16	21.01	-1.372	-2.231	-1.801	360.12
11.52	2.88	20.79	-1.345	-2.204	-1.775	355.00
10.35	2.59	20.59	-1.325	-2.170	-1.748	349.62
9.27	2.32	20.36	-1.303	-2.139	-1.722	344.37
8.21	2.05	20.13	-1.279	-2.103	-1.691	338.25
7.17	1.79	19.91	-1.259	-2.068	-1.664	332.75
6.08	1.52	19.68	-1.238	-2.028	-1.633	326.62
5.10	1.27	19.46	-1.214	-1.996	-1.607	321.37
4.17	1.04	19.24	-1.190	-1.961	-1.575	315.00
3.24	0.81	19.01	-1.163	-1.928	-1.547	309.37
2.30	0.57	18.79	-1.139	-1.893	-1.516	303.25
1.45	0.36	18.57	-1.113	-1.880	-1.497	299.37
0.64	0.16	18.35	-1.073	-1.873	-1.473	294.62
-0.12	-0.03	18.15	-1.045	-1.867	-1.458	291.50
-0.14	-0.03	18.10	-1.040	-1.863	-1.453	290.50

Series 2 - Normal Mix, 12 % Corrosion

Load (kN)	Moment (kN-m)	M.P. Displ. (mm)	E. Curv. LVDT (mm)	W. Curv. LVDT (mm)	Curv. LVDT Avg. (mm)	Curvature (1/km)
1.11	0.28	0.00	0.010	-0.014	-0.013	2.55
1.88	0.47	0.01	0.005	-0.061	-0.014	2.82
2.90	0.73	0.04	0.008	-0.028	-0.009	1.77
3.85	0.96	0.08	0.011	0.011	-0.012	2.40
4.77	1.19	0.10	0.002	0.015	-0.006	1.15
5.97	1.49	0.12	0.017	0.018	-0.010	2.03
7.01	1.75	0.16	0.011	-0.008	0.000	-0.05
8.11	2.03	0.18	0.003	0.014	-0.003	0.60
9.19	2.30	0.21	0.017	-0.005	-0.010	1.95
10.19	2.55	0.23	-0.004	0.031	-0.011	2.18
10.39	2.60	0.23	0.007	0.004	-0.011	2.23
10.54	2.63	0.24	0.017	0.002	-0.014	2.85
11.12	2.78	0.25	0.008	0.021	-0.004	0.75
11.69	2.92	0.26	-0.036	0.026	-0.010	2.03
12.21	3.05	0.28	0.011	0.016	-0.009	1.72
12.47	3.12	0.30	0.019	-0.017	-0.012	2.45
12.95	3.24	0.31	0.001	0.013	-0.015	2.95
13.49	3.37	0.33	0.025	0.031	-0.009	1.80
13.92	3.48	0.34	0.012	0.037	-0.012	2.48
14.22	3.56	0.35	0.023	0.022	-0.020	4.08
15.11	3.78	0.36	0.017	-0.009	-0.016	3.25
15.43	3.86	0.39	0.013	0.007	-0.012	2.40

16.26	4.07	0.42	0.002	0.005	-0.011	2.23
15.66	3.92	0.63	0.008	-0.019	-0.017	3.47
15.44	3.86	0.64	-0.031	0.010	-0.011	2.10
14.71	3.68	0.64	-0.004	0.011	-0.022	4.45
14.83	3.71	0.67	0.005	-0.019	-0.023	4.53
14.54	3.64	0.76	0.009	-0.002	-0.022	4.37
15.62	3.90	0.95	0.017	-0.026	-0.009	1.85
16.15	4.04	1.02	-0.001	0.020	-0.018	3.52
16.53	4.13	1.04	0.020	-0.001	-0.016	3.23
17.66	4.42	1.20	-0.005	0.012	-0.014	2.87
18.56	4.64	1.30	0.022	0.015	-0.019	3.70
18.63	4.66	1.30	0.018	0.009	-0.019	3.73
19.31	4.83	1.36	0.003	-0.026	-0.014	2.85
19.56	4.89	1.40	0.014	-0.006	-0.014	2.70
19.72	4.93	1.44	0.019	-0.022	-0.014	2.87
19.92	4.98	1.46	-0.008	-0.030	-0.020	3.98
20.76	5.19	1.53	0.006	0.001	-0.017	3.40
21.34	5.33	1.61	0.005	0.016	-0.007	1.43
22.28	5.57	1.71	0.002	-0.026	-0.020	4.03
22.23	5.56	1.90	-0.004	-0.037	-0.037	7.42
21.03	5.26	1.93	-0.005	-0.008	-0.047	9.48
19.79	4.95	1.96	-0.063	-0.070	-0.075	14.97
18.12	4.53	2.10	-0.063	-0.165	-0.125	24.95
16.61	4.15	2.11	-0.064	-0.148	-0.124	24.78
15.36	3.84	2.10	-0.055	-0.159	-0.131	26.20
14.22	3.56	2.14	-0.067	-0.171	-0.134	26.70
14.34	3.58	2.33	-0.083	-0.210	-0.165	33.00
15.11	3.78	2.50	-0.064	-0.269	-0.185	36.90
15.13	3.78	2.51	-0.101	-0.259	-0.190	37.90
15.23	3.81	2.60	-0.088	-0.259	-0.199	39.73
15.74	3.93	2.78	-0.103	-0.290	-0.225	45.00
16.33	4.08	2.92	-0.139	-0.358	-0.243	48.65
16.85	4.21	3.06	-0.111	-0.347	-0.268	53.57
17.26	4.32	3.27	-0.161	-0.389	-0.303	60.58
17.73	4.43	3.48	-0.163	-0.377	-0.316	63.27
18.33	4.58	3.71	-0.205	-0.445	-0.342	68.45
18.91	4.73	3.91	-0.224	-0.480	-0.370	74.00
19.31	4.83	4.11	-0.240	-0.528	-0.401	80.12
19.81	4.95	4.31	-0.274	-0.578	-0.425	84.95
19.99	5.00	4.52	-0.251	-0.588	-0.452	90.45
20.37	5.09	4.73	-0.292	-0.628	-0.477	95.30
20.26	5.07	4.97	-0.358	-0.657	-0.515	102.97
20.50	5.12	5.19	-0.396	-0.688	-0.547	109.35
20.04	5.01	5.40	-0.356	-0.743	-0.582	116.35
19.28	4.82	5.60	-0.433	-0.800	-0.610	121.90
18.20	4.55	5.75	-0.441	-0.814	-0.640	128.03
17.21	4.30	5.89	-0.424	-0.845	-0.669	133.73
16.30	4.07	5.97	-0.433	-0.870	-0.683	136.60

15.35	3.84	6.05	-0.503	-0.894	-0.691	138.25
14.45	3.61	6.15	-0.443	-0.895	-0.713	142.53
13.70	3.43	6.36	-0.499	-0.946	-0.741	148.25
13.11	3.28	6.54	-0.607	-0.943	-0.763	152.65
12.56	3.14	6.75	-0.605	-0.993	-0.791	158.20
11.99	3.00	6.95	-0.587	-1.009	-0.821	164.10
11.81	2.95	7.14	-0.601	-1.045	-0.848	169.68
11.52	2.88	7.34	-0.646	-1.076	-0.886	177.20
10.88	2.72	7.54	-0.632	-1.131	-0.927	185.32
9.90	2.48	7.76	-0.722	-1.166	-0.948	189.62
9.73	2.43	7.94	-0.709	-1.219	-0.980	196.05
9.30	2.32	8.13	-0.762	-1.214	-0.999	199.82
8.84	2.21	8.37	-0.753	-1.241	-1.036	207.25
8.48	2.12	8.54	-0.799	-1.319	-1.071	214.25
8.01	2.00	8.75	-0.880	-1.311	-1.095	219.00
7.73	1.93	8.91	-0.866	-1.375	-1.124	224.75
7.26	1.82	9.11	-0.828	-1.404	-1.154	230.75
6.64	1.66	9.30	-0.872	-1.384	-1.181	236.25
6.51	1.63	9.50	-0.933	-1.398	-1.204	240.75
6.19	1.55	9.70	-0.983	-1.483	-1.234	246.75
5.86	1.47	9.93	-0.961	-1.441	-1.263	252.50
5.55	1.39	10.06	-1.003	-1.548	-1.305	261.00
5.21	1.30	10.25	-1.050	-1.574	-1.333	266.50
4.88	1.22	10.41	-1.066	-1.545	-1.351	270.25
4.64	1.16	10.56	-1.096	-1.595	-1.368	273.50
4.33	1.08	10.82	-1.129	-1.584	-1.400	280.00
4.22	1.06	10.98	-1.144	-1.640	-1.423	284.50
3.78	0.94	11.18	-1.173	-1.684	-1.453	290.50
3.59	0.90	11.36	-1.173	-1.710	-1.473	294.50
3.52	0.88	11.59	-1.231	-1.730	-1.505	301.00
3.41	0.85	11.73	-1.296	-1.754	-1.540	308.00
3.19	0.80	11.87	-1.290	-1.795	-1.563	312.50
3.06	0.77	12.04	-1.308	-1.775	-1.590	318.00
3.09	0.77	12.23	-1.340	-1.863	-1.619	323.75
2.83	0.71	12.47	-1.356	-1.884	-1.656	331.25
2.62	0.66	12.69	-1.405	-1.914	-1.678	335.50
2.38	0.60	12.88	-1.379	-2.001	-1.710	342.00
2.43	0.61	13.10	-1.408	-1.966	-1.735	347.00
2.36	0.59	13.25	-1.484	-1.994	-1.764	352.75
1.94	0.49	13.32	-1.495	-1.993	-1.759	351.75

Series 2 - Silica Fume, Control

Load (kN)	Moment (kN-m)	M.P. Displ. (mm)	E. Curv. LVDT (mm)	W. Curv. LVDT (mm)	Curv. LVDT Avg. (mm)	Curvature (1/km)
-0.22	-0.05	0.00	0.001	0.006	0.002	-0.30
-0.04	-0.01	0.01	0.001	0.005	0.004	-0.76
1.05	0.26	0.02	0.001	0.005	0.002	-0.48
2.13	0.53	0.04	-0.001	0.001	0.002	-0.40
3.23	0.81	0.06	-0.001	0.003	0.002	-0.34
4.31	1.08	0.08	-0.003	0.005	0.001	-0.29
5.37	1.34	0.12	-0.001	0.003	0.001	-0.16
6.38	1.60	0.13	-0.003	0.003	0.001	-0.14
7.43	1.86	0.16	-0.003	0.002	0.000	0.00
8.45	2.11	0.18	-0.003	0.002	-0.000	0.04
9.52	2.38	0.21	-0.004	0.001	-0.002	0.40
10.59	2.65	0.25	-0.004	0.001	-0.001	0.28
11.61	2.90	0.25	-0.002	0.000	-0.002	0.31
12.73	3.18	0.31	-0.001	-0.000	-0.002	0.41
13.86	3.46	0.33	-0.004	-0.000	-0.002	0.45
14.81	3.70	0.35	-0.005	-0.002	-0.003	0.64
15.98	3.99	0.37	-0.003	-0.003	-0.005	1.06
14.83	3.71	0.49	-0.011	-0.020	-0.017	3.35
13.51	3.38	0.53	-0.013	-0.031	-0.021	4.24
12.32	3.08	0.55	-0.014	-0.038	-0.027	5.36
11.04	2.76	0.56	-0.015	-0.042	-0.028	5.50
9.91	2.48	0.58	-0.014	-0.045	-0.030	5.90
8.84	2.21	0.61	-0.015	-0.051	-0.033	6.58
7.68	1.92	0.65	-0.016	-0.058	-0.037	7.41
8.75	2.19	0.93	-0.026	-0.093	-0.061	12.26
9.96	2.49	1.05	-0.030	-0.111	-0.071	14.27
11.03	2.76	1.13	-0.036	-0.121	-0.079	15.79
12.12	3.03	1.26	-0.043	-0.134	-0.088	17.64
13.27	3.32	1.37	-0.049	-0.145	-0.096	19.24
14.37	3.59	1.45	-0.050	-0.155	-0.103	20.61
15.52	3.88	1.54	-0.048	-0.163	-0.106	21.15
16.62	4.16	1.65	-0.054	-0.174	-0.113	22.56
17.70	4.42	1.73	-0.057	-0.182	-0.120	23.91
18.77	4.69	1.82	-0.061	-0.189	-0.126	25.10
19.86	4.97	1.89	-0.067	-0.195	-0.131	26.21
21.00	5.25	1.99	-0.073	-0.202	-0.139	27.74
22.15	5.54	2.06	-0.079	-0.207	-0.143	28.68
23.22	5.80	2.16	-0.086	-0.213	-0.150	29.99
24.23	6.06	2.22	-0.093	-0.219	-0.156	31.14
25.25	6.31	2.33	-0.099	-0.227	-0.163	32.56
26.34	6.59	2.41	-0.105	-0.232	-0.165	33.03
27.36	6.84	2.49	-0.110	-0.236	-0.174	34.75
28.48	7.12	2.56	-0.116	-0.242	-0.175	35.08
29.52	7.38	2.65	-0.122	-0.248	-0.186	37.29

30.56	7.64	2.73	-0.129	-0.254	-0.192	38.30
31.55	7.89	2.85	-0.136	-0.260	-0.198	39.61
32.51	8.13	2.90	-0.143	-0.266	-0.205	40.90
33.55	8.39	2.97	-0.149	-0.271	-0.209	41.85
34.61	8.65	3.05	-0.153	-0.277	-0.215	43.01
35.74	8.93	3.14	-0.161	-0.285	-0.223	44.55
36.78	9.19	3.25	-0.167	-0.291	-0.229	45.83
37.76	9.44	3.32	-0.173	-0.298	-0.235	47.06
38.80	9.70	3.41	-0.180	-0.307	-0.244	48.76
39.85	9.96	3.49	-0.185	-0.316	-0.250	49.96
40.97	10.24	3.57	-0.187	-0.323	-0.255	51.09
41.95	10.49	3.66	-0.196	-0.334	-0.265	52.90
42.99	10.75	3.73	-0.202	-0.340	-0.271	54.26
44.12	11.03	3.85	-0.212	-0.351	-0.282	56.39
45.16	11.29	3.97	-0.222	-0.361	-0.285	56.91
46.20	11.55	4.09	-0.233	-0.372	-0.303	60.58
51.03	12.76	4.65	-0.294	-0.406	-0.351	70.19
52.15	13.04	4.78	-0.310	-0.418	-0.365	73.01
53.14	13.28	4.89	-0.324	-0.429	-0.377	75.40
54.15	13.54	5.05	-0.352	-0.443	-0.397	79.35
55.14	13.78	5.21	-0.383	-0.455	-0.419	83.84
56.28	14.07	5.37	-0.408	-0.466	-0.437	87.48
57.35	14.34	5.54	-0.431	-0.487	-0.458	91.51
58.39	14.60	5.73	-0.460	-0.505	-0.484	96.79
59.49	14.87	5.93	-0.489	-0.530	-0.511	102.12
60.56	15.14	6.21	-0.540	-0.565	-0.554	110.75
61.49	15.37	6.65	-0.627	-0.614	-0.622	124.37
62.45	15.61	7.06	-0.716	-0.680	-0.700	140.00
63.12	15.78	7.49	-0.797	-0.739	-0.768	153.50
63.52	15.88	7.88	-0.885	-0.798	-0.843	168.50
63.94	15.99	8.29	-0.968	-0.870	-0.920	184.00
64.21	16.05	8.69	-1.046	-0.930	-0.990	198.00
64.45	16.11	9.11	-1.138	-0.999	-1.070	214.00
64.75	16.19	9.53	-1.223	-1.065	-1.145	229.00
65.07	16.27	9.95	-1.313	-1.121	-1.219	243.88
65.25	16.31	10.37	-1.399	-1.190	-1.297	259.37
65.41	16.35	10.79	-1.491	-1.249	-1.371	274.25
65.79	16.45	11.21	-1.578	-1.318	-1.449	289.75
66.13	16.53	11.61	-1.671	-1.395	-1.535	307.00
66.00	16.50	12.01	-1.751	-1.463	-1.608	321.62
66.37	16.59	12.43	-1.850	-1.538	-1.696	339.12
66.51	16.63	12.85	-1.945	-1.601	-1.776	355.25
66.85	16.71	13.25	-2.037	-1.671	-1.856	371.13
66.96	16.74	13.65	-2.118	-1.733	-1.928	385.63
67.31	16.83	14.06	-2.210	-1.803	-2.009	401.75
67.63	16.91	14.46	-2.293	-1.870	-2.085	417.00
67.87	16.97	14.88	-2.380	-1.945	-2.165	433.00

68.24	17.06	15.29	-2.465	-2.020	-2.246	449.12
68.43	17.11	15.71	-2.555	-2.094	-2.328	465.50
68.64	17.16	16.13	-2.633	-2.159	-2.399	479.75
68.86	17.21	16.53	-2.720	-2.226	-2.476	495.25
69.20	17.30	16.94	-2.798	-2.294	-2.549	509.87
69.44	17.36	17.37	-2.883	-2.368	-2.628	525.50
68.21	17.05	17.41	-2.896	-2.366	-2.633	526.50
67.07	16.77	17.32	-2.881	-2.354	-2.618	523.63
65.76	16.44	17.21	-2.870	-2.339	-2.605	521.00
64.64	16.16	17.14	-2.858	-2.327	-2.594	518.87
63.33	15.83	17.05	-2.844	-2.310	-2.580	516.00
62.16	15.54	16.97	-2.833	-2.298	-2.568	513.50
60.96	15.24	16.89	-2.820	-2.285	-2.555	511.00
59.86	14.97	16.81	-2.803	-2.268	-2.539	507.88
58.77	14.69	16.69	-2.790	-2.252	-2.523	504.62
57.54	14.38	16.61	-2.775	-2.235	-2.508	501.50
56.37	14.09	16.51	-2.763	-2.217	-2.493	498.50
55.35	13.84	16.44	-2.753	-2.202	-2.479	495.75
54.20	13.55	16.35	-2.740	-2.185	-2.466	493.13
53.08	13.27	16.26	-2.731	-2.168	-2.453	490.50
52.04	13.01	16.18	-2.725	-2.153	-2.442	488.37
50.89	12.72	16.09	-2.718	-2.133	-2.428	485.50
49.88	12.47	16.01	-2.714	-2.115	-2.418	483.50
48.79	12.20	15.90	-2.703	-2.088	-2.399	479.75
45.10	11.28	15.89	-2.704	-2.085	-2.398	479.50
46.76	11.69	15.89	-2.704	-2.085	-2.398	479.50
47.85	11.96	15.88	-2.705	-2.085	-2.400	480.00
47.53	11.88	15.17	-2.553	-1.893	-2.204	440.75
44.73	11.18	15.05	-2.506	-1.849	-2.183	436.50
43.07	10.77	15.06	-2.513	-1.855	-2.187	437.38
41.77	10.44	15.05	-2.515	-1.855	-2.186	437.25
40.67	10.17	15.05	-2.515	-1.858	-2.189	437.75
39.34	9.83	14.46	-2.371	-1.733	-2.043	408.62
36.32	9.08	14.01	-2.273	-1.670	-1.970	394.00
32.99	8.25	13.34	-2.161	-1.523	-1.838	367.50
28.16	7.04	12.62	-2.089	-1.460	-1.773	354.50
22.66	5.66	11.98	-2.017	-1.415	-1.711	342.25
17.59	4.40	11.43	-1.942	-1.363	-1.649	329.87
12.38	3.09	10.85	-1.861	-1.315	-1.584	316.88
7.88	1.97	10.53	-1.812	-1.298	-1.557	311.37
4.85	1.21	10.49	-1.808	-1.293	-1.553	310.50
2.93	0.73	10.49	-1.805	-1.293	-1.551	310.12
1.69	0.42	10.47	-1.805	-1.292	-1.550	310.00
0.55	0.14	10.45	-1.802	-1.290	-1.549	309.75
-0.21	-0.05	10.39	-1.796	-1.285	-1.543	308.50

Series 2 - Silica Fume, 2 % Corrosion

Load (kN)	Moment (kN-m)	M.P. Displ. (mm)	E. Curv. LVDT (mm)	W. Curv. LVDT (mm)	Curv. LVDT Avg. (mm)	Curvature (1/km)
-0.09	-0.02	0.00	0.001	0.004	0.003	-0.61
0.96	0.24	0.03	-0.000	-0.005	-0.006	1.19
1.94	0.49	0.07	-0.001	-0.005	-0.006	1.12
0.76	0.19	0.19	0.041	0.017	0.029	-5.75
1.84	0.46	0.26	0.040	0.015	0.026	-5.26
2.90	0.73	0.31	0.043	0.018	0.028	-5.60
3.89	0.97	0.34	0.041	0.015	0.027	-5.35
4.86	1.21	0.35	0.042	0.019	0.030	-6.08
5.89	1.47	0.37	0.040	0.015	0.026	-5.20
6.94	1.74	0.41	0.041	0.017	0.029	-5.86
7.94	1.98	0.43	0.041	0.013	0.025	-4.98
8.95	2.24	0.46	0.040	0.016	0.028	-5.55
9.94	2.48	0.48	0.037	0.011	0.024	-4.83
10.97	2.74	0.51	0.040	0.014	0.027	-5.46
12.01	3.00	0.53	0.037	0.011	0.023	-4.66
13.04	3.26	0.56	0.038	0.013	0.027	-5.30
14.03	3.51	0.57	0.038	0.012	0.026	-5.21
15.09	3.77	0.59	0.036	0.010	0.023	-4.69
16.12	4.03	0.64	0.038	0.013	0.025	-5.06
17.15	4.29	0.64	0.037	0.012	0.022	-4.44
18.21	4.55	0.68	0.036	0.007	0.021	-4.11
19.25	4.81	0.70	0.036	0.010	0.024	-4.80
20.33	5.08	0.73	0.035	0.003	0.020	-3.90
19.16	4.79	0.81	0.026	-0.001	0.011	-2.20
17.90	4.48	0.84	0.022	0.001	0.009	-1.77
16.64	4.16	0.85	0.017	0.001	0.009	-1.76
15.37	3.84	0.86	0.014	0.000	-0.000	0.06
14.30	3.58	0.88	0.011	-0.003	0.004	-0.71
13.14	3.28	0.91	0.008	-0.006	0.001	-0.12
11.91	2.98	0.92	0.005	-0.008	-0.001	0.29
10.85	2.71	0.97	0.002	-0.011	-0.003	0.54
11.00	2.75	1.22	-0.025	-0.025	-0.025	5.05
12.04	3.01	1.40	-0.042	-0.027	-0.033	6.65
13.12	3.28	1.55	-0.059	-0.028	-0.044	8.75
14.13	3.53	1.70	-0.079	-0.031	-0.057	11.34
15.18	3.80	1.82	-0.099	-0.032	-0.065	13.01
16.20	4.05	1.96	-0.105	-0.031	-0.067	13.49
17.25	4.31	2.05	-0.119	-0.036	-0.078	15.64
18.31	4.58	2.18	-0.138	-0.036	-0.086	17.16
19.37	4.84	2.29	-0.153	-0.026	-0.089	17.76
20.36	5.09	2.41	-0.175	-0.019	-0.097	19.46
21.39	5.35	2.52	-0.194	-0.017	-0.112	22.41
22.42	5.60	2.63	-0.212	-0.011	-0.113	22.56
23.43	5.86	2.75	-0.227	-0.007	-0.117	23.34

24.37	6.09	2.84	-0.245	-0.004	-0.124	24.79
25.41	6.35	2.95	-0.263	0.000	-0.131	26.15
26.47	6.62	3.06	-0.282	0.005	-0.138	27.68
27.49	6.87	3.18	-0.304	0.003	-0.150	29.99
28.58	7.15	3.30	-0.325	0.011	-0.159	31.76
29.62	7.41	3.43	-0.369	0.036	-0.166	33.25
30.64	7.66	3.54	-0.404	0.048	-0.178	35.60
31.65	7.91	3.66	-0.442	0.082	-0.180	36.09
32.77	8.19	3.78	-0.472	0.092	-0.190	38.02
33.79	8.45	3.92	-0.509	0.108	-0.202	40.31
34.77	8.69	4.05	-0.552	0.127	-0.213	42.58
35.82	8.95	4.19	-0.585	0.143	-0.222	44.40
36.78	9.19	4.31	-0.623	0.159	-0.233	46.60
37.87	9.47	4.45	-0.675	0.181	-0.248	49.58
38.88	9.72	4.58	-0.766	0.193	-0.287	57.44
39.90	9.97	4.72	-0.816	0.211	-0.303	60.56
40.99	10.25	4.86	-0.862	0.227	-0.318	63.65
42.09	10.52	5.01	-0.913	0.241	-0.338	67.54
43.10	10.78	5.16	-0.973	0.263	-0.356	71.13
44.12	11.03	5.30	-1.025	0.275	-0.376	75.25
45.10	11.28	5.43	-1.073	0.285	-0.395	78.91
46.06	11.52	5.57	-1.131	0.294	-0.420	83.93
47.13	11.78	5.70	-1.193	0.305	-0.444	88.80
48.15	12.04	5.86	-1.249	0.315	-0.468	93.62
49.19	12.30	6.00	-1.363	0.323	-0.520	104.00
50.23	12.56	6.14	-1.406	0.214	-0.594	118.87
51.21	12.80	6.29	-1.464	0.222	-0.623	124.50
52.28	13.07	6.46	-1.565	0.223	-0.673	134.50
53.24	13.31	6.64	-1.623	0.233	-0.695	139.00
54.28	13.57	6.82	-1.708	0.240	-0.733	146.50
55.32	13.83	7.02	-1.773	0.199	-0.788	157.50
56.31	14.08	7.26	-1.860	0.206	-0.827	165.38
57.38	14.34	7.50	-1.937	0.211	-0.865	173.00
58.29	14.57	7.76	-2.018	0.213	-0.903	180.50
59.11	14.78	8.01	-2.098	0.214	-0.942	188.37
59.73	14.93	8.26	-2.178	0.215	-0.980	196.00
60.26	15.07	8.51	-2.248	0.214	-1.018	203.50
60.69	15.17	8.76	-2.438	0.211	-1.114	222.87
61.12	15.28	9.00	-2.508	0.124	-1.192	238.37
61.44	15.36	9.26	-2.583	0.117	-1.233	246.50
61.65	15.41	9.51	-2.658	0.106	-1.278	255.50
61.76	15.44	9.77	-2.729	0.082	-1.325	265.00
62.05	15.51	10.02	-2.863	0.067	-1.399	279.75
62.08	15.52	10.27	-2.931	0.053	-1.440	288.00
62.24	15.56	10.53	-3.008	0.027	-1.493	298.50
62.26	15.57	10.77	-3.128	0.018	-1.556	311.25
61.25	15.31	10.91	-3.185	0.018	-1.584	316.88

60.26	15.07	10.89	-3.186	0.024	-1.583	316.50
59.19	14.80	10.85	-3.185	0.031	-1.578	315.62
58.07	14.52	10.77	-3.180	0.038	-1.573	314.50
56.95	14.24	10.71	-3.175	0.045	-1.566	313.25
55.91	13.98	10.65	-3.171	0.051	-1.560	312.00
54.90	13.72	10.58	-3.164	0.055	-1.556	311.13
53.75	13.44	10.52	-3.158	0.061	-1.550	310.00
52.66	13.16	10.46	-3.153	0.067	-1.545	309.00
51.59	12.90	10.38	-3.145	0.073	-1.538	307.62
50.41	12.60	10.27	-3.135	0.083	-1.528	305.50
49.19	12.30	10.19	-3.126	0.091	-1.518	303.62
48.07	12.02	10.13	-3.118	0.096	-1.513	302.63
46.92	11.73	10.05	-3.110	0.103	-1.503	300.63
45.80	11.45	9.99	-3.103	0.110	-1.498	299.50
44.60	11.15	9.92	-3.094	0.117	-1.489	297.87
43.55	10.89	9.86	-3.086	0.123	-1.483	296.50
42.43	10.61	9.79	-3.079	0.130	-1.475	295.00
41.39	10.35	9.72	-3.072	0.138	-1.466	293.12
39.90	9.97	9.72	-3.073	0.139	-1.468	293.50
40.99	10.25	9.72	-3.072	0.139	-1.465	293.00
39.87	9.97	9.51	-3.040	0.165	-1.438	287.50
38.80	9.70	9.50	-3.038	0.167	-1.438	287.63
37.66	9.41	9.22	-2.988	0.204	-1.393	278.50
36.08	9.02	9.05	-2.952	0.221	-1.365	273.00
34.83	8.71	8.92	-2.920	0.235	-1.340	268.00
33.39	8.35	8.73	-2.875	0.248	-1.313	262.50
31.92	7.98	8.57	-2.849	0.255	-1.295	259.00
30.40	7.60	8.40	-2.808	0.260	-1.273	254.62
28.77	7.19	8.23	-2.764	0.263	-1.249	249.87
27.17	6.79	8.05	-2.725	0.265	-1.230	246.00
25.35	6.34	7.88	-2.689	0.266	-1.210	242.00
23.49	5.87	7.71	-2.656	0.266	-1.194	238.87
21.62	5.40	7.55	-2.620	0.264	-1.177	235.37
19.72	4.93	7.37	-2.583	0.261	-1.159	231.75
17.95	4.49	7.21	-2.543	0.257	-1.141	228.12
16.32	4.08	7.04	-2.505	0.253	-1.125	225.00
14.75	3.69	6.89	-2.465	0.247	-1.108	221.50
13.32	3.33	6.74	-2.429	0.242	-1.093	218.62
11.89	2.97	6.58	-2.388	0.235	-1.075	215.00
10.57	2.64	6.44	-2.348	0.229	-1.058	211.62
9.33	2.33	6.29	-2.308	0.221	-1.043	208.50
7.90	1.97	6.12	-2.258	0.212	-1.021	204.12
6.50	1.63	5.92	-2.204	0.201	-1.000	200.00
5.18	1.29	5.72	-2.018	0.190	-0.913	182.50
3.95	0.99	5.53	-1.959	0.178	-0.889	177.75
2.77	0.69	5.34	-1.903	0.165	-0.867	173.37
1.50	0.37	5.11	-1.832	0.195	-0.816	163.25

0.33	0.08	5.02	-1.795	0.197	-0.800	160.00
-2.24	-0.56	4.95	-1.776	0.191	-0.793	158.50
-1.14	-0.28	4.94	-1.775	0.191	-0.793	158.50
-0.40	-0.10	4.93	-1.773	0.190	-0.791	158.13

Series 2 - Silica Fume, 5 % Corrosion

Load (kN)	Moment (kN-m)	M.P. Displ. (mm)	E. Curv. LVDT (mm)	W. Curv. LVDT (mm)	Curv. LVDT Avg. (mm)	Curvature (1/km)
0.76	0.19	0.00	***	***	***	0.00
0.09	0.02	-0.02	***	***	***	-0.18
1.21	0.30	0.02	***	***	***	0.11
2.29	0.57	0.03	***	***	***	0.18
3.38	0.85	0.05	***	***	***	0.40
4.42	1.11	0.07	***	***	***	0.55
5.50	1.38	0.12	***	***	***	0.84
6.55	1.64	0.14	***	***	***	1.02
7.58	1.89	0.18	***	***	***	1.27
8.64	2.16	0.20	***	***	***	1.42
9.72	2.43	0.22	***	***	***	1.60
10.79	2.70	0.25	***	***	***	1.82
11.87	2.97	0.28	***	***	***	2.00
12.99	3.25	0.31	***	***	***	2.25
14.09	3.52	0.34	***	***	***	2.44
15.12	3.78	0.37	***	***	***	2.65
16.24	4.06	0.38	***	***	***	2.76
17.31	4.33	0.41	***	***	***	2.94
18.37	4.59	0.44	***	***	***	3.16
19.40	4.85	0.48	***	***	***	3.45
18.11	4.53	0.60	***	***	***	4.36
16.41	4.10	0.66	***	***	***	4.76
14.73	3.68	0.70	***	***	***	5.05
13.12	3.28	0.78	***	***	***	5.63
11.61	2.90	0.81	***	***	***	5.89
10.50	2.63	0.83	***	***	***	6.03
9.38	2.34	0.89	***	***	***	6.51
9.28	2.32	1.10	***	***	***	8.00
10.20	2.55	1.30	***	***	***	9.45
11.13	2.78	1.51	***	***	***	10.98
12.18	3.05	1.70	***	***	***	12.32
13.23	3.31	1.88	***	***	***	13.63
14.30	3.58	2.04	***	***	***	14.83
15.42	3.85	2.23	***	***	***	16.25
16.47	4.12	2.44	***	***	***	17.70
17.56	4.39	2.62	***	***	***	19.01
18.62	4.66	2.82	***	***	***	20.47

19.67	4.92	3.02	***	***	***	21.96
20.64	5.16	3.22	***	***	***	23.41
21.67	5.42	3.44	***	***	***	24.97
22.66	5.66	3.68	***	***	***	26.72
23.46	5.86	3.88	***	***	***	28.21
24.10	6.02	4.09	***	***	***	29.73
24.85	6.21	4.29	***	***	***	31.19
25.57	6.39	4.50	***	***	***	32.68
26.05	6.51	4.70	***	***	***	34.13
26.21	6.55	4.90	***	***	***	35.59
25.97	6.49	5.10	***	***	***	37.08
26.21	6.55	5.32	***	***	***	38.64
26.45	6.61	5.54	***	***	***	40.24
26.53	6.63	5.74	***	***	***	41.69
26.66	6.67	5.96	***	***	***	43.29
26.69	6.67	6.16	***	***	***	44.75
26.69	6.67	6.36	***	***	***	46.24
26.69	6.67	6.56	***	***	***	47.65
26.66	6.67	6.78	***	***	***	49.25
26.53	6.63	6.98	***	***	***	50.71
26.45	6.61	7.19	***	***	***	52.23
26.42	6.61	7.40	***	***	***	53.76
26.31	6.58	7.62	***	***	***	55.36
26.29	6.57	7.82	***	***	***	56.82
26.15	6.54	8.03	***	***	***	58.38
26.15	6.54	8.24	***	***	***	59.87
26.07	6.52	8.45	***	***	***	61.43
25.99	6.50	8.66	***	***	***	62.92
25.91	6.48	8.86	***	***	***	64.41
25.83	6.46	9.08	***	***	***	65.98
25.78	6.45	9.28	***	***	***	67.43
25.75	6.44	9.48	***	***	***	68.88
25.62	6.41	9.68	***	***	***	70.34
25.62	6.41	9.90	***	***	***	71.94
25.57	6.39	10.11	***	***	***	73.50
25.54	6.39	10.32	***	***	***	75.03
25.49	6.37	10.52	***	***	***	76.44
25.43	6.36	10.72	***	***	***	77.90
25.35	6.34	10.93	***	***	***	79.42
25.43	6.36	11.14	***	***	***	80.99
25.35	6.34	11.36	***	***	***	82.55
25.35	6.34	11.56	***	***	***	84.00
25.25	6.31	11.76	***	***	***	85.46
25.19	6.30	11.97	***	***	***	86.99
25.11	6.28	12.18	***	***	***	88.51
25.17	6.29	12.38	***	***	***	89.97
25.14	6.29	12.58	***	***	***	91.42

25.09	6.27	12.78	***	***	***	92.87
25.11	6.28	12.99	***	***	***	94.40
25.06	6.27	13.20	***	***	***	95.93
25.06	6.27	13.42	***	***	***	97.53
25.11	6.28	13.62	***	***	***	99.02
25.22	6.31	13.82	***	***	***	100.47
25.17	6.29	14.04	***	***	***	102.03
25.25	6.31	14.24	***	***	***	103.49
25.22	6.31	14.46	***	***	***	105.09
25.30	6.33	14.68	***	***	***	106.69
25.27	6.32	14.89	***	***	***	108.25
25.19	6.30	15.10	***	***	***	109.78
25.22	6.31	15.32	***	***	***	111.34
25.19	6.30	15.54	***	***	***	112.94
25.25	6.31	15.75	***	***	***	114.47
25.25	6.31	16.02	***	***	***	116.43
25.33	6.33	16.23	***	***	***	117.96
25.35	6.34	16.44	***	***	***	119.49
25.33	6.33	16.65	***	***	***	121.06
25.35	6.34	16.86	***	***	***	122.60
25.33	6.33	17.08	***	***	***	124.20
25.35	6.34	17.29	***	***	***	125.73
25.43	6.36	17.51	***	***	***	127.30
25.41	6.35	17.72	***	***	***	128.84
25.43	6.36	17.93	***	***	***	130.34
25.49	6.37	18.14	***	***	***	131.86
25.43	6.36	18.35	***	***	***	133.43
25.51	6.38	18.56	***	***	***	134.95
25.59	6.40	18.79	***	***	***	136.57
25.54	6.39	19.00	***	***	***	138.12
25.57	6.39	19.21	***	***	***	139.63
25.62	6.41	19.42	***	***	***	141.21
25.62	6.41	19.64	***	***	***	142.75
25.59	6.40	19.85	***	***	***	144.29
25.65	6.41	20.06	***	***	***	145.84
25.67	6.42	20.27	***	***	***	147.38
25.65	6.41	20.51	***	***	***	149.10
25.70	6.43	20.73	***	***	***	150.69
25.70	6.43	20.95	***	***	***	152.33
25.78	6.45	21.17	***	***	***	153.93
25.67	6.42	21.41	***	***	***	155.65
25.54	6.39	21.64	***	***	***	157.31
25.38	6.35	21.85	***	***	***	158.86
25.09	6.27	22.07	***	***	***	160.45
25.03	6.26	22.29	***	***	***	162.04
24.50	6.12	22.49	***	***	***	163.51
23.59	5.90	22.71	***	***	***	165.11

22.79	5.70	22.93	***	***	***	166.70
22.68	5.67	23.14	***	***	***	168.26
23.01	5.75	23.36	***	***	***	169.80
23.41	5.85	23.56	***	***	***	171.26
23.78	5.94	23.78	***	***	***	172.89
23.91	5.98	23.99	***	***	***	174.43
23.99	6.00	24.22	***	***	***	176.04
23.97	5.99	24.44	***	***	***	177.64
23.99	6.00	24.66	***	***	***	179.24
24.05	6.01	24.87	***	***	***	180.80
24.10	6.02	25.10	***	***	***	182.44
24.07	6.02	25.32	***	***	***	184.08
24.10	6.02	25.54	***	***	***	185.64
24.13	6.03	25.75	***	***	***	187.20
24.18	6.04	25.97	***	***	***	188.77
24.15	6.04	26.20	***	***	***	190.44
24.18	6.04	26.40	***	***	***	191.93
24.18	6.04	26.62	***	***	***	193.49
24.18	6.04	26.82	***	***	***	194.98
24.23	6.06	27.12	***	***	***	197.13
24.18	6.04	27.32	***	***	***	198.58
24.15	6.04	27.53	***	***	***	200.11
24.13	6.03	27.74	***	***	***	201.63
24.15	6.04	27.94	***	***	***	203.09
24.21	6.05	28.14	***	***	***	204.58
24.13	6.03	28.38	***	***	***	206.29
24.15	6.04	28.60	***	***	***	207.92
24.18	6.04	28.82	***	***	***	209.49
24.15	6.04	29.04	***	***	***	211.12
24.26	6.06	29.26	***	***	***	212.68
24.31	6.08	29.48	***	***	***	214.28
24.42	6.10	29.70	***	***	***	215.92
24.42	6.10	29.94	***	***	***	217.63
24.45	6.11	30.28	***	***	***	220.10
24.42	6.10	30.52	***	***	***	221.84
24.50	6.12	30.74	***	***	***	223.44
24.45	6.11	30.98	***	***	***	225.22
24.47	6.12	31.22	***	***	***	226.93
24.50	6.12	31.46	***	***	***	228.68
24.61	6.15	31.70	***	***	***	230.42
24.61	6.15	31.95	***	***	***	232.28
24.69	6.17	32.18	***	***	***	233.95
24.63	6.16	32.45	***	***	***	235.91
24.69	6.17	32.70	***	***	***	237.69
24.74	6.18	32.94	***	***	***	239.44
24.71	6.18	33.16	***	***	***	241.04
24.82	6.20	33.40	***	***	***	242.78

24.82	6.20	33.72	***	***	***	245.11
24.90	6.22	33.95	***	***	***	246.78
24.87	6.22	34.18	***	***	***	248.45
24.93	6.23	34.39	***	***	***	249.98
25.03	6.26	34.63	***	***	***	251.72
25.03	6.26	34.86	***	***	***	253.43
25.03	6.26	35.10	***	***	***	255.14
25.03	6.26	35.32	***	***	***	256.74
25.09	6.27	35.56	***	***	***	258.52
25.03	6.26	35.80	***	***	***	260.27
25.03	6.26	36.04	***	***	***	262.01
25.03	6.26	36.28	***	***	***	263.76
25.03	6.26	36.51	***	***	***	265.39
25.09	6.27	36.76	***	***	***	267.21
25.11	6.28	37.01	***	***	***	269.06
25.11	6.28	37.26	***	***	***	270.84
25.17	6.29	37.50	***	***	***	272.59
25.17	6.29	37.75	***	***	***	274.44
25.25	6.31	38.00	***	***	***	276.22
25.27	6.32	38.24	***	***	***	277.97
25.33	6.33	38.47	***	***	***	279.64
25.30	6.33	38.83	***	***	***	282.29
25.33	6.33	39.06	***	***	***	283.97
25.38	6.35	39.30	***	***	***	285.67
25.38	6.35	39.55	***	***	***	287.49
25.38	6.35	39.77	***	***	***	289.13
25.41	6.35	40.02	***	***	***	290.91
25.43	6.36	40.27	***	***	***	292.76
25.43	6.36	40.51	***	***	***	294.47
25.46	6.37	40.73	***	***	***	296.11
25.49	6.37	40.96	***	***	***	297.74
25.49	6.37	41.19	***	***	***	299.45
25.46	6.37	41.42	***	***	***	301.09
25.49	6.37	41.66	***	***	***	302.87
25.54	6.39	41.90	***	***	***	304.58
25.51	6.38	42.14	***	***	***	306.32
25.46	6.37	42.36	***	***	***	307.92
24.45	6.11	42.47	***	***	***	308.72
23.25	5.81	42.46	***	***	***	308.65
22.10	5.52	42.28	***	***	***	307.34
20.92	5.23	42.10	***	***	***	306.03
19.81	4.95	41.90	***	***	***	304.58
18.71	4.68	41.70	***	***	***	303.12
17.66	4.42	41.48	***	***	***	301.52
16.75	4.19	41.26	***	***	***	299.96
15.95	3.99	41.06	***	***	***	298.47
15.21	3.80	40.86	***	***	***	297.05

14.66	3.66	40.68	***	***	***	295.71
14.32	3.58	40.10	***	***	***	291.49
13.21	3.30	39.68	***	***	***	288.44
12.13	3.03	39.69	***	***	***	288.51
11.57	2.89	39.06	***	***	***	283.93
9.76	2.44	37.06	***	***	***	269.39
7.16	1.79	35.19	***	***	***	255.79
4.65	1.16	33.82	***	***	***	245.84
2.86	0.71	33.78	***	***	***	245.54
1.59	0.40	33.72	***	***	***	245.11
0.44	0.11	33.70	***	***	***	244.96
0.11	0.03	33.56	***	***	***	243.94

*** Curvature based on Midpoint Deflection as problem with data acquisition.

Series 2 - Silica Fume, 8 % Corrosion

Load (kN)	Moment (kN-m)	M.P. Displ. (mm)	E. Curv. LVDT (mm)	W. Curv. LVDT (mm)	Curv. LVDT Avg. (mm)	Curvature (1/km)
-0.31	-0.08	0.00	0.005	-0.011	-0.010	1.98
1.62	0.40	-0.00	0.010	-0.009	-0.013	2.58
0.18	0.04	0.00	0.010	-0.003	-0.009	1.72
1.29	0.32	0.02	0.004	-0.058	-0.009	1.87
2.44	0.61	0.06	0.010	-0.007	-0.013	2.55
3.51	0.88	0.08	0.006	-0.105	-0.065	12.98
4.57	1.14	0.11	0.022	-0.109	-0.063	12.53
5.58	1.39	0.13	0.007	-0.108	-0.063	12.58
6.65	1.66	0.16	-0.013	-0.118	-0.068	13.52
7.67	1.92	0.20	0.009	-0.156	-0.064	12.73
8.72	2.18	0.21	0.002	-0.109	-0.064	12.80
9.78	2.44	0.23	0.005	-0.113	-0.065	12.90
10.80	2.70	0.26	0.007	-0.171	-0.068	13.65
11.85	2.96	0.28	-0.003	-0.093	-0.069	13.80
12.96	3.24	0.32	-0.001	-0.111	-0.066	13.20
14.07	3.52	0.34	-0.005	-0.092	-0.070	13.95
15.09	3.77	0.38	-0.003	-0.177	-0.075	14.90
16.20	4.05	0.39	-0.002	-0.071	-0.067	13.45
17.26	4.31	0.43	-0.009	-0.035	-0.072	14.37
18.39	4.60	0.46	-0.011	-0.193	-0.074	14.80
19.46	4.87	0.48	-0.013	-0.108	-0.070	13.92
20.55	5.14	0.52	0.003	-0.111	-0.071	14.17
19.10	4.78	0.64	-0.004	-0.114	-0.075	14.90
17.19	4.30	0.68	-0.006	-0.131	-0.080	16.05
15.84	3.96	0.70	-0.008	-0.142	-0.085	16.90
14.60	3.65	0.72	0.005	-0.186	-0.092	18.48

13.45	3.36	0.77	0.006	-0.142	-0.079	15.80
12.33	3.08	0.88	0.011	-0.149	-0.084	16.87
12.01	3.00	1.08	-0.009	-0.170	-0.085	16.93
12.80	3.20	1.28	0.005	-0.175	-0.089	17.73
13.83	3.46	1.45	-0.003	-0.321	-0.098	19.57
14.91	3.73	1.62	0.014	-0.192	-0.093	18.62
15.96	3.99	1.78	0.029	-0.221	-0.095	19.08
17.09	4.27	1.92	0.031	-0.157	-0.104	20.70
18.12	4.53	2.07	0.038	-0.211	-0.097	19.47
19.17	4.79	2.22	0.055	-0.235	-0.100	20.00
20.24	5.06	2.37	0.059	-0.227	-0.097	19.43
21.31	5.33	2.53	0.059	-0.231	-0.096	19.23
22.42	5.60	2.68	0.102	-0.240	-0.098	19.62
23.41	5.85	2.83	0.112	-0.240	-0.098	19.52
24.50	6.12	2.98	0.071	-0.320	-0.095	18.90
25.59	6.40	3.15	0.115	-0.214	-0.095	18.93
26.61	6.65	3.32	0.112	-0.225	-0.092	18.35
27.62	6.91	3.47	0.150	-0.250	-0.095	19.08
28.64	7.16	3.64	0.110	-0.369	-0.097	19.43
29.65	7.41	3.81	0.140	-0.276	-0.101	20.10
30.69	7.67	3.99	0.102	-0.274	-0.101	20.12
31.73	7.93	4.18	0.112	-0.292	-0.103	20.68
32.69	8.17	4.37	0.046	-0.298	-0.116	23.12
33.57	8.39	4.56	0.060	-0.284	-0.123	24.62
34.59	8.65	4.78	0.075	-0.302	-0.141	28.20
35.41	8.85	4.98	0.056	-0.357	-0.127	25.42
36.24	9.06	5.18	0.080	-0.342	-0.140	28.07
36.99	9.25	5.38	0.064	-0.413	-0.170	33.93
37.50	9.37	5.58	0.051	-0.420	-0.196	39.27
37.84	9.46	5.77	0.037	-0.397	-0.178	35.53
38.30	9.57	5.97	0.022	-0.393	-0.201	40.15
38.72	9.68	6.17	0.009	-0.456	-0.217	43.42
39.28	9.82	6.37	-0.015	-0.427	-0.236	47.15
39.66	9.91	6.58	0.009	-0.448	-0.232	46.40
39.82	9.95	6.79	-0.020	-0.503	-0.255	50.95
39.82	9.95	6.98	-0.038	-0.439	-0.265	52.95
39.95	9.99	7.19	-0.045	-0.444	-0.283	56.60
40.35	10.09	7.39	-0.079	-0.516	-0.327	65.30
40.43	10.11	7.60	-0.095	-0.526	-0.323	64.62
40.38	10.09	7.80	-0.126	-0.573	-0.348	69.50
40.03	10.01	8.00	-0.152	-0.565	-0.369	73.73
39.10	9.77	8.21	-0.176	-0.585	-0.393	78.50
37.98	9.49	8.41	-0.206	-0.605	-0.436	87.27
37.04	9.26	8.63	-0.210	-0.580	-0.431	86.15
36.56	9.14	8.87	-0.277	-0.685	-0.492	98.40
36.03	9.01	9.12	-0.357	-0.741	-0.539	107.80
34.67	8.67	9.30	-0.406	-0.662	-0.574	114.72

33.73	8.43	9.34	-0.418	-0.691	-0.595	118.97
32.53	8.13	9.43	-0.436	-0.748	-0.602	120.32
31.65	7.91	9.63	-0.462	-0.737	-0.617	123.37
31.31	7.83	9.83	-0.490	-0.785	-0.655	130.90
30.72	7.68	10.03	-0.523	-0.831	-0.690	138.00
30.26	7.57	10.24	-0.557	-0.827	-0.727	145.37
29.78	7.45	10.44	-0.559	-0.849	-0.756	151.15
29.54	7.39	10.63	-0.593	-0.924	-0.784	156.80
29.20	7.30	10.84	-0.626	-0.961	-0.820	164.03
28.82	7.21	11.06	-0.652	-1.020	-0.849	169.78
28.58	7.15	11.26	-0.657	-1.109	-0.878	175.65
28.21	7.05	11.48	-0.692	-1.099	-0.913	182.60
27.92	6.98	11.70	-0.732	-1.141	-0.947	189.30
27.73	6.93	11.90	-0.764	-1.168	-0.983	196.62
27.62	6.91	12.13	-0.770	-1.204	-1.005	201.00
27.41	6.85	12.34	-0.789	-1.241	-1.034	206.75
27.30	6.83	12.54	-0.820	-1.288	-1.060	212.00
27.03	6.76	12.74	-0.846	-1.270	-1.094	218.75
26.93	6.73	12.94	-0.871	-1.335	-1.118	223.50
26.77	6.69	13.18	-0.886	-1.365	-1.140	228.00
26.55	6.64	13.38	-0.923	-1.408	-1.171	234.25
26.37	6.59	13.59	-0.934	-1.440	-1.201	240.25
26.26	6.57	13.79	-0.957	-1.473	-1.229	245.75
26.02	6.51	14.00	-0.948	-1.493	-1.268	253.50
25.86	6.47	14.20	-1.047	-1.599	-1.283	256.50
25.75	6.44	14.40	-1.044	-1.555	-1.314	262.75
25.62	6.41	14.60	-1.013	-1.589	-1.350	270.00
25.51	6.38	14.80	-1.110	-1.615	-1.381	276.25
25.30	6.33	15.00	-1.128	-1.635	-1.396	279.25
25.19	6.30	15.20	-1.185	-1.668	-1.438	287.50
25.09	6.27	15.40	-1.196	-1.685	-1.465	293.00
25.19	6.30	15.59	-1.231	-1.710	-1.481	296.25
25.06	6.27	15.80	-1.203	-1.729	-1.490	298.00
24.90	6.22	15.99	-1.256	-1.794	-1.519	303.75
24.74	6.18	16.19	-1.268	-1.786	-1.544	308.75
24.61	6.15	16.38	-1.301	-1.804	-1.576	315.25
24.42	6.10	16.59	-1.330	-1.823	-1.586	317.25
24.31	6.08	16.78	-1.276	-1.819	-1.615	323.00
24.21	6.05	17.00	-1.374	-1.899	-1.646	329.25
24.15	6.04	17.21	-1.343	-1.878	-1.666	333.25
24.13	6.03	17.42	-1.401	-1.940	-1.689	337.75
24.05	6.01	17.63	-1.405	-1.948	-1.734	346.75
24.15	6.04	17.82	-1.410	-1.966	-1.748	349.50
24.26	6.06	18.04	-1.514	-2.015	-1.784	356.75
23.94	5.98	18.24	-1.548	-2.020	-1.816	363.25
23.94	5.98	18.44	-1.575	-2.045	-1.825	365.00
23.99	6.00	18.64	-1.605	-2.068	-1.850	370.00

23.62	5.90	18.84	-1.590	-2.081	-1.854	370.75
23.75	5.94	19.06	-1.620	-2.100	-1.875	375.00
23.89	5.97	19.25	-1.666	-2.099	-1.909	381.75
23.65	5.91	19.45	-1.685	-2.110	-1.931	386.25
23.81	5.95	19.65	-1.716	-2.163	-1.960	392.00
23.73	5.93	19.85	-1.721	-2.180	-1.968	393.50
23.62	5.90	20.04	-1.753	-2.195	-1.988	397.50
23.62	5.90	20.25	-1.768	-2.164	-1.996	399.25
23.33	5.83	20.48	-1.794	-2.259	-2.025	405.00
23.22	5.80	20.67	-1.823	-2.201	-2.056	411.25
23.25	5.81	20.86	-1.855	-2.258	-2.076	415.25
22.98	5.74	21.05	-1.845	-2.274	-2.078	415.50
23.27	5.82	21.25	-1.880	-2.314	-2.113	422.50
22.98	5.74	21.46	-1.910	-2.306	-2.110	422.00
22.76	5.69	21.67	-1.938	-2.328	-2.134	426.75
22.66	5.66	21.87	-1.949	-2.284	-2.120	424.00
22.44	5.61	22.06	-1.978	-2.308	-2.159	431.75
22.26	5.56	22.27	-1.991	-2.298	-2.156	431.25
22.26	5.56	22.46	-2.010	-2.306	-2.161	432.25
21.56	5.39	22.68	-2.033	-2.275	-2.188	437.50
21.16	5.29	22.87	-2.058	-2.298	-2.213	442.50
20.87	5.22	23.07	-2.083	-2.293	-2.206	441.25
20.34	5.08	23.25	-2.084	-2.308	-2.205	441.00
20.32	5.08	23.46	-2.110	-2.309	-2.221	444.25
20.32	5.08	23.66	-2.130	-2.296	-2.244	448.75
20.17	5.04	23.86	-2.120	-2.319	-2.229	445.75
20.38	5.10	24.05	-2.138	-2.311	-2.250	450.00
20.02	5.00	24.25	-2.140	-2.348	-2.250	450.00
20.27	5.07	24.45	-2.156	-2.334	-2.281	456.25
19.93	4.98	24.65	-2.178	-2.333	-2.274	454.75
20.20	5.05	24.84	-2.169	-2.340	-2.273	454.50
20.15	5.04	25.05	-2.196	-2.349	-2.294	458.75
20.13	5.03	25.26	-2.208	-2.378	-2.305	461.00
20.00	5.00	25.45	-2.231	-2.384	-2.319	463.75
20.07	5.02	25.66	-2.245	-2.388	-2.339	467.75
19.99	5.00	25.86	-2.280	-2.409	-2.356	471.25
19.78	4.94	26.05	-2.290	-2.420	-2.374	474.75
20.05	5.01	26.25	-2.246	-2.434	-2.354	470.75
20.11	5.03	26.43	-2.266	-2.439	-2.389	477.75
19.63	4.91	26.63	-2.296	-2.455	-2.389	477.75
19.79	4.95	26.83	-2.305	-2.471	-2.405	481.00
19.92	4.98	27.04	-2.318	-2.486	-2.415	483.00
19.46	4.86	27.25	-2.335	-2.501	-2.438	487.50
19.55	4.89	27.45	-2.366	-2.506	-2.446	489.25
19.53	4.88	27.65	-2.338	-2.530	-2.453	490.50
19.42	4.86	27.85	-2.359	-2.546	-2.473	494.50
19.42	4.86	28.03	-2.385	-2.560	-2.495	499.00

19.27	4.82	28.23	-2.378	-2.581	-2.500	500.00
19.25	4.81	28.42	-2.413	-2.593	-2.520	504.00
19.38	4.85	28.63	-2.424	-2.615	-2.534	506.75
19.32	4.83	28.83	-2.428	-2.594	-2.525	505.00
19.24	4.81	29.03	-2.444	-2.611	-2.554	510.75
19.12	4.78	29.25	-2.466	-2.628	-2.568	513.50
19.17	4.79	29.46	-2.489	-2.639	-2.589	517.75
19.03	4.76	29.65	-2.506	-2.658	-2.599	519.75
19.01	4.75	29.85	-2.451	-2.678	-2.585	517.00
18.86	4.72	30.06	-2.476	-2.685	-2.593	518.50
19.00	4.75	30.26	-2.509	-2.705	-2.628	525.50
18.99	4.75	30.46	-2.523	-2.724	-2.646	529.25
18.79	4.70	30.66	-2.544	-2.746	-2.683	536.50
18.74	4.69	30.87	-2.569	-2.781	-2.684	536.75
18.79	4.70	31.06	-2.600	-2.801	-2.705	541.00
18.70	4.67	31.27	-2.615	-2.816	-2.739	547.75
18.52	4.63	31.48	-2.623	-2.844	-2.744	548.75
18.63	4.66	31.70	-2.646	-2.878	-2.780	556.00
18.39	4.60	31.91	-2.680	-2.926	-2.814	562.75
18.52	4.63	32.11	-2.678	-2.956	-2.836	567.25
18.43	4.61	32.29	-2.703	-2.915	-2.829	565.75
18.34	4.58	32.48	-2.736	-2.923	-2.843	568.50
18.26	4.56	32.69	-2.759	-2.961	-2.880	576.00
18.60	4.65	32.90	-2.785	-2.986	-2.905	581.00
18.44	4.61	33.09	-2.810	-3.013	-2.933	586.50
18.04	4.51	33.29	-2.846	-3.048	-2.960	592.00
17.98	4.49	33.50	-2.803	-3.071	-2.943	588.50
18.12	4.53	33.70	-2.825	-3.094	-2.985	597.00
18.27	4.57	33.91	-2.860	-3.139	-3.009	601.75
18.28	4.57	34.11	-2.883	-3.159	-3.053	610.50
18.32	4.58	34.33	-2.914	-3.169	-3.078	615.50
18.33	4.58	34.53	-2.930	-3.231	-3.096	619.25
18.29	4.57	34.74	-2.933	-3.264	-3.123	624.50
18.41	4.60	34.94	-2.979	-3.294	-3.166	633.25
18.36	4.59	35.15	-3.006	-3.306	-3.194	638.75
18.33	4.58	35.34	-3.035	-3.348	-3.206	641.25
18.38	4.60	35.55	-3.059	-3.368	-3.240	648.00
18.50	4.63	35.76	-3.065	-3.405	-3.253	650.50
18.44	4.61	35.97	-3.091	-3.434	-3.278	655.50
18.59	4.65	36.18	-3.144	-3.468	-3.326	665.25
18.53	4.63	36.39	-3.160	-3.504	-3.364	672.75
18.65	4.66	36.60	-3.220	-3.519	-3.361	672.25
18.48	4.62	36.83	-3.220	-3.556	-3.405	681.00
18.68	4.67	37.05	-3.269	-3.594	-3.450	690.00
18.55	4.64	37.26	-3.261	-3.640	-3.473	694.50
18.61	4.65	37.47	-3.296	-3.661	-3.506	701.25
18.68	4.67	37.68	-3.334	-3.701	-3.533	706.50

18.63	4.66	37.88	-3.351	-3.728	-3.549	709.75
18.73	4.68	38.08	-3.393	-3.739	-3.598	719.50
18.69	4.67	38.28	-3.359	-3.766	-3.585	717.00
18.78	4.69	38.45	-3.408	-3.795	-3.625	725.00
18.78	4.69	38.65	-3.401	-3.831	-3.656	731.25
18.84	4.71	38.86	-3.430	-3.839	-3.658	731.50
18.91	4.73	39.07	-3.464	-3.881	-3.694	738.75
18.82	4.71	39.28	-3.505	-3.910	-3.710	742.00
18.80	4.70	39.48	-3.525	-3.925	-3.748	749.50
18.84	4.71	39.69	-3.539	-3.955	-3.768	753.50
18.92	4.73	39.90	-3.569	-3.994	-3.796	759.25
18.72	4.68	40.08	-3.604	-4.024	-3.843	768.50
18.88	4.72	40.28	-3.600	-4.026	-3.863	772.50
18.86	4.72	40.51	-3.620	-4.083	-3.878	775.50
18.80	4.70	40.72	-3.644	-4.114	-3.905	781.00
18.89	4.72	40.92	-3.690	-4.110	-3.895	779.00
18.87	4.72	41.14	-3.698	-4.131	-3.924	784.75
18.94	4.74	41.34	-3.720	-4.168	-3.975	795.00
18.93	4.73	41.55	-3.746	-4.206	-3.989	797.75
19.05	4.76	41.76	-3.774	-4.241	-4.015	803.00
19.00	4.75	41.96	-3.783	-4.251	-4.019	803.75
19.08	4.77	42.17	-3.820	-4.281	-4.039	807.75
18.96	4.74	42.37	-3.831	-4.300	-4.104	820.75
19.01	4.75	42.56	-3.858	-4.340	-4.114	822.75
19.14	4.79	42.76	-3.871	-4.356	-4.140	828.00
19.20	4.80	43.00	-3.893	-4.381	-4.150	830.00
19.19	4.80	43.20	-3.928	-4.421	-4.193	838.50
18.83	4.71	43.40	-3.931	-4.439	-4.204	840.75
17.85	4.46	43.56	-3.929	-4.479	-4.239	847.75
16.72	4.18	43.71	-3.958	-4.516	-4.229	845.75
15.47	3.87	43.81	-3.965	-4.568	-4.288	857.50
14.42	3.61	43.91	-3.974	-4.588	-4.291	858.25
13.95	3.49	44.11	-3.990	-4.624	-4.306	861.25
13.84	3.46	44.32	-4.015	-4.654	-4.356	871.25
13.94	3.49	44.53	-4.036	-4.674	-4.379	875.75
13.89	3.47	44.74	-4.004	-4.694	-4.364	872.75
13.92	3.48	44.99	-4.014	-4.738	-4.385	877.00
14.21	3.55	45.20	-4.043	-4.755	-4.431	886.25
14.37	3.59	45.41	-4.056	-4.778	-4.423	884.50
14.35	3.59	45.62	-4.076	-4.790	-4.435	887.00
13.18	3.29	45.54	-4.060	-4.796	-4.443	888.50
11.81	2.95	45.36	-4.055	-4.781	-4.421	884.25
10.75	2.69	45.17	-4.038	-4.778	-4.421	884.25
9.93	2.48	45.03	-4.028	-4.765	-4.420	884.00
9.11	2.28	44.16	-3.954	-4.681	-4.341	868.25
7.84	1.96	43.59	-3.944	-4.651	-4.301	860.25
6.78	1.69	43.60	-3.954	-4.641	-4.316	863.25

5.67	1.42	42.95	-3.890	-4.585	-4.255	851.00
4.81	1.20	41.11	-3.729	-4.513	-4.143	828.50
3.63	0.91	39.57	-3.608	-4.416	-4.044	808.75
2.58	0.65	38.22	-3.514	-4.348	-3.923	784.50
1.81	0.45	36.84	-3.485	-4.286	-3.866	773.25
1.14	0.29	36.38	-3.465	-4.265	-3.868	773.50
0.15	0.04	36.28	-3.443	-4.266	-3.886	777.25

Series 2 - Silica Fume, 10 % Corrosion

Load (kN)	Moment (kN-m)	M.P. Displ. (mm)	E. Curv. LVDT (mm)	W. Curv. LVDT (mm)	Curv. LVDT Avg. (mm)	Curvature (1/km)
0.00	0.00	0.00	****	****	****	0.00
3.13	0.78	0.01	****	****	****	0.05
9.50	2.38	0.14	****	****	****	1.02
16.13	4.03	0.29	****	****	****	2.10
19.30	4.82	0.34	****	****	****	2.50
20.81	5.20	0.40	****	****	****	2.93
20.09	5.02	0.50	****	****	****	3.61
18.48	4.62	0.59	****	****	****	4.27
16.57	4.14	0.63	****	****	****	4.59
14.42	3.60	0.66	****	****	****	4.78
12.17	3.04	0.69	****	****	****	5.03
9.72	2.43	0.73	****	****	****	5.34
8.49	2.12	0.75	****	****	****	5.43
7.43	1.86	0.88	****	****	****	6.40
6.56	1.64	1.17	****	****	****	8.51
5.79	1.45	1.43	****	****	****	10.40
5.35	1.34	1.56	****	****	****	11.37
6.21	1.55	2.09	****	****	****	15.19
7.05	1.76	2.78	****	****	****	20.21
7.37	1.84	3.16	****	****	****	22.98
8.51	2.13	3.85	****	****	****	28.01
9.21	2.30	4.16	****	****	****	30.21
10.12	2.53	4.50	****	****	****	32.70
9.96	2.49	4.92	****	****	****	35.75
8.65	2.16	5.60	****	****	****	40.68
7.01	1.75	6.22	****	****	****	45.20
6.31	1.58	6.53	****	****	****	47.49
4.61	1.15	7.32	****	****	****	53.23
3.85	0.96	8.00	****	****	****	58.17
3.40	0.85	8.41	****	****	****	61.15
3.82	0.96	9.05	****	****	****	65.82
2.94	0.74	9.61	****	****	****	69.90
3.23	0.81	10.43	****	****	****	75.83
3.25	0.81	10.84	****	****	****	78.77

2.99	0.75	10.92	****	****	****	79.40
2.97	0.74	11.16	****	****	****	81.13
2.63	0.66	11.29	****	****	****	82.10
2.25	0.56	11.86	****	****	****	86.24
1.74	0.43	13.35	****	****	****	97.06
1.41	0.35	14.47	****	****	****	105.23
1.65	0.41	15.35	****	****	****	111.63
1.65	0.41	16.10	****	****	****	117.04
1.85	0.46	16.96	****	****	****	123.32
1.89	0.47	17.68	****	****	****	128.56
1.90	0.48	18.77	****	****	****	136.45
1.89	0.47	19.55	****	****	****	142.09
1.87	0.47	19.95	****	****	****	145.03

**** Curvature based upon Midpoint deflection as problem with data acquistion

Series 3 - 14.5 % Corrosion

Load (kN)	Moment (kN-m)	M.P. Displ. (mm)	E. Curv. LVDT (mm)	W. Curv. LVDT (mm)	Curv. LVDT Avg. (mm)	Curvature (1/km)
0.84	0.21	0.00	0.004	0.003	-0.007	-0.68
1.88	0.47	0.01	-0.004	0.007	-0.006	-1.43
2.80	0.70	0.04	0.007	-0.002	-0.006	0.48
3.87	0.97	0.04	0.002	-0.006	-0.006	1.15
4.93	1.23	0.09	0.003	0.001	-0.008	-0.20
5.93	1.48	0.12	0.006	-0.001	-0.007	0.12
6.99	1.75	0.14	0.006	0.002	-0.007	-0.48
8.06	2.02	0.18	0.005	0.000	-0.007	-0.05
7.97	1.99	0.18	0.003	-0.004	-0.007	0.88
8.96	2.24	0.20	0.006	0.000	-0.007	0.00
9.79	2.45	0.21	0.005	-0.004	-0.006	0.80
9.97	2.49	0.24	-0.003	-0.002	-0.006	0.35
10.53	2.63	0.22	0.004	0.002	-0.006	-0.35
11.64	2.91	0.26	0.006	-0.000	-0.007	0.08
12.97	3.24	0.29	-0.000	-0.002	-0.007	0.48
14.17	3.54	0.30	0.008	-0.007	-0.007	1.35
15.43	3.86	0.31	0.003	-0.008	-0.007	1.65
16.52	4.13	0.30	0.008	-0.001	-0.007	0.28
17.76	4.44	0.30	0.004	-0.000	-0.006	0.03
18.87	4.72	0.30	0.004	-0.006	-0.006	1.10
20.14	5.03	0.31	0.006	-0.007	-0.006	1.35
19.04	4.76	0.33	0.009	-0.003	-0.007	0.60
20.17	5.04	0.35	0.007	-0.007	-0.007	1.45
21.48	5.37	0.39	0.005	-0.014	-0.008	2.75
20.31	5.08	0.37	0.012	-0.009	-0.007	1.75
21.54	5.38	0.40	0.012	-0.012	-0.008	2.45
22.82	5.70	0.42	0.008	-0.008	-0.008	1.50
23.97	5.99	0.41	0.012	-0.005	-0.008	1.05
25.14	6.29	0.42	0.007	-0.007	-0.009	1.35
26.23	6.56	0.41	0.004	-0.006	-0.007	1.15
26.85	6.71	0.41	0.011	-0.005	-0.008	0.98
25.54	6.39	0.41	0.009	-0.006	-0.007	1.15
26.42	6.61	0.41	0.008	-0.009	-0.008	1.83
24.10	6.02	0.41	0.009	-0.006	-0.008	1.20
25.19	6.30	0.42	0.010	-0.007	-0.008	1.37
27.01	6.75	0.42	0.012	-0.014	-0.008	2.80
25.65	6.41	0.42	0.007	-0.005	-0.006	1.07
26.69	6.67	0.44	0.003	-0.003	-0.008	0.65
25.49	6.37	0.43	0.005	-0.014	-0.008	2.70
27.20	6.80	0.43	0.009	-0.007	-0.009	1.30
26.15	6.54	0.43	0.007	-0.010	-0.008	1.98
27.49	6.87	0.46	0.007	-0.007	-0.010	1.40
25.99	6.50	0.45	0.012	-0.013	-0.008	2.55
24.95	6.24	0.44	0.007	-0.012	-0.008	2.37

26.21	6.55	0.46	0.006	-0.016	-0.008	3.28
25.14	6.29	0.46	0.009	-0.007	-0.009	1.37
24.15	6.04	0.45	0.009	-0.007	-0.009	1.48
25.19	6.30	0.47	0.009	-0.007	-0.009	1.40
24.07	6.02	0.46	0.009	-0.007	-0.009	1.35
25.17	6.29	0.48	0.011	-0.007	-0.009	1.35
26.26	6.57	0.49	0.010	-0.014	-0.009	2.78
25.14	6.29	0.48	0.009	-0.007	-0.010	1.43
24.05	6.01	0.48	0.003	-0.014	-0.009	2.88
25.14	6.29	0.51	0.008	-0.008	-0.010	1.57
26.34	6.59	0.53	0.010	-0.012	-0.010	2.37
27.65	6.91	0.55	0.004	-0.011	-0.011	2.18
28.85	7.21	0.57	0.007	-0.010	-0.012	1.93
29.92	7.48	0.54	0.004	-0.013	-0.010	2.50
31.04	7.76	0.58	0.005	-0.007	-0.011	1.32
29.94	7.49	0.57	0.008	-0.010	-0.011	1.93
31.01	7.75	0.62	0.002	-0.018	-0.011	3.52
32.16	8.04	0.67	0.004	-0.010	-0.011	2.08
33.20	8.30	0.72	0.002	-0.003	-0.011	0.58
34.32	8.58	0.75	0.003	-0.011	-0.013	2.13
34.75	8.69	0.98	0.001	-0.036	-0.025	7.25
36.03	9.01	1.05	-0.012	-0.039	-0.031	7.80
37.18	9.29	1.10	-0.005	-0.038	-0.031	7.58
38.32	9.58	1.17	0.000	-0.046	-0.032	9.18
39.36	9.84	1.21	0.003	-0.045	-0.032	9.05
40.62	10.15	1.25	0.009	-0.062	-0.033	12.30
39.55	9.89	1.27	0.007	-0.054	-0.034	10.72
40.62	10.15	1.44	0.012	-0.065	-0.038	12.98
41.90	10.48	1.52	0.008	-0.073	-0.040	14.65
42.97	10.74	1.50	0.016	-0.075	-0.039	15.05
41.95	10.49	1.52	0.011	-0.072	-0.041	14.37
43.13	10.78	1.53	0.009	-0.080	-0.040	16.08
44.36	11.09	1.56	0.007	-0.077	-0.041	15.40
45.50	11.38	1.56	0.014	-0.075	-0.040	15.03
46.49	11.62	1.56	0.012	-0.074	-0.043	14.82
45.21	11.30	1.58	0.011	-0.076	-0.042	15.10
46.70	11.68	1.63	0.012	-0.081	-0.042	16.13
47.99	12.00	1.65	0.014	-0.077	-0.043	15.40
46.78	11.70	1.65	0.013	-0.078	-0.043	15.62
45.66	11.42	1.65	0.013	-0.081	-0.045	16.18
44.52	11.13	1.83	0.014	-0.100	-0.052	19.98
44.54	11.14	2.05	0.006	-0.127	-0.063	25.30
45.72	11.43	2.18	0.006	-0.127	-0.069	25.45
46.92	11.73	2.31	0.006	-0.143	-0.075	28.53
48.01	12.00	2.44	0.010	-0.150	-0.079	29.93
49.16	12.29	2.57	0.005	-0.156	-0.085	31.15
50.25	12.56	2.66	0.004	-0.163	-0.088	32.52

51.27	12.82	2.86	-0.006	-0.205	-0.112	40.93
52.44	13.11	2.97	0.001	-0.212	-0.116	42.45
53.14	13.28	3.20	-0.002	-0.230	-0.123	46.05
54.23	13.56	3.32	-0.006	-0.231	-0.126	46.12
54.87	13.72	3.54	-0.006	-0.255	-0.134	50.98
55.91	13.98	3.72	-0.009	-0.260	-0.138	52.08
56.82	14.20	3.91	-0.008	-0.270	-0.144	54.00
57.78	14.44	4.10	-0.006	-0.277	-0.151	55.30
58.13	14.53	4.32	-0.001	-0.299	-0.158	59.80
56.79	14.20	4.16	-0.006	-0.287	-0.150	57.45
54.34	13.58	4.03	0.001	-0.272	-0.146	54.40
52.01	13.00	3.96	0.003	-0.268	-0.142	53.67
50.63	12.66	3.96	0.001	-0.274	-0.143	54.80
49.40	12.35	3.92	-0.001	-0.272	-0.141	54.43
50.47	12.62	4.00	-0.003	-0.271	-0.147	54.15
51.67	12.92	4.07	-0.003	-0.275	-0.150	55.03
52.71	13.18	4.09	-0.004	-0.283	-0.149	56.57
53.86	13.46	4.18	-0.004	-0.283	-0.155	56.60
54.98	13.74	4.22	-0.007	-0.291	-0.155	58.27
56.10	14.02	4.28	-0.005	-0.293	-0.157	58.55
57.14	14.28	4.37	-0.006	-0.291	-0.159	58.10
58.23	14.56	4.53	-0.009	-0.299	-0.165	59.82
59.33	14.83	4.69	-0.010	-0.309	-0.170	61.82
60.42	15.11	4.86	-0.012	-0.312	-0.172	62.48
61.54	15.39	4.99	-0.008	-0.324	-0.175	64.85
62.69	15.67	5.15	-0.012	-0.331	-0.181	66.13
64.00	16.00	5.19	-0.011	-0.334	-0.183	66.83
65.41	16.35	5.35	-0.008	-0.389	-0.218	77.83
62.80	15.70	5.41	-0.017	-0.543	-0.295	108.68
59.62	14.91	5.48	-0.022	-0.651	-0.349	130.25
57.54	14.38	5.48	-0.018	-0.692	-0.368	138.43
55.94	13.98	5.50	-0.024	-0.720	-0.382	143.98
54.60	13.65	5.52	-0.025	-0.744	-0.397	148.72
53.35	13.34	5.66	-0.042	-0.809	-0.434	161.78
51.88	12.97	5.69	-0.031	-0.821	-0.437	164.28
50.65	12.66	5.72	-0.017	-0.838	-0.439	167.58
49.53	12.38	5.79	-0.032	-0.859	-0.458	171.83
47.90	11.98	5.81	-0.038	-0.869	-0.466	173.87
46.81	11.70	5.90	-0.054	-0.897	-0.485	179.45
45.66	11.42	5.98	-0.085	-0.948	-0.522	189.68
44.68	11.17	6.07	-0.086	-0.987	-0.538	197.35
43.63	10.91	6.16	-0.076	-1.000	-0.549	199.97
42.54	10.64	6.27	-0.089	-1.040	-0.567	208.00
41.10	10.27	6.34	-0.086	-1.051	-0.580	210.25
41.53	10.38	6.59	-0.108	-1.116	-0.624	223.25
40.41	10.10	6.77	-0.136	-1.165	-0.665	233.00
39.26	9.81	6.94	-0.179	-1.210	-0.695	242.00

38.00	9.50	7.02	-0.164	-1.238	-0.709	247.50
37.34	9.33	7.26	-0.193	-1.281	-0.749	256.25
36.48	9.12	7.46	-0.201	-1.340	-0.783	268.00
37.20	9.30	7.68	-0.206	-1.398	-0.818	279.50
36.78	9.19	7.92	-0.231	-1.455	-0.857	291.00
35.66	8.91	8.11	-0.248	-1.505	-0.890	301.00
35.23	8.81	8.32	-0.271	-1.545	-0.926	309.00
34.00	8.50	8.35	-0.274	-1.565	-0.933	313.00
33.47	8.37	8.56	-0.310	-1.609	-0.973	321.75
33.31	8.33	8.78	-0.322	-1.675	-1.015	335.00
32.93	8.23	9.02	-0.360	-1.743	-1.059	348.50
32.80	8.20	9.26	-0.377	-1.814	-1.108	362.75
33.25	8.31	9.50	-0.395	-1.839	-1.126	367.75
33.39	8.35	9.72	-0.394	-1.913	-1.171	382.50
32.83	8.21	9.96	-0.428	-1.973	-1.214	394.50
32.08	8.02	10.19	-0.453	-1.975	-1.225	395.00
31.55	7.89	10.43	-0.464	-2.046	-1.265	409.25
31.44	7.86	10.66	-0.474	-2.098	-1.305	419.50
31.47	7.87	10.90	-0.498	-2.165	-1.344	433.00
31.52	7.88	11.13	-0.518	-2.226	-1.385	445.25
31.47	7.87	11.36	-0.554	-2.295	-1.439	459.00
31.36	7.84	11.55	-0.550	-2.226	-1.400	445.25
31.33	7.83	11.75	-0.565	-2.280	-1.435	456.00
31.49	7.87	11.97	-0.630	-2.325	-1.490	465.00
31.65	7.91	12.18	-0.644	-2.378	-1.529	475.50
32.03	8.01	12.39	-0.656	-2.448	-1.576	489.50
32.53	8.13	12.59	-0.669	-2.508	-1.603	501.50
32.61	8.15	12.80	-0.683	-2.531	-1.620	506.25
32.75	8.19	13.01	-0.696	-2.590	-1.655	518.00
33.25	8.31	13.22	-0.709	-2.635	-1.688	527.00
33.89	8.47	13.44	-0.724	-2.708	-1.730	541.50
34.77	8.69	13.64	-0.739	-2.770	-1.768	554.00
34.40	8.60	13.85	-0.751	-2.805	-1.799	561.00
34.88	8.72	14.05	-0.760	-2.859	-1.825	571.75
35.17	8.79	14.25	-0.772	-2.900	-1.850	580.00
35.31	8.83	14.47	-0.784	-2.955	-1.885	591.00
35.60	8.90	14.67	-0.796	-2.966	-1.895	593.25
35.82	8.95	14.91	-0.806	-3.045	-1.936	609.00
35.66	8.91	15.11	-0.823	-3.100	-1.970	620.00
35.44	8.86	15.35	-0.842	-3.151	-2.010	630.25
35.33	8.83	15.55	-0.856	-3.208	-2.048	641.50
35.17	8.79	15.77	-0.869	-3.236	-2.076	647.25
34.64	8.66	15.98	-0.889	-3.285	-2.100	657.00
34.67	8.67	16.19	-0.904	-3.324	-2.130	664.75
34.35	8.59	16.41	-0.932	-3.360	-2.161	672.00
33.71	8.43	16.63	-0.945	-3.398	-2.193	679.50
33.57	8.39	16.85	-0.972	-3.445	-2.225	689.00

33.47	8.37	17.06	-0.992	-3.496	-2.256	699.25
33.57	8.39	17.26	-1.004	-3.528	-2.286	705.50
33.89	8.47	17.47	-1.029	-3.580	-2.315	716.00
34.37	8.59	17.68	-1.040	-3.610	-2.340	722.00
34.91	8.73	17.90	-1.053	-3.654	-2.371	730.75
34.43	8.61	18.11	-1.070	-3.695	-2.400	739.00
34.16	8.54	18.33	-1.078	-3.744	-2.428	748.75
34.21	8.55	18.54	-1.094	-3.788	-2.455	757.50
34.27	8.57	18.76	-1.105	-3.819	-2.479	763.75
34.45	8.61	18.98	-1.120	-3.864	-2.505	772.75
34.64	8.66	19.19	-1.129	-3.903	-2.530	780.50
34.72	8.68	19.41	-1.134	-3.953	-2.560	790.50
34.69	8.67	19.62	-1.155	-3.996	-2.590	799.25
34.80	8.70	19.83	-1.161	-4.039	-2.616	807.75
34.45	8.61	20.05	-1.164	-4.079	-2.641	815.75
33.87	8.47	20.26	-1.170	-4.118	-2.664	823.50
33.63	8.41	20.47	-1.179	-4.173	-2.685	834.50
33.52	8.38	20.69	-1.180	-4.198	-2.705	839.50
33.41	8.35	20.90	-1.183	-4.249	-2.730	849.75
33.23	8.31	21.12	-1.190	-4.275	-2.758	855.00
33.07	8.27	21.33	-1.204	-4.330	-2.780	866.00
32.96	8.24	21.54	-1.206	-4.371	-2.805	874.25
33.07	8.27	21.76	-1.210	-4.410	-2.826	882.00
33.15	8.29	21.97	-1.219	-4.454	-2.850	890.75
33.17	8.29	22.19	-1.215	-4.490	-2.875	898.00
33.23	8.31	22.41	-1.223	-4.538	-2.909	907.50
33.47	8.37	22.62	-1.230	-4.574	-2.918	914.75
33.52	8.38	22.83	-1.238	-4.605	-2.936	921.00
33.52	8.38	23.04	-1.234	-4.640	-2.955	928.00
33.52	8.38	23.25	-1.238	-4.680	-2.974	936.00
33.31	8.33	23.46	-1.230	-4.716	-2.990	943.25
32.24	8.06	23.62	-1.219	-4.391	-2.829	878.25
30.88	7.72	22.33	-1.116	-4.260	-2.694	852.00
21.16	5.29	21.43	-1.079	-4.318	-2.714	863.50
16.46	4.12	21.44	-1.076	-4.244	-2.676	848.75
14.37	3.59	21.46	-1.085	-4.301	-2.720	860.25
13.26	3.31	21.48	-1.084	-4.190	-2.653	838.00
12.78	3.20	20.95	-1.034	-4.135	-2.580	827.00
8.83	2.21	19.59	-0.866	-4.049	-2.471	809.75
4.60	1.15	19.20	-0.822	-4.039	-2.448	807.75
2.45	0.61	19.18	-0.813	-4.041	-2.445	808.25
1.25	0.31	19.16	-0.816	-4.038	-2.441	807.50
0.53	0.13	19.09	-0.800	-4.008	-2.420	801.50

** Curvature based soley on West Curvature-meter as results no good from east meter as a crack passed through anchorage point.

IMAGE EVALUATION TEST TARGET (QA-3)

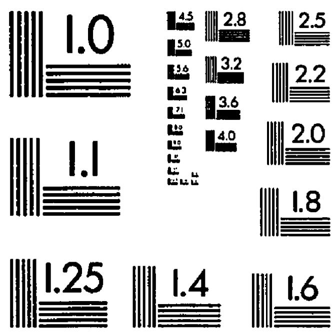

150mm

6″

APPLIED IMAGE, Inc
1653 East Main Street
Rochester, NY 14609 USA
Phone: 716/482-0300
Fax: 716/288-5989